January 1967

The structure of turbulence in an open channel with large spherical roughness elements

Farooq Nazir

Report WG34-1T

THE STRUCTURE OF TURBULENCE IN AN OPEN CHANNEL WITH LARGE SPHERICAL ROUGHNESS ELEMENTS

by

Farooq Nazir

This study was supported by funds from the
National Science Foundation
Grant GK-734

Utah Water Research Laboratory
College of Engineering
Utah State University
Logan, Utah

1967

ACKNOWLEDGMENTS

The author wishes to express his sincere appreciation to Dr. Calvin G. Clyde, his major professor and advisor for suggesting the research problem and supervising the research work. He considers that without his continuous assistance and encouragement and valuable criticism the study could not be completed. The author is especially indebted to him for providing timely financial assistance.

Gratitude is also expressed to Mr. Gaylord V. Skogerboe for the help rendered in setting up the research equipment and construction of "false bed".

The author is very much thankful to Mr. Mohammad Aslam Rasheed, his old friend, who spent his valuable time in reading the proofs of the thesis and making suggestions.

Thanks are also due to Mr. Edmond Cheng, Mr. Yousaf Chaudry, Mr. Nasim Ahmad and Mr. Kenneth Steele and his staff of the Utah Water Research Laboratory for their valuable help in conducting this study.

Farooq Nazir

TABLE OF CONTENTS

TABLE OF CONTENTS CONTINUED

LIST OF FIGURES

LIST OF FIGURES CONTINUED

LIST OF FIGURES CONTINUED

ABSTRACT

The Structure of Turbulence in an Open

Channel with Large Spherical

Roughness Elements

by

Farooq Nazir

Utah State University, 1967

Major Professor: Dr. Calvin G. Clyde
Department: Civil Engineering

The present status of knowledge of turbulent flow is inadequate, especially in the case of rough open channels, for the formulation of a general theory. It is believed that more experimental data and the subsequent interpretation of these data are necessary before a workable theory can be formulated. Hence, a description of the turbulence present in a rough open channel can be valuable.

For this study an artificially roughened bed 48 feet in length was placed in a channel 8 feet wide and 6 feet deep. Measurements were made of the following properties of turbulence at three different slopes:

1. Intensity of turbulence.
2. Autocorrelation and cross-correlation coefficients.
3. Microscale and macroscale of turbulence.
4. One-dimensional energy and dissipation spectra.

All the measurements were taken with a piezoelectric total head tube in combination with necessary electronics equipment.

The results have been presented in the form of dimensionless curves as far as possible. These curves are compared with published data.

(113 pages)

CHAPTER I

INTRODUCTION

Fluid flow may be classified as laminar or turbulent, steady or unsteady, and uniform or nonuniform. These classifications are based on the motion of fluid particles. The most commonly observed flow is that found in open channels. This flow in most cases is turbulent. Rouse (1938) defines turbulent flow as "a flow characterized primarily by a continuous mixing action of the eddies whereby small fluid masses are constantly being moved into regions of different velocity causing a more uniform velocity distribution as compared with that in laminar flow." In 1921 Taylor and von Karman gave the following definition: "Turbulence is an irregular motion which in general makes its appearance in fluids, gaseous or liquid, when they flow past solid surfaces or even when neighbouring streams of the same fluid flow past or over one another."

The phenomenon of turbulent flow is not limited to open channels, but is also observed in under sea currents, tital currents, in the atmosphere, pipe flow, and lubricants lying between two rapidly moving parts of machines.

Due to the common occurrence of the phenomenon of turbulence in fluid flow problems, hydraulicians have always wished to get as complete knowledge as possible about its production, convection, diffusion,

distribution, and dissipation. The first prominent person who tried to understand this problem was Reynolds (1911). During the years of 1900 to 1915 many people, realizing that a knowledge of fluctuations occurring during turbulent flow would add materially to the understanding of turbulence, suggested various empirical theories. The theories proposed by Boussinesq, Prandtl and von Karman were widely accepted.

In 1921, Taylor introduced the idea that the velocity of fluid in turbulent motion was a random function of position and time. He applied principles of statistical mechanics to this random continuous function and in 1935 published his classic series of papers on statistical theories of turbulence. This represented a new approach to the understanding of turbulence which the previous investigators had not considered.

Some of the prominent workers in the field of statistical theory of turbulence are von Karman (1931-1948) who also made important contributions to Prandtl's (1926) empirical mixing length theory, Kolmogoroff (1941), Burgers (1953), Townsend (1947), Dryden (1929-1937), Batchelor (1946), Lin (1947), Chandrasekhar (1949), Laufer (1951), Ippen (1955), Einstein (1959), Li (1959), Clyde (1961), and Eagleson et al. (1961). A Majority of the above mentioned scientists studied the turbulence created in air flow by screens of various sizes in a wind tunnel. Very few attempted to observe the properties of turbulence present in an open channel, especially with large roughness. The necessity of knowing more about this type of turbulence was always present. Hence an attempt was made in this investigation to complete

the following objectives in an artificially roughened open channel:

1. To find out the effect of large roughness on the mean velocity distribution in a turbulent flow field.

2. To observe the distribution of relative intensity of turbulence as a function of relative depth for different slopes.

3. To determine the autocorrelation function and the distribution of mean macroscale of turbulence as a function of relative depth.

4. To obtain the distribution of microscale as a function of depth and slope.

5. To get the cross-correlation for different depths and slopes.

6. To determine the energy spectral distribution and if possible to determine the spectral laws of locally isotropic turbulence.

Most of the quantities mentioned above are spatial vectors. Due to the limitation imposed by the instruments available, it is not possible to measure all the components. Hence the study will be restricted to the measurement of only one component.

CHAPTER II

EQUATION OF MOTION AND SEMIEMPIRICAL THEORIES

The phenomenon of turbulent flow cannot be fully understood without a knowledge of the equations governing it. These equations will be briefly reviewed in the following pages.

The equation of conservation of mass (the continuity equation) reads as follows

$$\frac{\partial \rho}{\partial t} + \frac{\partial(\rho U_1)}{\partial x_1} + \frac{\partial(\rho U_2)}{\partial x_2} + \frac{\partial(\rho U_3)}{\partial x_3} = 0 \quad . \quad . \quad . \quad (2\text{-}1)$$

This holds only for an instant in a turbulent flow.

Substituting the following expressions in equation (2-1),

$$\rho = \bar{\rho} + \rho' \quad . \quad . \quad . \quad . \quad . \quad . \quad . \quad . \quad (2\text{-}2)$$

$$U_1 = \bar{U}_1 + u_1 \quad . \quad . \quad . \quad . \quad . \quad . \quad . \quad . \quad (2\text{-}3)$$

$$U_2 = \bar{U}_2 + u_2 \quad . \quad . \quad . \quad . \quad . \quad . \quad . \quad (2\text{-}4)$$

$$U_3 = \bar{U}_3 + u_3 \quad . \quad . \quad . \quad . \quad . \quad . \quad . \quad (2\text{-}5)$$

and taking the average

$$\overline{\frac{\partial(\bar{\rho}+\rho')}{\partial t}} = -\overline{\frac{\partial}{\partial x_1}(\bar{\rho}+\rho')(\bar{U}_1+u_1)} - \overline{\frac{\partial}{\partial x_2}(\bar{\rho}+\rho')(\bar{U}_2+u_2)} - \overline{\frac{\partial}{\partial x_3}(\bar{\rho}+\rho')(\bar{U}_3+u_3)} \quad . \quad (2\text{-}6)$$

Applying the properties of averaging as given in the Appendix B the following equation is obtained.

$$\frac{\partial \bar{\rho}}{\partial t} + \frac{\partial}{\partial x_1}\left(\bar{\rho}\bar{U}_1 + \overline{\rho' u_1}\right) + \frac{\partial}{\partial x_2}\left(\bar{\rho}\bar{U}_2 + \overline{\rho' u_2}\right) + \frac{\partial}{\partial x_3}\left(\bar{\rho}\bar{U}_3 + \overline{\rho' u_3}\right) = 0 \quad \ldots\ldots \quad (2\text{-}7)$$

For incompressible fluids ρ is a constant quantity and the continuity equation becomes

$$\frac{\partial u_1}{\partial x_1} + \frac{\partial u_2}{\partial x_2} + \frac{\partial u_3}{\partial x_3} = 0 \quad \ldots\ldots \quad (2\text{-}8)$$

Next, consider the momentum equations (Navier-Stokes equations). For flow in the x_1-direction at any instant

$$a_{x_1} = \frac{\partial U_1}{\partial t} + U_1\frac{\partial U_1}{\partial x_1} + U_2\frac{\partial U_1}{\partial x_2} + U_3\frac{\partial U_1}{\partial x_3}$$

$$= -\frac{\partial}{\partial x_1}\left(\frac{P}{\rho} + gh\right) + \nu\left(\frac{\partial^2 U_1}{\partial x_1^2} + \frac{\partial^2 U_1}{\partial x_2^2} + \frac{\partial^2 U_1}{\partial x_3^2}\right) \quad \ldots\ldots \quad (2\text{-}9)$$

Taking the time averages

$$\bar{a}_{x_1} = \frac{\partial \bar{U}_1}{\partial t} + \overline{U_1\frac{\partial U_1}{\partial x_1}} + \overline{U_2\frac{\partial U_1}{\partial x_2}} + \overline{U_3\frac{\partial U_1}{\partial x_3}}$$

$$= -\frac{\partial}{\partial x_1}\left(\frac{\bar{P}}{\rho} + gh\right) + \nu\left(\frac{\partial^2 \bar{U}_1}{\partial x_1^2} + \frac{\partial^2 \bar{U}_1}{\partial x_2^2} + \frac{\partial^2 \bar{U}_1}{\partial x_3^2}\right)$$

If the flow is steady $\frac{\partial \bar{U}_1}{\partial t} = 0$ and h is not a function of time.

Then using equation (1) to (5) from Appendix B

$$\overline{U_2 \frac{\partial U_1}{\partial x_2}} = \overline{(\bar{U}_2 + u_2)\frac{\partial(\bar{U}_1 + u_1)}{\partial x_2}} = \overline{\bar{U}_2 \frac{\partial U_1}{\partial x_2}} + \overline{u_2 \frac{\partial \bar{U}_1}{\partial x_2}}$$

$$\overline{\bar{U}_2 \frac{\partial u_1}{\partial x_2}} + \overline{u_2 \frac{\partial u_1}{\partial x_2}} = \bar{U}_2 \frac{\partial \bar{U}_1}{\partial x_2} + \bar{u}_2 \frac{\partial \bar{U}_1}{\partial x_2} + \bar{U}_2 \frac{\partial \bar{u}_1}{\partial x_2} + \overline{u_2 \frac{\partial u_1}{\partial x_2}}$$

$$= \bar{U}_2 \frac{\partial \bar{U}_1}{\partial x_2} + \overline{u_2 \frac{\partial u_1}{\partial x_2}}$$

because

$$\bar{u}_1 = \bar{u}_2 = 0$$

Thus

$$\bar{a}_{x_1} = \overline{U_1 \frac{\partial U_1}{\partial x_1}} + \overline{U_2 \frac{\partial U_1}{\partial x_2}} + \overline{U_3 \frac{\partial U_1}{\partial x_3}}$$

$$= \bar{U}_1 \frac{\partial \bar{U}_1}{\partial x_1} + \bar{U}_2 \frac{\partial \bar{U}_1}{\partial x_2} + \bar{U}_3 \frac{\partial \bar{U}_1}{\partial x_3}$$

$$+ \overline{u_1 \frac{\partial u_1}{\partial x_1}} + \overline{u_2 \frac{\partial u_1}{\partial x_2}} + \overline{u_3 \frac{\partial u_1}{\partial x_3}}$$

But

$$u_1 \frac{\partial u_1}{\partial x_1} + u_2 \frac{\partial u_1}{\partial x_2} + u_3 \frac{\partial u_1}{\partial x_3}$$

$$= \left[\frac{\partial u_1 u_1}{\partial x_1} - u_1 \frac{\partial u_1}{\partial x_1}\right] + \left[\frac{\partial u_1 u_2}{\partial x_2} - u_1 \frac{\partial u_2}{\partial x_2}\right]$$

$$+ \left[\frac{\partial u_1 u_3}{\partial x_3} - u_1 \frac{\partial u_3}{\partial x_3}\right]$$

$$= \frac{\partial u_1 u_1}{\partial x_1} + \frac{\partial u_1 u_2}{\partial x_2} + \frac{\partial u_1 u_3}{\partial x_3} - u_1\left(\frac{\partial u_1}{\partial x_1} + \frac{\partial u_2}{\partial x_2} + \frac{\partial u_3}{\partial x_3}\right)$$

According to equation (2-8) $\quad \frac{\partial u_1}{\partial x_1} + \frac{\partial u_2}{\partial x_2} + \frac{\partial u_3}{\partial x_3} = 0$

Then $\quad \overline{u_1 \frac{\partial u_1}{\partial x_1}} + \overline{u_2 \frac{\partial u_1}{\partial x_2}} + \overline{u_3 \frac{\partial u_1}{\partial x_3}} = \frac{\partial \overline{u_1 u_1}}{\partial x_1} + \frac{\partial \overline{u_1 u_2}}{\partial x_2} + \frac{\partial \overline{u_1 u_3}}{\partial x_3}$

Thus the Navier-Stokes equation for steady turbulent incompressible flow can be written as

$$\overline{a}_{x_1} = \overline{U}_1 \frac{\partial \overline{U}_1}{\partial x_1} + \overline{U}_2 \frac{\partial \overline{U}_1}{\partial x_2} + \overline{U}_3 \frac{\partial \overline{U}_1}{\partial x_3}$$

$$+ \frac{\partial \overline{u_1 u_1}}{\partial x_1} + \frac{\partial \overline{u_2 u_1}}{\partial x_2} + \frac{\partial \overline{u_3 u_1}}{\partial x_3}$$

$$= - \frac{\partial}{\partial x_1} \left(\frac{\overline{P}}{\rho} + gh \right) + \nu \left(\frac{\partial^2 \overline{U}_1}{\partial x_1} + \frac{\partial^2 \overline{U}_1}{\partial x_2} + \frac{\partial^2 \overline{U}_1}{\partial x_3} \right) . \quad (2\text{-}10)$$

Similarily, the equations for other directions can be written as

$$\overline{a}_{x_2} = \overline{U}_1 \frac{\partial \overline{U}_2}{\partial x_1} + \overline{U}_2 \frac{\partial \overline{U}_2}{\partial x_2} + \overline{U}_3 \frac{\partial \overline{U}_2}{\partial x_3} + \frac{\partial \overline{u_1 u_2}}{\partial x_1} + \frac{\partial \overline{u_2 u_2}}{\partial x_2} + \frac{\partial \overline{u_3 u_2}}{\partial x_3}$$

$$= - \frac{\partial}{\partial x_2} \left(\frac{\overline{P}}{\rho} + gh \right) + \nu \left(\frac{\partial^2 \overline{U}_2}{\partial x_1} + \frac{\partial^2 \overline{U}_2}{\partial x_2^2} + \frac{\partial^2 \overline{U}_2}{\partial x_3} \right) . \quad (2\text{-}11)$$

$$\overline{a}_{x_3} = \overline{U}_1 \frac{\partial \overline{U}_3}{\partial x_1} + \overline{U}_2 \frac{\partial \overline{U}_3}{\partial x_2} + \overline{U}_3 \frac{\partial \overline{U}_3}{\partial x_3} + \frac{\partial \overline{u_3 u_1}}{\partial x_1} + \frac{\partial \overline{u_3 u_2}}{\partial x_2} + \frac{\partial \overline{u_3 u_3}}{\partial x_3}$$

$$= - \frac{\partial}{\partial x_3} \left(\frac{\overline{P}}{\rho} + gh \right)$$

$$+ \nu \left(\frac{\partial^2 U_3}{\partial x_1^2} + \frac{\partial^2 U_3}{\partial x_2^2} + \frac{\partial^3 U_3}{\partial x_3^2} \right) . \quad (2\text{-}12)$$

The instantaneous quantities in equation (2-9) have been replaced by mean quantities, and three additional terms have been added in each equation which involve the fluctuating components of the velocity.

If equation (2-10) is multiplied by ρ the results are

$$\rho \overline{a}_{x_1} = \rho \overline{U}_1 \frac{\partial \overline{U}_1}{\partial x_1} + \rho \overline{U}_2 \frac{\partial \overline{U}_1}{\partial x_2} + \rho \overline{U}_3 \frac{\partial \overline{U}_1}{\partial x_3}$$

$$+ \rho \frac{\partial u_1 u_1}{\partial x_1} + \rho \frac{\partial u_1 u_2}{\partial x_2} + \rho \frac{\partial u_2 u_1}{\partial x_3}$$

$$= - \frac{\partial}{\partial x_1} \left(\rho \overline{P} + \rho g h \right) + \mu \left(\frac{\partial^2 \overline{U}_1}{\partial x_1} + \frac{\partial^2 \overline{U}_1}{\partial x_2} + \frac{\partial^2 \overline{U}_1}{\partial x_3} \right) . \quad (2\text{-}13)$$

The term

$$\mu\left(\frac{\partial^2\bar{U}_1}{\partial x_1^2}+\frac{\partial^2\bar{U}_1}{\partial x_2^2}+\frac{\partial^2\bar{U}_1}{\partial x_3^2}\right)$$

gives the stresses in the fluid due to mean velocity $\bar{U}_1$ and molecular viscosity μ . The terms $\frac{\partial \rho\overline{u_1u_2}}{\partial x_1}$, $\frac{\partial \rho\overline{u_1u_2}}{\partial x_2}$, $\frac{\partial \rho\overline{u_3u_1}}{\partial x_3}$, give the stress in the fluid caused by turbulent fluctuations. In all three equations (2-10), (2-11) and (2-12) the following nine new quantities are involved

$$\rho\overline{u_1u_1}\ ,\quad \rho\overline{u_1u_2}\ ,\quad \rho\overline{u_1u_3}$$

$$\rho\overline{u_2u_1}\ ,\quad \rho\overline{u_2u_1}\ ,\quad \rho\overline{u_2u_3}$$

$$\rho\overline{u_3u_1}\ ,\quad \rho\overline{u_3u_2}\ ,\quad \rho\overline{u_3u_3}$$

These are called Reynolds, or eddy, stresses. These also represent the rate of transfer of momentum across corresponsind surfaces.

The solution of the Reynolds equations can represent the turbulent flow fully but there are only four available equations involving ten unknown quantities.

In order to obtain definite results from the Reynolds equations further hypotheses about the Reynolds stresses are necessary.

Many different ways for determining the Reynolds stresses have been proposed by different people. A few important and interesting methods are given in the following few pages.

Consider the case of simple two-dimensional parallel turbulent flow having mean flow in x_1 direction only.

Then

$$\overline{U}_1 = \overline{U}_1(x_2) \qquad \overline{U}_2 = 0 \qquad \overline{U}_3 = 0$$

and equation (2-10) gives

$$\frac{\partial \overline{P}}{\partial x_1} = -\rho \frac{\partial}{\partial x_2} \overline{u_1 u_2} \quad . \quad . \quad . \quad . \quad . \quad . \quad (2\text{-}14)$$

This can only be solved if the value of $\overline{u_1 u_2}$ is known. Boussinesq (1877) assumed that

$$\overline{u_1 u_2} = -\epsilon_t \frac{\partial \overline{U}_1}{\partial x_2} \quad . \quad . \quad . \quad . \quad . \quad . \quad . \quad . \quad (2\text{-}15)$$

where ϵ_t is called the turbulent exchange coefficient. This provides a means of getting the distribution of $\overline{U}_1$. Comparing the equation (2-15) with Newton's viscosity equation

$$\tau = \mu \frac{d\overline{U}_1}{dx_2} \quad . \quad . \quad . \quad . \quad . \quad . \quad . \quad (2\text{-}16)$$

it was found that $\epsilon_t = \mu + \eta$ where η is an additional factor known as eddy viscosity which depends upon the intensity of turbulence and boundary conditions of the flow. The determination of the exact value of ϵ_t is a tedious problem so the Boussinesq theory cannot be readily applied.

Another semiempirical theory about turbulence which is the most successful and best known is Prandtl's (1925) mixing length theory which is based on following assumptions:

1. The turbulent shear stress between two fluid layers is due to exchange of momentum.

2. The instantaneous velocity in the x_1-direction is given by the following relationship:

$$u_1 = \bar{U}_1 + \ell_i \frac{d\bar{U}_1}{dx_2} - \bar{U}_1 = \ell_i \frac{d\bar{U}_1}{dx_2}$$

where ℓ_i is a constant known as the mixing length.

3. $|u_1| = |u_2|$ (The vertical bars show that only the magnitude is being considered and no consideration is given to the sign.)

According to the first assumption the instantaneous shear stress is given by the transfer of momentum through a unit area.

Hence

$$\tau_i = m(\bar{U}_A + \bar{U}_B)$$

$$= \rho u_2 u_1$$

$$= \rho u_2 \ell_i \frac{d\bar{U}_1}{dx_2} = \rho \left(\ell_i \frac{d\bar{U}_1}{dx_2} \right)^2 . \qquad (2\text{-}17)$$

Then

$$\tau = \rho \overline{u_2 u_1} = \rho \left(\ell \frac{d\bar{U}_1}{dx_2} \right)^2 \quad . \quad . \qquad (2\text{-}18)$$

Taylor (1932) suggested that the assumption of conservation of momentum during the turbulent mixing process over the length ℓ is not valid. He proposed a new theory on the basis of following assumptions.

1. The turbulent shear stress between two fluid layers is due to exchange of moment of momentum (or vorticity).

2. The instantaneous vorticity

$$w = \ell \frac{d\bar{\omega}}{dx_2} = \ell \frac{d^2\bar{U}_1}{dx_2^2} \quad \ldots\ldots \quad (2\text{-}19)$$

From equation (2-10)

$$\frac{\partial \bar{P}}{\partial x_1} = -\rho \frac{\partial}{\partial x_1} (\overline{u_1 u_2}) = -\rho \overline{u_2 \omega}$$

$$= \rho u_2 \ell \frac{d\bar{\omega}}{dx_2}$$

$$= \rho u_2 \ell \frac{d^2\bar{U}_1}{dx_2^2} \quad \ldots\ldots \quad (2\text{-}20)$$

Perhaps the most satisfactory approach is that embodied in von Karman's (1930) hypothesis of turbulent similitude based upon these two assumptions.

1. The mechanism of turbulence is independent of viscosity except in the immediate neighborhood of the flow boundaries.

2. The pattern of secondary flow is statistically similar from point to point varying only in time and length scales.

If this hypothesis is applied to the case of two-dimensional uniform motion as shown by von Karman, the following three conclusions will be reached.

1. The components of fluctuation will be proportional to the length ℓ and to the gradient $\partial \bar{U}_1 / \partial x_2$

2. The intensity of shear is proportional to $\rho \ell^2 (\partial \bar{U}_1 / \partial x_2)$

3. The length ℓ will be proportional to

$$\frac{\partial \bar{U}_1 / \partial x_2}{\partial^2 U_1 / \partial^2 x_2}$$

From these the following is obtained

$$\tau = \rho \ell^2 \left(\frac{\partial \bar{U}_1}{\partial x_2} \right)^2$$

$$= K^2 \rho \frac{\left(\partial \bar{U}_1 / \partial x_2 \right)^4}{\left(\partial^2 \bar{U}_1 / \partial^2 x_2 \right)^2} \quad . \quad . \quad . \quad . \quad (2\text{-}21)$$

CHAPTER III

STATISTICAL THEORY OF TURBULENCE

The various semiempirical theories described in Chapter II can define only the distribution of the mean velocity of flow. These theories give no idea about the size of the eddies or the production, distribution, and dissipation of turbulence energies. A detailed analysis was always needed to solve the various problems faced in this flow phenomenon. In 1921 Taylor published his work, commonly known as the statistical theory of turbulence, which opened a new way of treating this flow problem and became the foundation of modern turbulence studies.

Taylor's theory was further developed by von Karman (1931, 1937, 1938, 1948), Kolmogoroff (1941), Heisenberg (1948), and several other scientists. These scientists assumed that the fluctuating quantities met in turbulence are random in nature and that it is possible to apply statistical mechanics to them and get average values of each fluctuating function and then to deduce practically useful results.

The turbulence which is usually met in fluid flow problems is such that its mathematical analysis is nearly impossible. Thus, Taylor and his followers while developing their theories considered an idealized homogeneous and isotropic flow.

In a turbulent flow if each of the fluctuating quantities have the same values at all points in the flow field then this flow field is said to have homogeneous turbulence.

In an isotropic turbulent flow field, the mean value of any function of the velocity components and space derivatives is unaltered by any rotation or reflection of reference areas.

Thus

$$\overline{u_1^2} = \overline{u_2^2} = \overline{u_3^2} \quad . \quad . \quad . \quad . \quad . \quad (3\text{-}1)$$

and

$$\overline{u_1 u_3} = \overline{u_3 u_2} = \overline{u_1 u_2} = 0 \quad . \quad . \quad (3\text{-}2)$$

When

$$\overline{u_1^2} \neq \overline{u_2^2} \neq \overline{u_3^2}$$

the turbulence becomes anisotropic.

Taylor defined certain terms which can describe the behavior of turbulent flow intelligently. A brief description of these terms follows.

Intensity of Turbulence

At any point in a turbulent flow field, the velocity vector does not have a constant value. It is always changing in magnitude and direction. This vector can be assumed to be a sum of two velocities $\overline{U}$ and u, $\overline{U}$ refers to the average movement while u refers to the fluctuations. Schematically, the velocity u might be considered

as the relative velocity within an eddy at the point of observation and $\overline{U}$ as the velocity with which the eddy is carried past this point by the flow. Hence for a turbulent flow, the velocity vector is

$$U = \overline{U} + u \quad . \quad . \quad . \quad . \quad . \quad . \quad . \quad . \quad (3\text{-}3)$$

Considering the components of U along three coordinate axes, $U_i = \overline{U}_i + u_i$ where $i = 1, 2, 3$ represent the three coordinate axes. The mean square of the fluctuating velocity is referred to as the intensity of turbulence and can be defined mathematically as

$$u'_i = \left[\int_{\infty}^{\infty} u_i^2 \, f(u_i) \, du_i \right]^{\frac{1}{2}} \quad . \quad . \quad (3\text{-}4)$$

It is seen that the statistical average of u_i gives u'_i but such an average is almost impossible to obtain. This can be obtained only by having an infinite number of channels of exactly the same size, shape, and flow conditions, and then measuring u_i in all channels at a geometrical similar point and taking their average.

According to certain theorems it has been proven that for a random variable (u'_i is considered a random variable), the statistical average of a quantity is the same as the time average of that quantity. Hence

$$u'_i = \sqrt{\overline{u_i^2}} = \left[\frac{1}{\Delta t} \int_{o}^{\Delta t} u_i^2 \, dt \right]^{\frac{1}{2}} . \quad (3\text{-}5)$$

The relative intensity of turbulence is defined as

$$\frac{\sqrt{\overline{u_i^2}}}{\overline{U}_i} \quad i.e. \quad \frac{u'_i}{\overline{U}_i} \qquad i = 1, 2, 3.$$

The intensity of turbulence is a means of describing the strength of the turbulence.

Correlation Coefficients

While developing the statistical theory of turbulence, Taylor and others correlated various fluctuating quantities in a turbulent flow field and described many types of correlations. These correlations provide useful information regarding size and strength of eddies and turbulent stresses, etc.

The most commonly used correlations are velocity correlations because these are easy to measure and it is possible to express pressure correlations in terms of these.

The correlation between two velocities at two points x and $(x + \vec{r})$ is as follows

$$R_{ij}(\vec{r}) = \overline{u_i(x)\, u_j(x + r)} \quad . \qquad (3\text{-}6)$$

Von Karman suggested that equation (3-6) forms a second order tensor.

Triple velocity correlation may also be defined as suggested by Hinze (1959)

$$(S_{ijk})_{AB} = \overline{(u_i)_A\, (u_k)_B\, (u_j)_B} \quad . \quad . \qquad (3\text{-}7)$$

This is a third order tensor.

The pressure correlations are defined as follows.

$$L_a = \frac{1}{\rho}\, \overline{p u_i} \quad . \quad . \quad . \quad . \quad . \quad . \quad . \qquad (3\text{-}8)$$

Another type of correlation very commonly used in diffusion problems is the Eulerian time correlation also known as the autocorrelation and defined as

$$R_{E_1}(\tau) = \frac{\overline{u_1(\tau)\, u_1(\tau - \Delta t)}}{\overline{u_1^2}} \quad . \quad . \quad . \quad . \quad . \quad (3\text{-}9)$$

where

u_1 - velocity of a particle at time

τ - time at which u_1 was recorded

$u_1(\tau - \Delta t)$-velocity of the particle at the same point at $(\tau - \Delta t)$ time

If the turbulence is assumed to be homogeneous then

$$\overline{u_{1_A}^2} = \overline{u_{1_B}^2} = \overline{u_1^2(t)}$$

where $\overline{u_1^2}$ is only a function of time and does not depend on the position. If isotrophy is also assumed the correlation functions $R_{ij}(\vec{r})$, L_a, $(S_{ijk})_{AB}$ become invariant for any rotation of axes.

Under these conditions, the correlation tensor

$$R_{ij}(\vec{r}) = \overline{u_i(x)\, u_j(x + \vec{r})} \quad . \quad . \quad . \quad . \quad (3\text{-}6)$$

loses its full identity leaving behind only two terms.

$$R_{11}(r) \quad \text{and} \quad R_{22}(r)$$

where $R_{11}(r)$ is the longitudinal double-velocity correlation and $R_{22}(r)$ is the lateral double-velocity correlation function

$$R_{11}(r) = \overline{u_{1A}\, u_{1B}} = \overline{u_1^2}\, f(r) \quad . \quad . \quad . \quad (3\text{-}10)$$

$$R_{22}(r) = \overline{u_{2A}\, u_{2B}} = \overline{u_2^2}\, g(r) \quad (3\text{-}11)$$

It was found by von Karman and Howarth (1938) that

$$g(r) = \left[f(r) - \frac{r}{2} f'(r) \right] \quad . \quad . \quad . \quad . \quad (3\text{-}12)$$

Since both g(r) and f(r) can be measured and if it is found that equation (3-12) holds good, then turbulence can be said to be homogeneous and isotropic.

The various correlation coefficients have been found useful in determining the scales of turbulence, eddy stress distribution of fluctuating velocity components, etc. Extensive use of $R_{ij}(\vec{r})$ and $R_E(r)$ have been made in determining the scale of turbulence. In fact, macroscale of turbulence can be measured only by the help of corss-correlation curves.

Microscale of Turbulence

It is always of interest to measure in some way the maximum and minimum size of eddies present in a particular type of turbulence. Many different types of scales have been defined which relate the size of eddies to linear dimensions but the scales described by Taylor (1921) have attained the widest popularity.

Consider homogeneous turbulence so that

$$\overline{u_1(\xi_2)\, u_1(\xi_2 + x_2)} = \overline{u_1(\xi_2 - x_2)\, u_1(\xi_2)}$$

or

$$\overline{u_1(\xi_2) \frac{\partial u_1(\xi_2 + x_2)}{\partial(\xi_2 + x_2)}} = -\overline{\frac{\partial u_1(\xi_2 - x_2)}{\partial(\xi_2 - x_2)} u_1(\xi_2)}$$

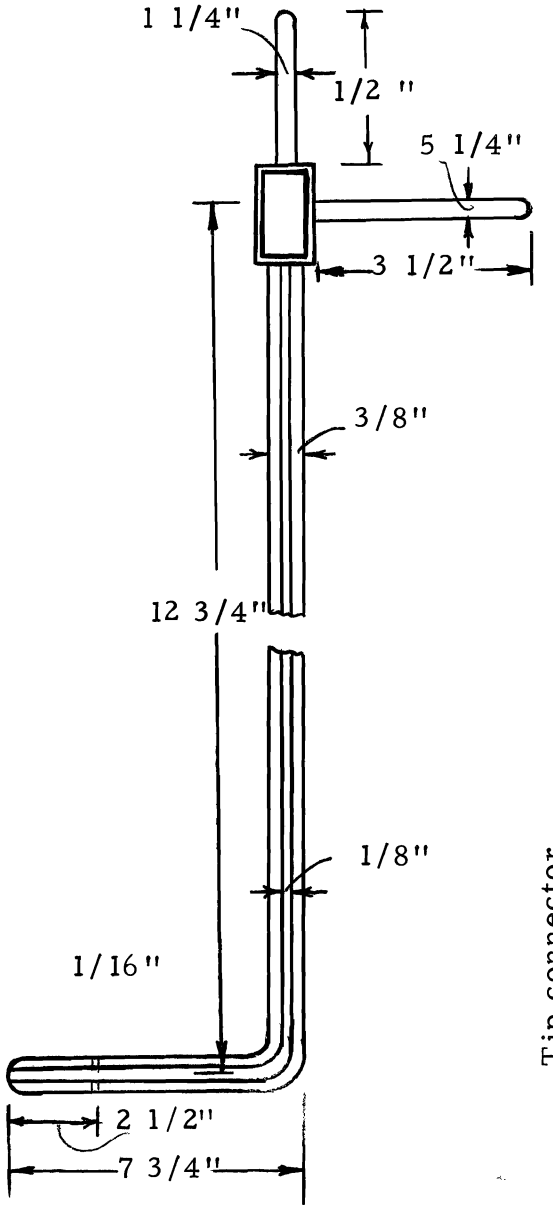

Figure 1. Pitot tube

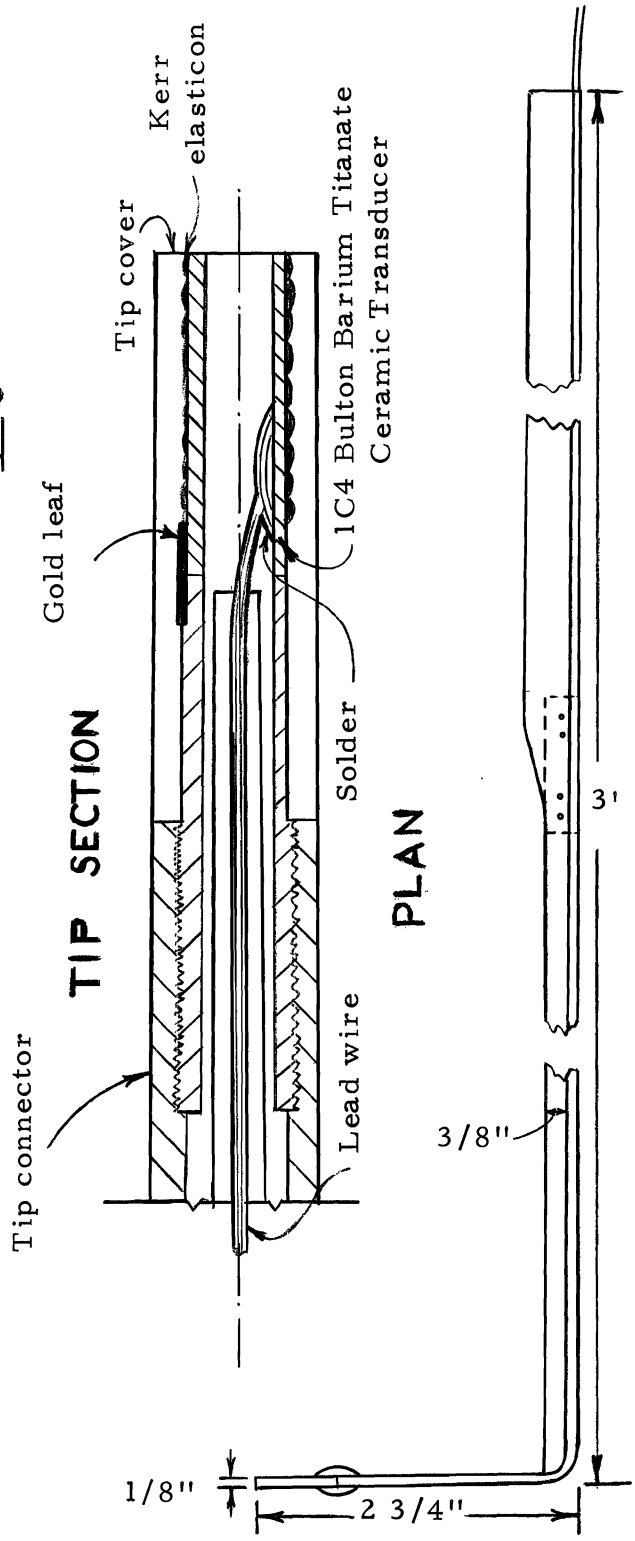

Figure 2. Total head transducer probe

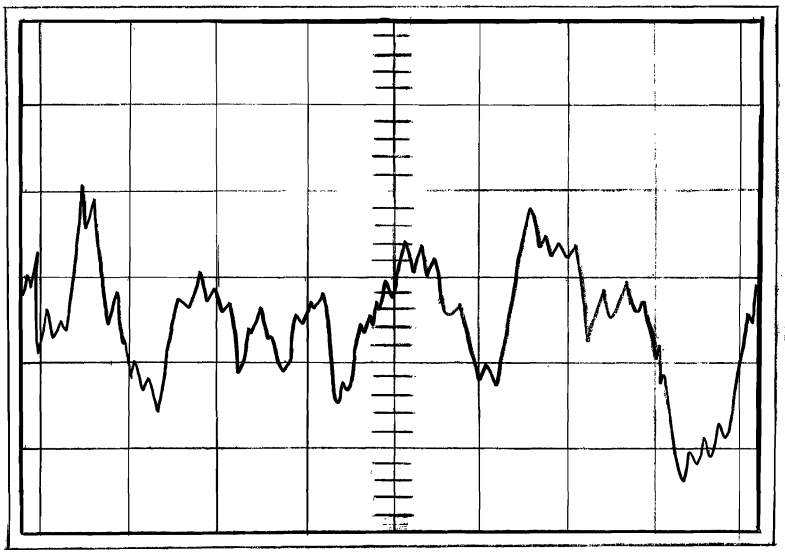

Figure 3. Typical oscilloscope picture of turbulent total head fluctuations.

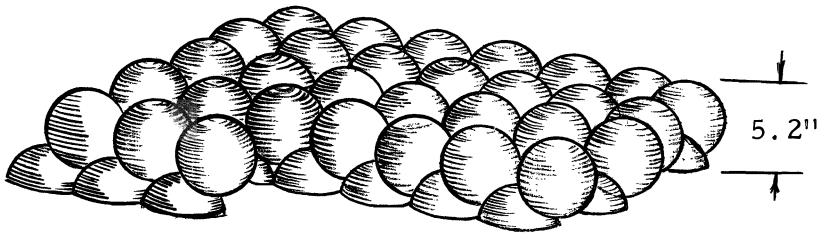

Figure 4. Spherical roughness element.

to selectively reject certain frequencies of the signal with the amplifers. During experiments all frequencies lying above 1000 cps and below 0.8 cps were rejected because turbulence frequencies are rarely out of this range. Any signal whose frequency is above 1000 cps or below 0.8 cps is not caused by turbulence. The voltage gain for all measurements was kept at 100 except for spectrum analysis for which a gain of 1000 was used.

Random Signal Indicator and Correlator

This instrument is designed for measuring the root-mean-square value (R.M.S.) of the voltage of two electrical input signals as well as the correlation coefficient relating the two signals. In this study it was used to measure the following properties of turbulence:

1. Intensity of turbulence
2. Autocorrelation coefficient
3. Cross-correlation coefficient
4. Microscale of turbulence.

Two electrical meters are fixed at the face of the instrument. The R.M.S. meter is capable of measuring the root mean square value of either signal A or B separately, the time derivative of signal A, R.M.S. value of the sum and difference of the signal A and B regardless of wave form. The other meter gives $\frac{A}{B}$, $\frac{A}{\tau \frac{dA}{dt}}$ and $\frac{A+B}{A-B}$ and is therefore called the ratio meter.

Operation of the instrument is summarized below.

The random signal A is first fed into a variable gain preamplifier, then it passes through an isolation amplifier, an output amplifier, and finally through a squaring and averaging network. The circuit for channel B is similar to the circuit of A except that it contains a sign invertor. The instrument has, in addition, two circuits for adding voltages, a differentiator, and a squaring and averaging network.

This instrument has the frequency response of 3 cps to 200 k cps.

The instrument was adjusted completely, before it was used, in accordance with its instruction manual. The gain controls were always kept at the recommended position while making measurements of intensity of turbulence. For other measurements the adjustments were in accordance with the instruction manual.

Spectrum Analyser

The instrument used for spectrum measurement was manufactured by Quan Tech Laboratory. This instrument was basically a combination of filters with an R.M.S. voltmeter. Thus it gives the R.M.S. voltage of an input signal after passing through adjustable filters. The range of frequency response of the instrument is from 30 cps to 100 K cps. Band pass width is adjustable at 10 cps or 30 cps. Ten different ranges are available on the R.M.S. meter by operating the voltage gain switch. The instrument is equipped with two input terminals X1 and X10 and it is also provided with a meter-multiplier which is to be set to a range higher than the signals to be measured. For taking absolute readings in millivolts, the reading on the R.M.S. meter should be multiplied by the meter multiplier factor when gain control is fully clockwise.

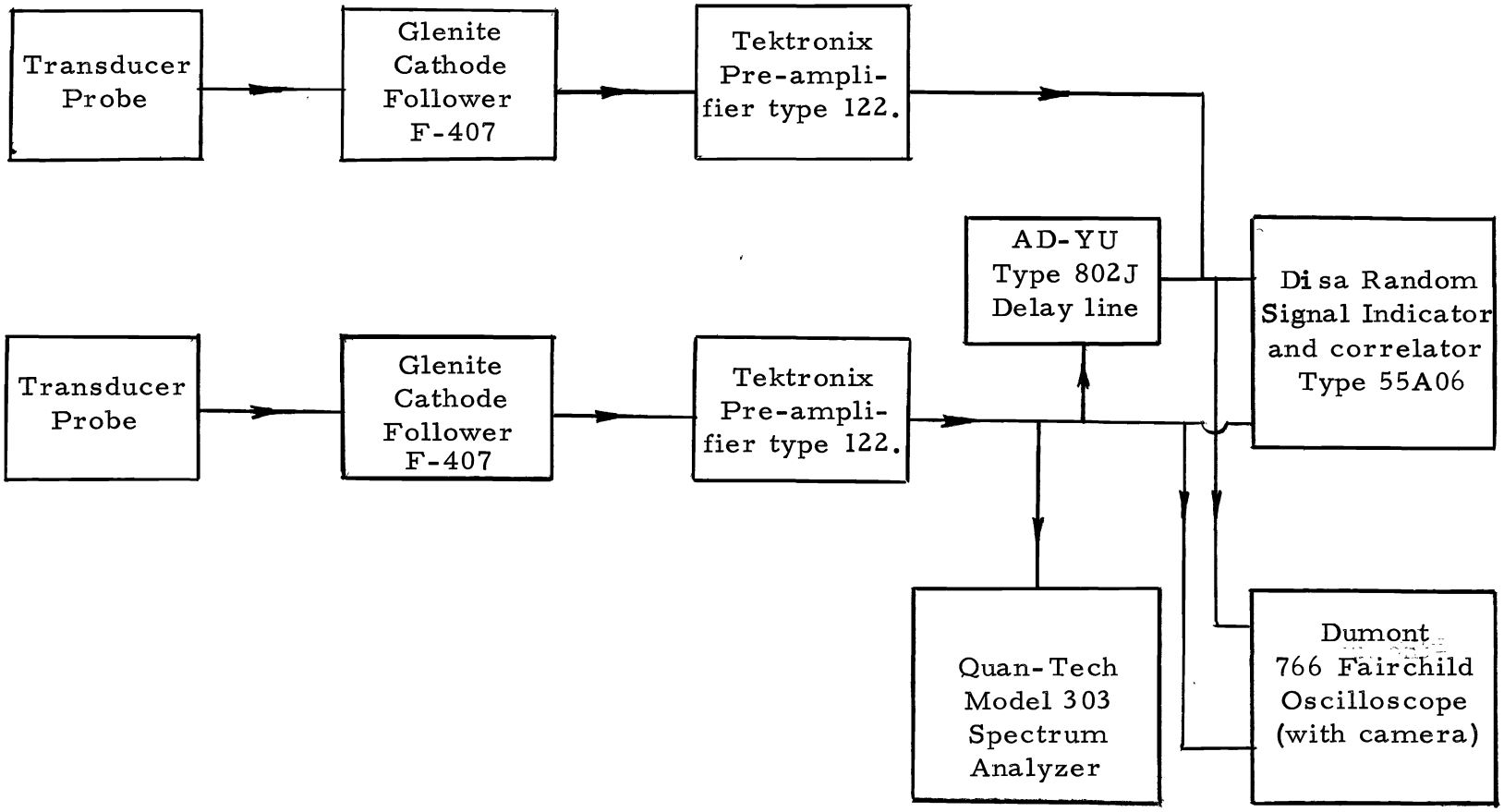

Figure 5. Block diagram of the transducer probe and associated electronic instrumentation.

Variable Time Delay

For measuring the autocorrelation coefficient it was necessary to delay the output signal of the probe system. This was done by a delay line manufactured by AD-YU Electronics Inc., which was capable of providing a delay ranging from 2 milliseconds to 200,000 milliseconds. The instrument was basically a series of selected coils with switches. If the impendence of the delay line does not match with the impendence of the input circuit, the signal may be distorted while passing through. This makes it necessary to place two variable resistors in parallel across the input and output terminals of delay line.

Oscilloscope

For visual observations and for permanent check on the form of signals coming from the probes a dual-trace Dumont Type 766 transistorized oscilloscope was placed in the measuring circuit. Wide range of voltage gain and frequency change were possible. A polaroid camera was available for photographing the signals.

General Considerations

The complete system used for measuring the turbulence properties is shown in Figure 5. All the connections in the circuit were made with coaxial shielded cables and each instrument was carefully grounded. This was done to minimize the interference due to 60 cycle noise pickup.

Observation of Data

Mean velocity measurement

The purpose of measuring the mean velocity distribution was two-fold. First, these measurements were required for the calculations of relative intensity of turbulence and for the spectrum function. Second, the effect of large scale roughness on the shape of the velocity profiles was to be determined. A simple pitot tube and a manometer with water as a fluid was used. For each discharge a series of velocities at varying depths were measured at three different locations; one at the center line and the others at a distance of 1.5 feet on either side of center. The reading of the manometer was stabilized by pinching the tubing connecting the manometer to the pitot tube.

The pitot tube used for these experiments had an outer diameter of 3/8 inch. The inner diameter of the tube was 1/8 inch. Various other dimensions are shown in Figure 1.

Measurement of intensity of turbulence

The root mean square of the fluctuating velocity component in the x_1-direction is defined as the intensity of turbulence in that direction. This fluctuating velocity produces a voltage proportional to the velocity in the piezoelectric probe. This voltage was applied to the random signal indicator, after due amplification, for the determination of the value of $\sqrt{\overline{u}_1^2}$ with a true R.M.S. voltmeter. For each discharge the intensity readings as a function of depth were taken at two

different locations. For some measurements the top of the spheres was considered to be at zero whereas for others, the zero was taken as the point of contact of two adjacent spheres.

Measurement of autocorrelation and macroscale

For this measurement both channels of the random signal indicator were employed. The channel A was fed by a signal coming directly from the Tektronix preamplifier whereas channel B was fed with the same signal after this was passed through the delay line. Then the gain control and meter volts were adjusted to obtain the recommended deflection on the R.M.S. meter for channel A as well as for B. The ratio meter then gave the correlation coefficient when it was set on the correlation coefficient position. It was not possible to measure the macroscale of the turbulence directly. This quantity was derived from the area under the autocorrelation curve.

Measurement of spatial correlation

The spatial correlation between the velocity fluctuations at two points in turbulent flow field was observed by placing probes at the desired two points. Signals from these probes were fed into channel A and B, then the cross correlation was measured directly from the R.M.S. meter. The cross correlation was observed in vertical and horizontal directions for each flow depth on different slopes.

Measurement of longitudinal microscale of turbulence

The method suggested by Townsend (1947) was used to measure the microscale. Townsend observed experimentally that the mean square of the time derivative of the fluctuating velocity is proportional to the space derivative of the same quantity. He proved that

$$\overline{\left[\frac{\partial u_1}{\partial t}\right]^2} = \overline{U_1}^2 \overline{\left[\frac{\partial u_1}{\partial x_1}\right]^2} \quad \ldots\ldots \quad (4\text{-}1)$$

Also Taylor found that

$$\overline{\left[\frac{\partial u_1}{\partial x_2}\right]^2} = 2 \overline{\left[\frac{\partial u_1}{\partial x_1}\right]^2} \quad \ldots\ldots \quad (4\text{-}2)$$

By equations (3-19), (4-1), and (4-2)

$$\frac{1}{\lambda_g^2} = \frac{1}{2\overline{u_1^2}} 2\overline{\left(\frac{\partial u_1}{\partial x_1}\right)^2} = \frac{1}{\overline{U_1}^2 \overline{u_1^2}} \overline{\left(\frac{\partial u_1}{\partial t}\right)^2}$$

or

$$\lambda_g = \overline{U_1} \frac{\sqrt{\overline{u_1^2}}}{\sqrt{\overline{\left(\frac{\partial u_1}{\partial t}\right)^2}}} \quad \ldots\ldots \quad (4\text{-}3)$$

The quantity $\dfrac{\sqrt{\overline{u_1^2}}}{\sqrt{\overline{\left(\frac{\partial u_1}{\partial t}\right)^2}}}$ can be measured directly on R.M.S. indicator by selecting a predetermined time constant and setting the controls in the proper positions.

Measurement of turbulence energy spectrum

The spectrum analyzer is quite similar to the random signal indicator in operation. The random signal indicator gives the R.M.S. reading of all the frequencies feed into it. But the spectrum analyzer gives the R.M.S. value of the selected range of frequencies of the signal.

For all measurements the band width was kept at 30 cps and a value of 10 was used for the meter multiplier.

Data Processing

Relative intensity of turbulence

The observations for intensity measurements were read in volts from the random signal indicator. These observations were a combination of the voltages produced in the probe due to turbulent fluctuations, the pressure fluctuations in the flow (assumed to be small compared to the velocity fluctuations) and noise voltage picked up by the circuit from various sources such as vibrations, 60 cycle hum, etc.

Then

$$V_T = V_R + V_N \quad . \quad . \quad . \quad . \quad . \quad . \quad . \quad . \quad . \quad . \quad (4\text{-}4)$$

$$V_T^2 = V_R^2 + V_N^2 + 2V_R V_N \quad . \quad . \quad . \quad . \quad . \quad .$$

Taking the average,

$$\overline{V_T^2} = \overline{V_R^2} + \overline{V_N^2} + \overline{2V_R V_N} \quad . \quad . \quad . \quad . \quad . \quad . \quad . \quad . \quad (4\text{-}5)$$

As V_R and V_n are two completely independent signals, therefore, no correlation exists between them.

Hence

$$\overline{V_R V_N} = 0$$

Thus

$$\overline{V_T^2} = \overline{V_R^2} + \overline{V_N^2} \quad . \quad . \quad . \quad . \quad . \quad . \quad . \quad . \quad . \quad . \quad (4\text{-}6)$$

This equation can be employed for separating noise voltage from turbulence voltage.

From Appendix A

$$V_R' = \frac{c\, u_1' \overline{U}_1}{g}$$

$$u_1' = \frac{g\, V_R'}{c\, \overline{U}_1} \quad . \quad . \quad . \quad . \quad . \quad . \quad . \quad . \quad (4\text{-}7)$$

where u_1' is the intensity of turbulence. If V_R and $\overline{U}_1$ are known, the intensity can be measured.

The value of V_R for 9 inches depth of flow at a depth of 0.1 feet and slope of 3.72 percent was observed to be 0.13 volts. This reading while passing through the amplifer has increased by 100.

Hence the acutal V_R = 0.0013 volts. From calibration C equals 7.14 millivolts per foot. So

$$u_1' = 0.956 \text{ ft/sec}$$

One-Dimensional Energy Spectrum

The spectrum curves are usually drawn as K_1 Vs $E_1(K_1)$ where wave number K_1 is defined as

$$K_1 = \frac{2\pi n}{\overline{U}_1}$$

and $E_1(K_1)$ is the energy carried by a certain frequency band of voltage signal produced by the probe.

From Appendix A

$$E_1(K_1) = \frac{g\,\overline{\Delta V_R^2(K)}}{C\,\overline{U}_1\,2\pi\,\Delta n} \qquad (4\text{-}8)$$

It was observed that for $x_2/\bar{h} = 0$ at a slope of 6.2 percent when $\overline{U}_2 = 4.1$ ft/sec., with a band width 30,

$$K_1 = 15.35 \text{ ft.}^{-1}$$

$$E_1(K_1) = 0.0129 \text{ ft}^3/\text{sec}^2$$

Measurement of Scales of Turbulence

Referring to chapter IV it is seen that macroscale is proportional to the area enclosed by the Eulerian correlation curve plotted on the cartesian coordinates axis. Hence

$$\ell_1 \propto A$$

$$\ell_1 = \overline{U}_1 A \qquad (4\text{-}9)$$

The area enclosed by the curve was measured with the help of graph paper.

The microscale can be calculated directly by the following equation

$$\lambda_f = \overline{U}_1 \tau R \qquad (4\text{-}10)$$

where

τ = preselected time factor (This can have any of the following values 0.05, 0.1, 0.2, 0.5, 1, 2, 5.)

R = the ratio observed from the R.M.S. meter.

CHAPTER V

RESULTS AND DISCUSSION

Mean Velocity Profile

The Figures 6 to 12 show the velocity profiles for three different slopes at different Reynolds numbers. Figure 13 shows Figures 6(a) and 11 as dimensionless plots along with curves taken from Bazin (1865) and Prandtl. Bazin obtained curve No. 3 in a large open channel of moderate aspect ratio and small size of absolute roughness. The curve No. 4 is a theoretical curve drawn on the basis of the Prandtl-von Karman universal velocity distribution law which is as follows:

$$\bar{U}_1 = 5.75\, U_f \log \frac{30\, y}{e} \quad . \quad . \quad . \quad (5\text{-}1)$$

This figure is given for comparing the observed velocity profiles with published data and shows that the present data agree closely with the Bazin and Prandtl logrithmic curves. There is, however, some difference near the channel bed. First, the roughness is very large and some flow is below the top of the spheres which was considered as the datum. Another reason is that the pitot tube used was not small enough as to be very close to the bed of the channel. Thus the velocity which occurred at zero bed level was actually larger than zero velocity.

From these relationships, it can also be inferred that a change in Reynolds number or slope does not have much effect on the shape of the curves.

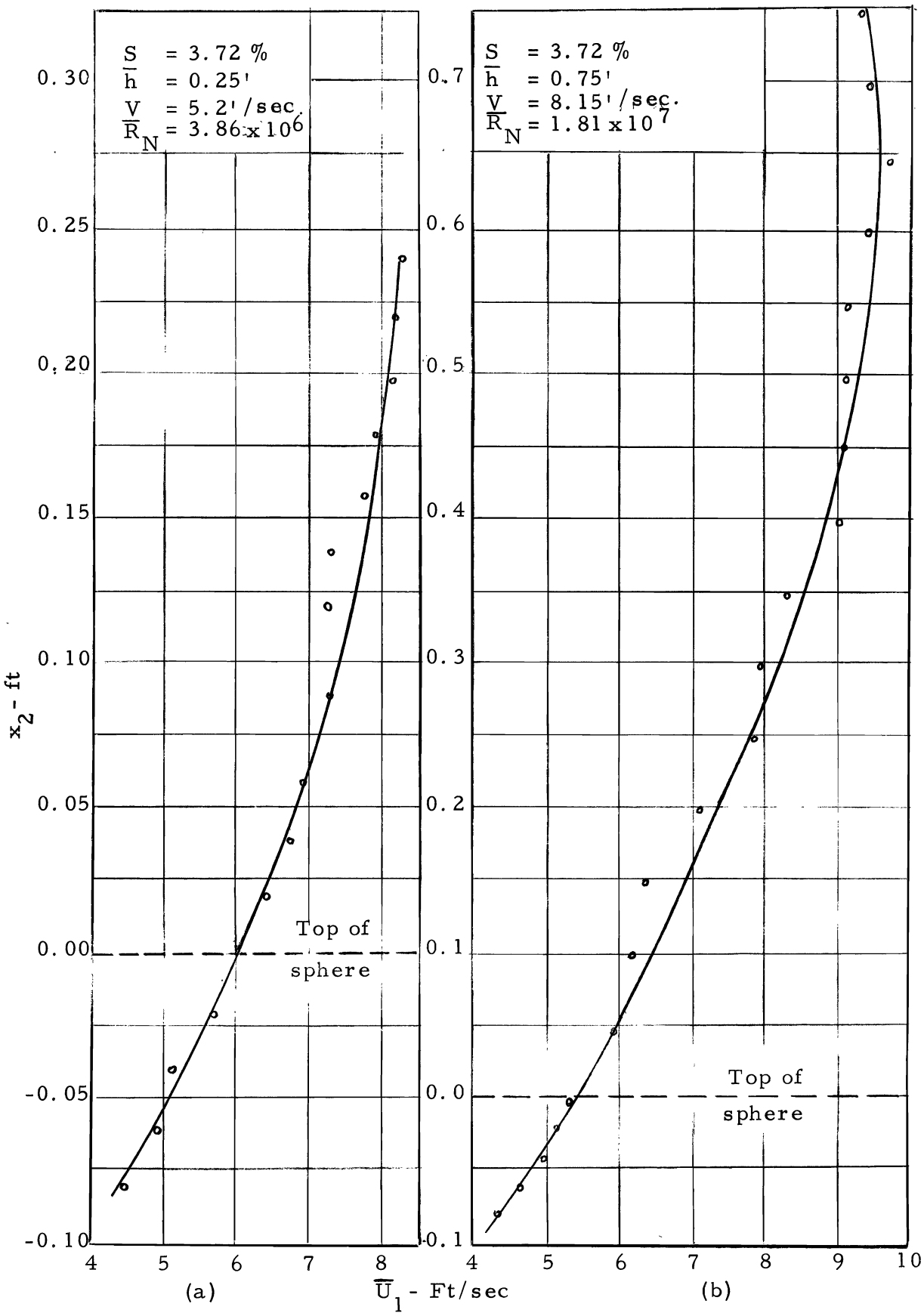

Figure 6. Variation of mean velocity as a function of depth at ℄

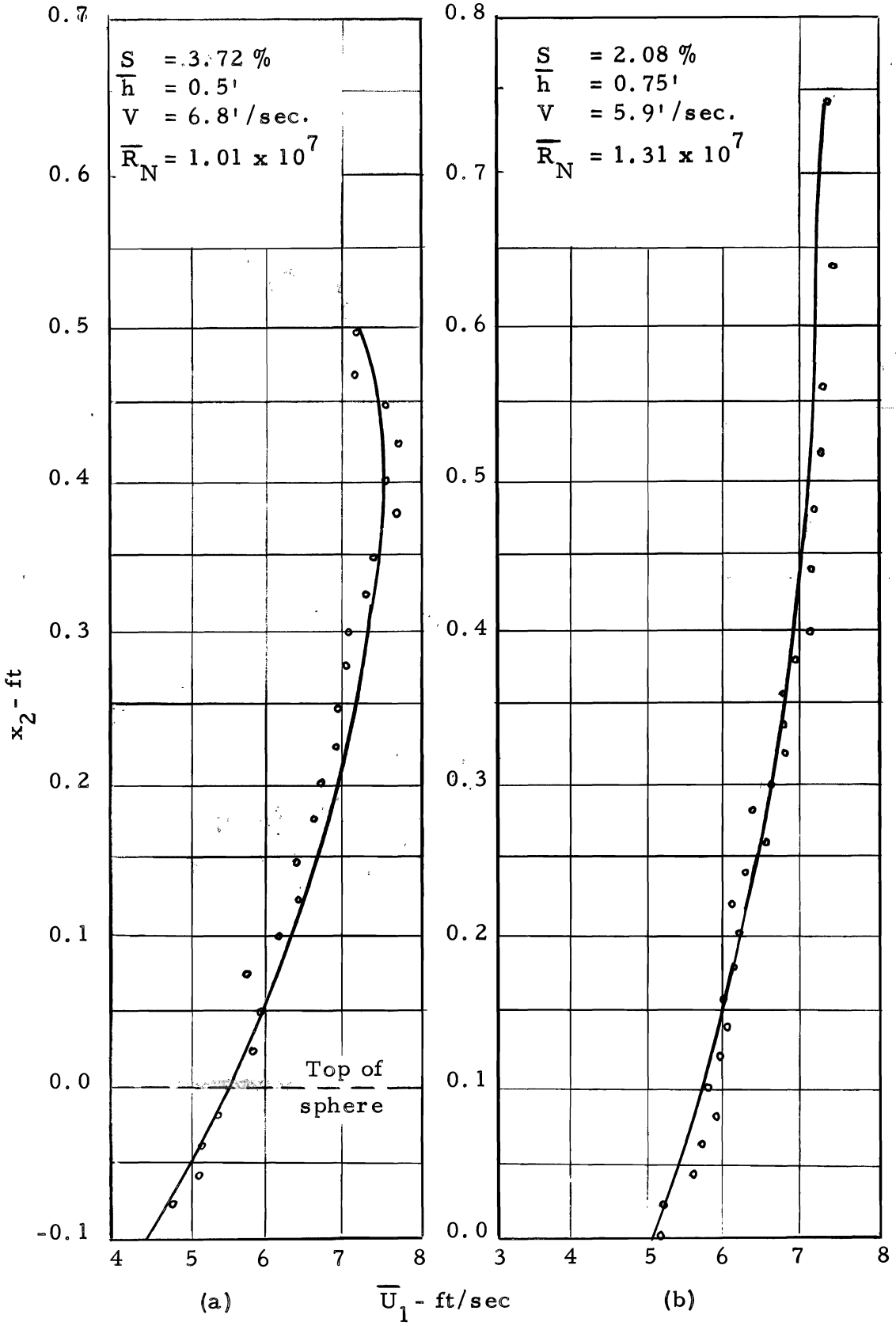

Figure 7. Variation of mean velocity as a function of depth at ℄

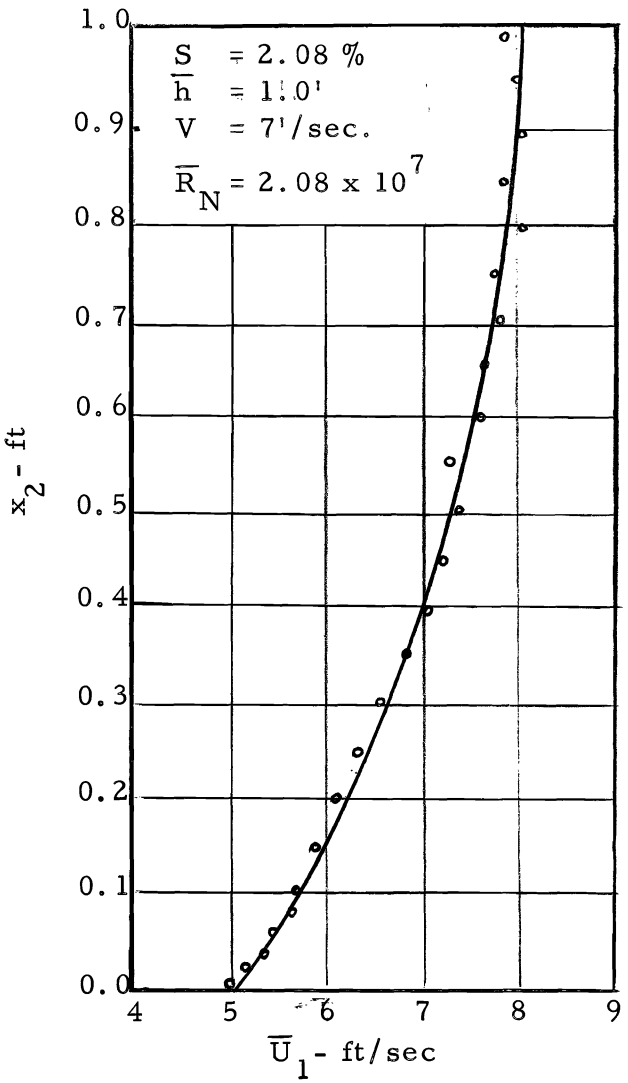

Figure 8. Variation of mean velocity as a function of depth at ℄

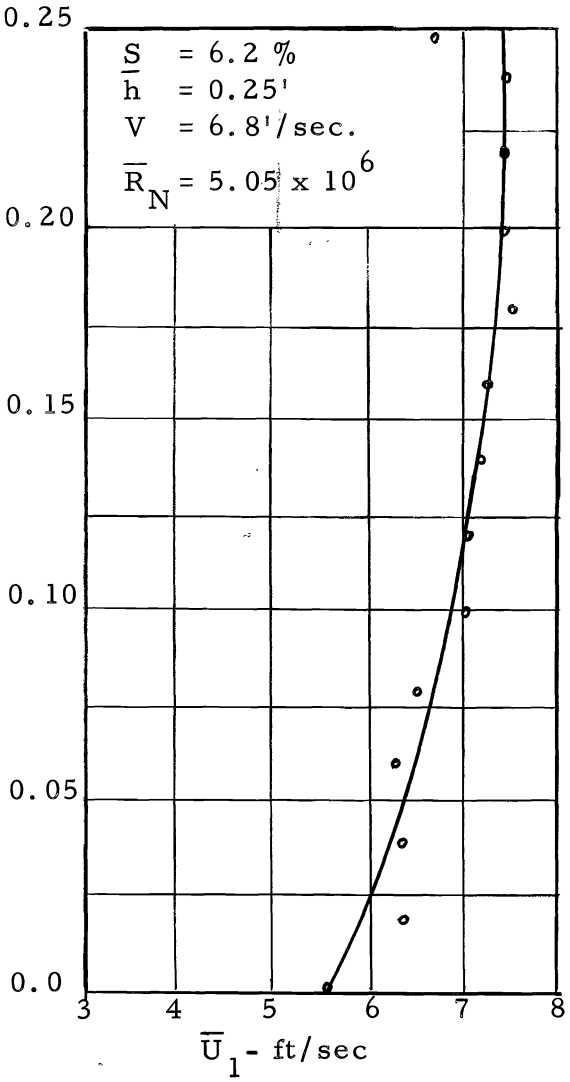

Figure 9. Variation of mean velocity as a function of depth at 1.5 ft left of ℄ looking downstream

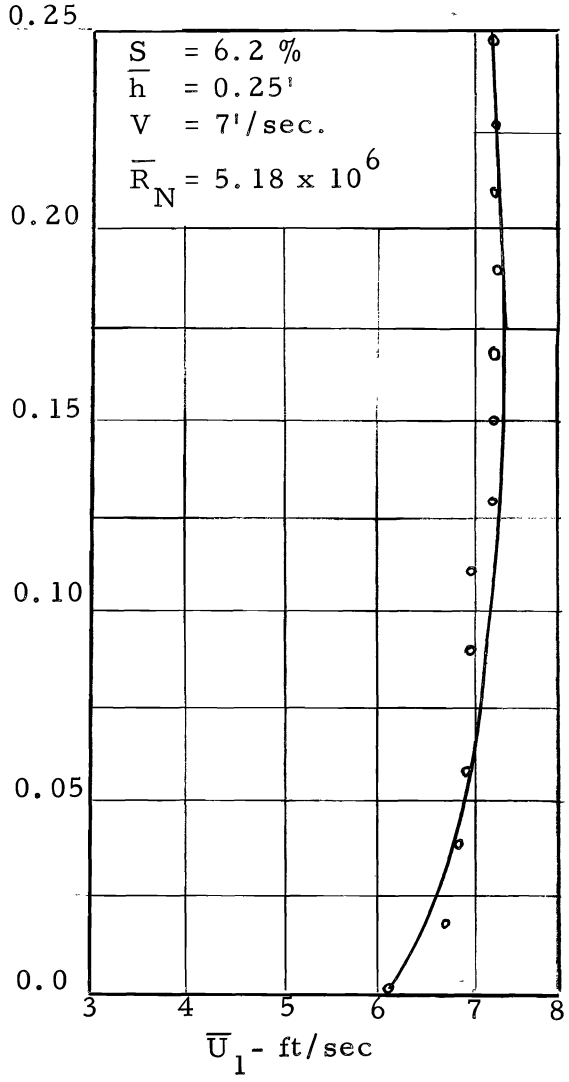

Figure 10. Variation of mean velocity as a function of depth at 1.5 ft right of ℄ looking downstream

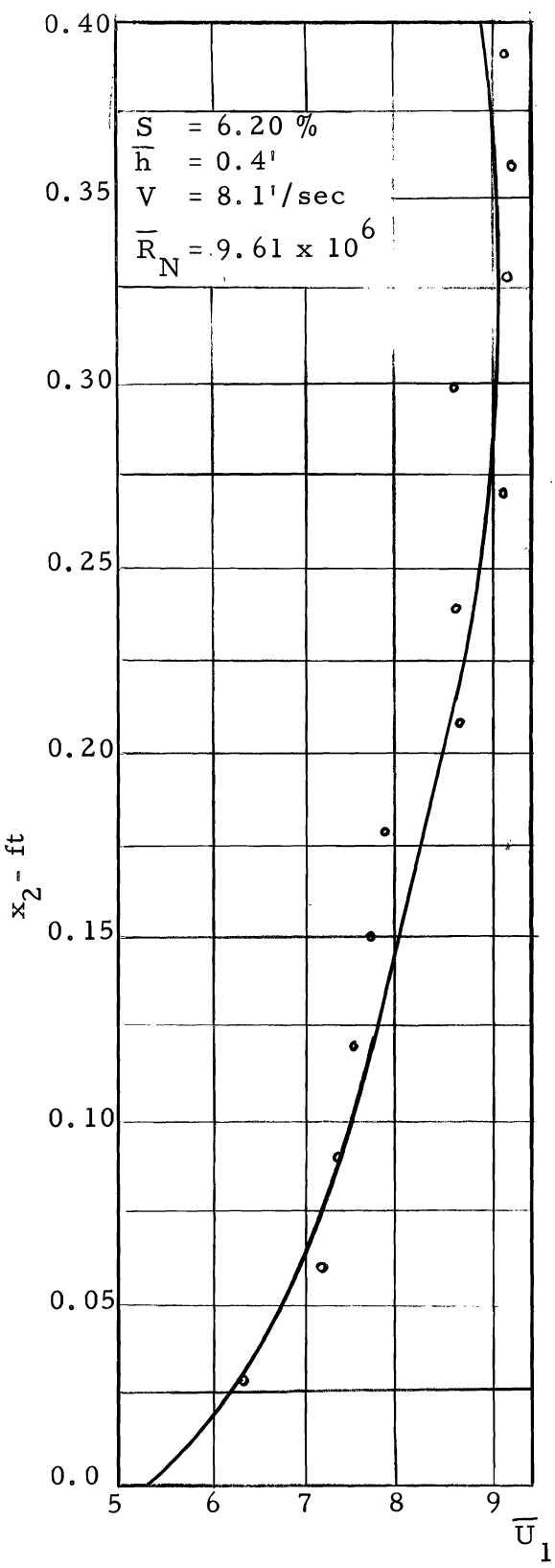

Figure 11. Variation of mean velocity as a function of depth x_2 at 1.5 ft. right of ℄ looking downstream

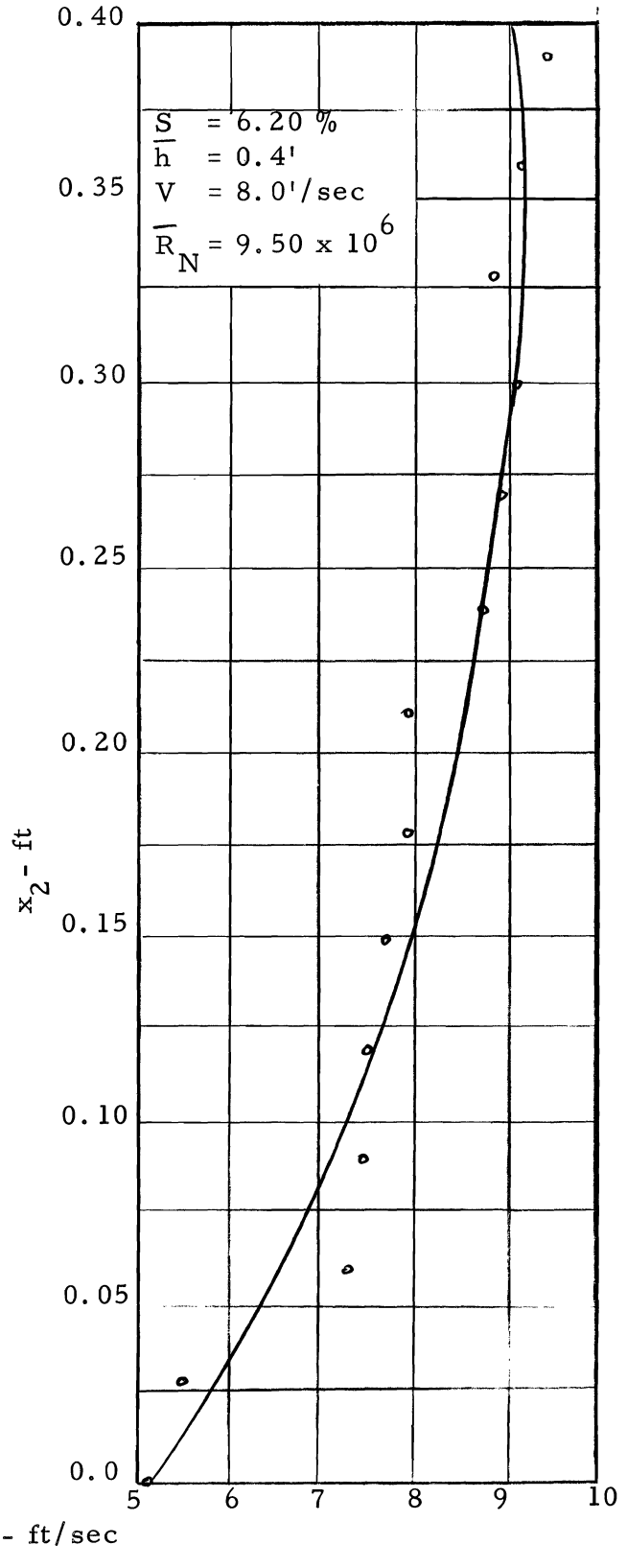

Figure 12. Variation of mean velocity as a function of depth x_2 at 1.5 ft. right of ℄ looking downstream

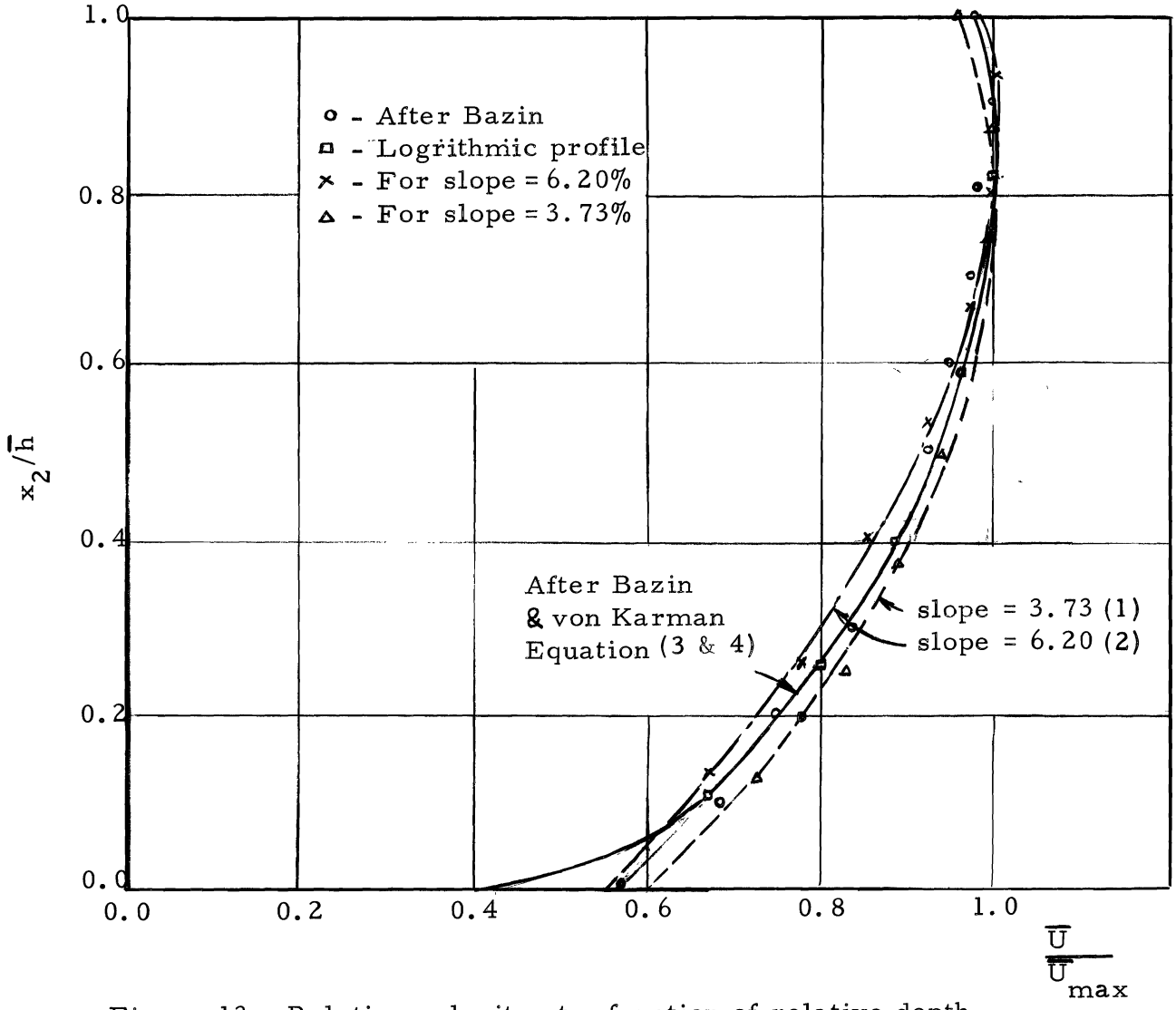

Figure 13. Relative velocity at a function of relative depth

Relative Intensity of Turbulence

The intensities of turbulence were measured for at least two discharges on each slope. The figures given on pages 48 to 50 show the relative intensity curves drawn as a function of relative depth for the fully developed turbulent flow conditions. The measurements for Figures 14 to 15 were made right on the top of the sphere whereas figure 16 shows turbulent intensity above the point of contact of two adjacent spheres. The shapes of all these curves, except 16, are similar and show a maximum value near the wall which keeps on decreasing as the surface is approached. The rate of decrease of intensity is greater near the bed but small near the surface. This shows that near the surface the Reynolds number does not have much effect. The shape of curves on page 50 is similar to the rest of the figures over their major portion. They differ only near the bottom by showing a maximum value a little above the wall.

These curves can be compared with the work of Laufer (1951), Brookshire (1951), and Rao (1965). The present measurements agree well in the outer region but close to the wall show a higher value of turbulence intensity and a greater rate of decrease of intensity. This is due to the presence of very large roughness elements. Laufer's work which was performed in smooth pipes show that maximum intensity occurs at the edge of laminar sublayer. Figure 16 shows that the maximum intensity is obtained at the point where maximum production of turbulence is taking place, that is near the top of the sphere where eddies are added.

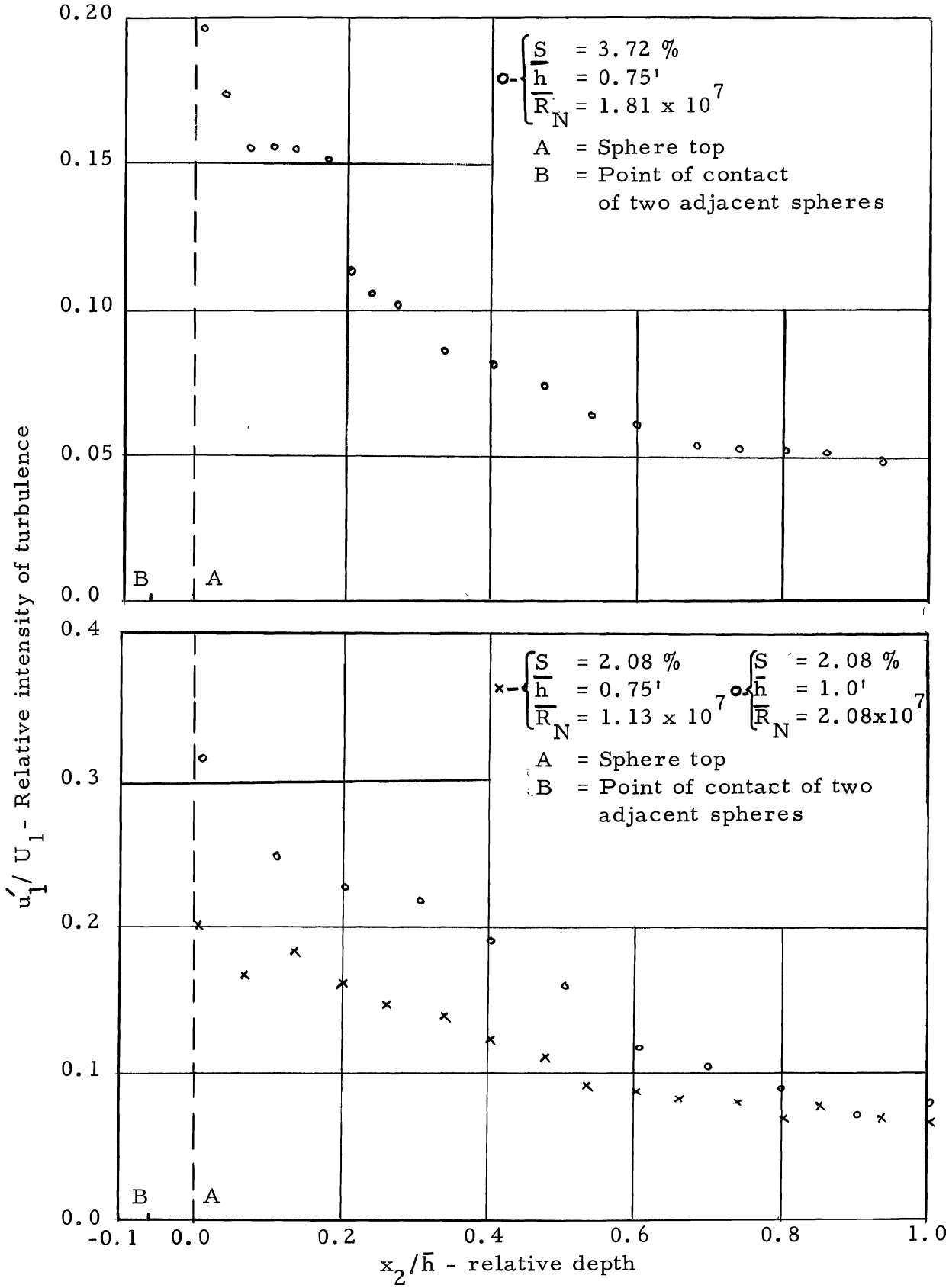

Figure 14. Distribution of relative intensity as a function of relative depth at ℄

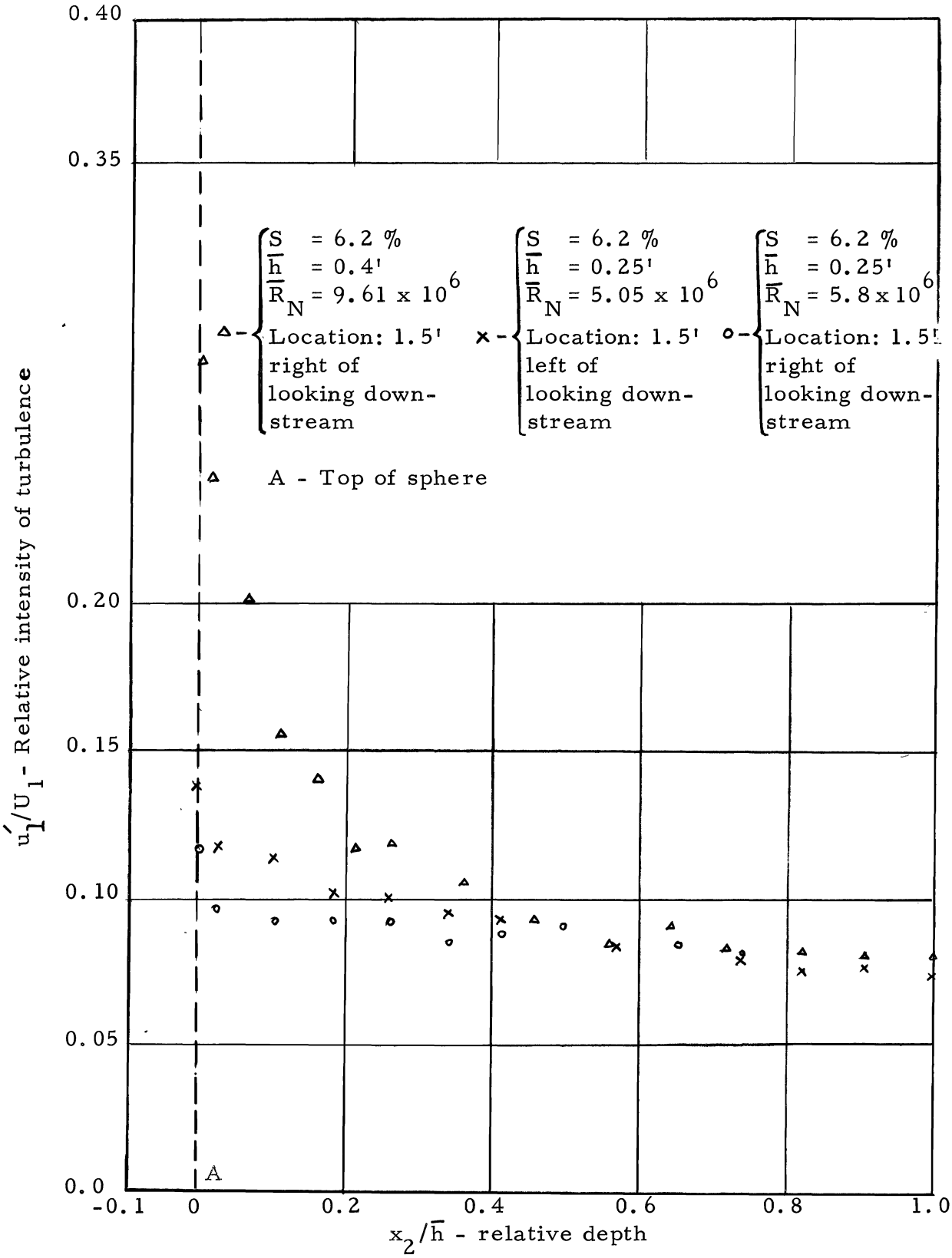

Figure 15. Distribution of relative intensity as a function of relative depth.

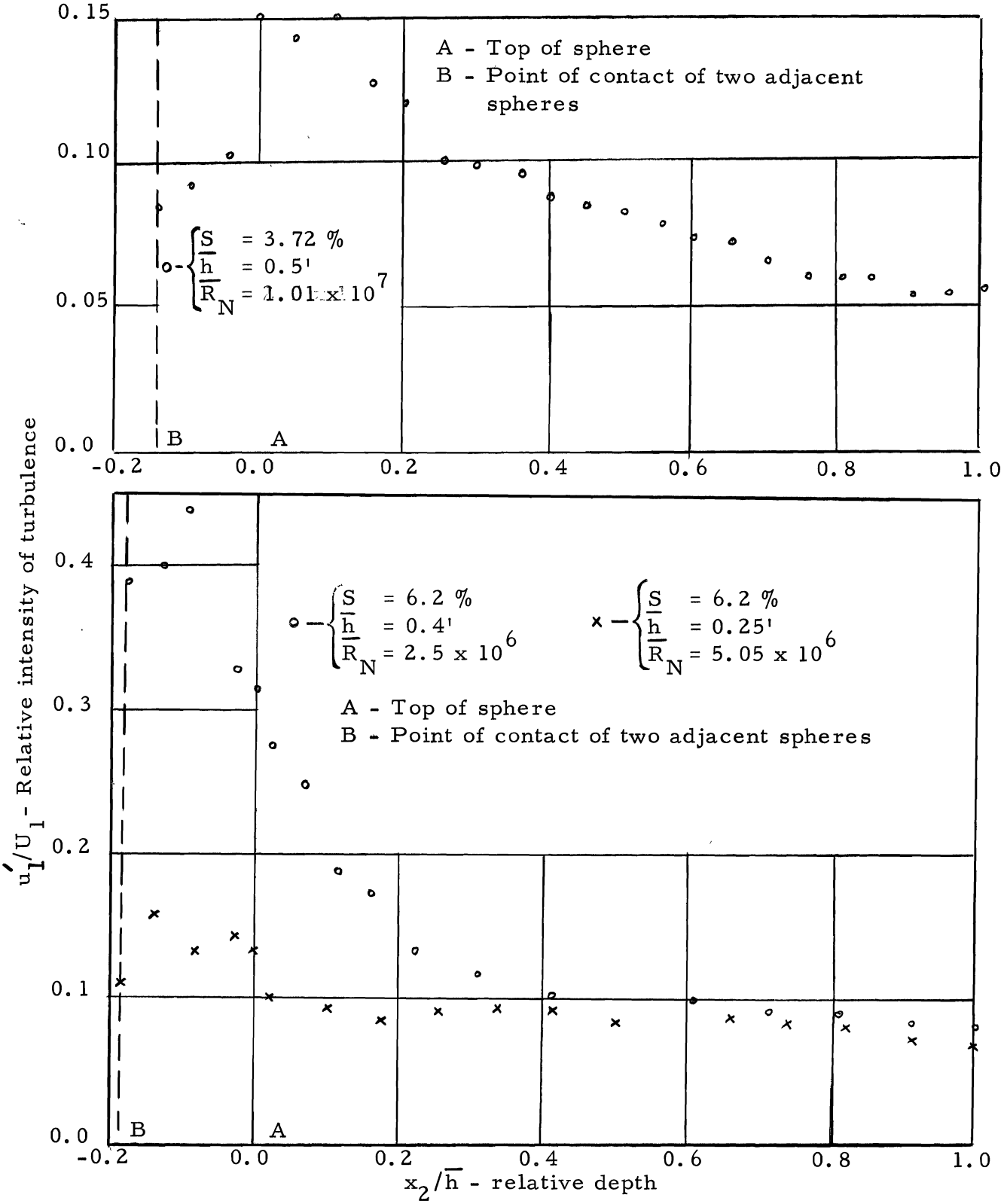

Figure 16. Distribution of relative intensity as a function of relative depth at £

The effect of slope on the intensity is quite clear. A higher slope causes more intense turbulence.

Autocorrelation Curves

Autocorrelation curves or Eulerian time correlations measured at different points in the flow for different discharges and slopes are shown in Figures 17 to 25. These curves were mainly recorded to determine the Eulerian longitudinal integral scale. The shape of all the curves is similar. At zero time interval the correlation is nearly one but falls rapidly and is zero when the delay is about 20 milliseconds. Thereafter the value of correlation coefficient becomes negative but oscillates. This part of the curve does not agree with the work of other investigators. Favre's (1953) autocorrelation curves given in Hinze (1959) show that after attaining a zero value, the autocorrelation coefficient reaches a negative maximum and consequently becomes zero. On the other hand these curves do appear similar to the observations of Rao (1965) and Lee (1966) who used the same type of equipment. The fluctuations in the autocorrelation curves appear to come from the following sources: the vibrations induced in the probe by impact of water, 60 cycle per second noise picked up by exposed connections, and by time delay network. For improving the correlation curves, probes and instruments of higher quality are needed.

It may be mentioned here that similar correlation curves were also obtained by Martin (1963) for the flow of water in pipes.

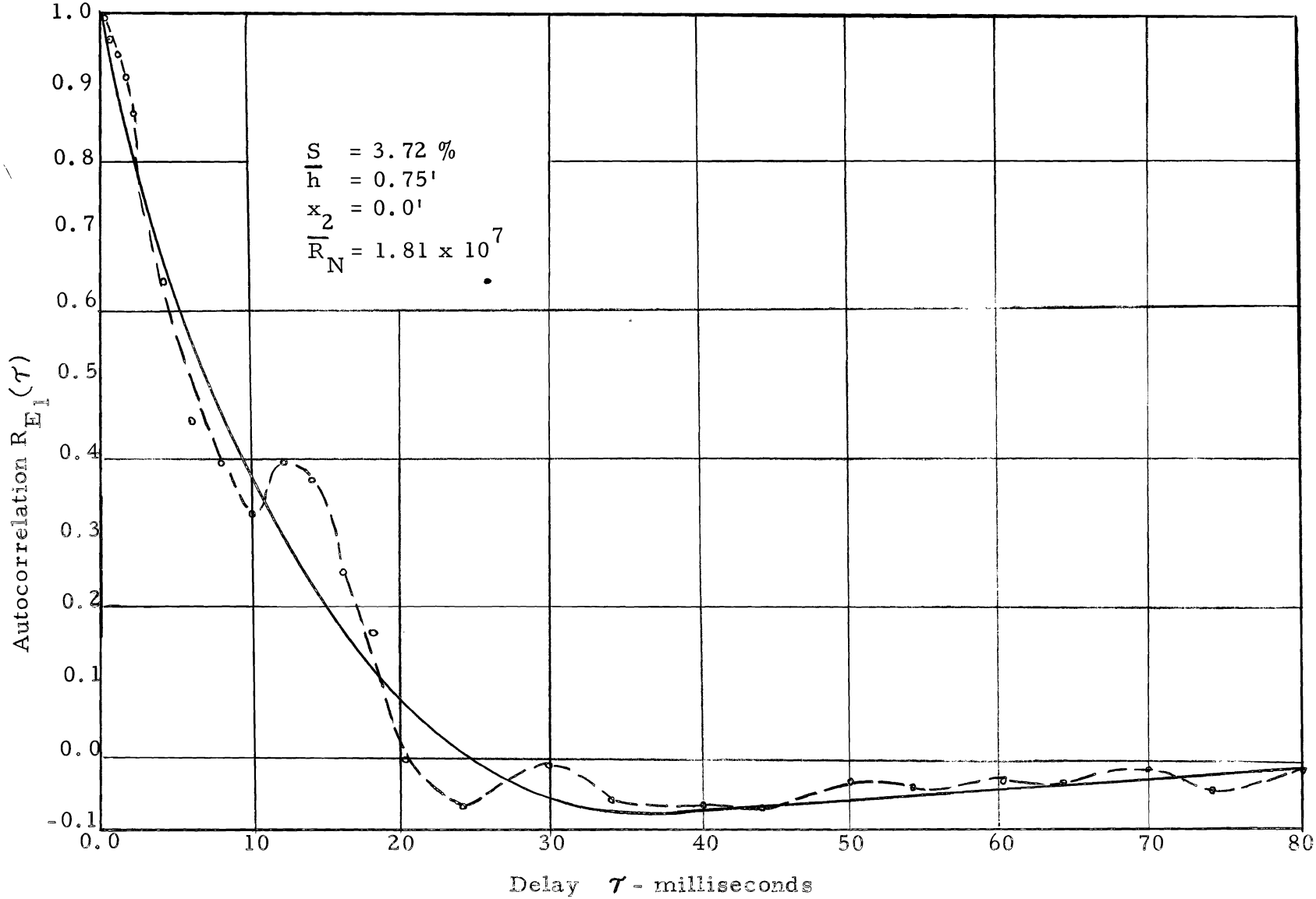

Figure 17. Autocorrelation curve

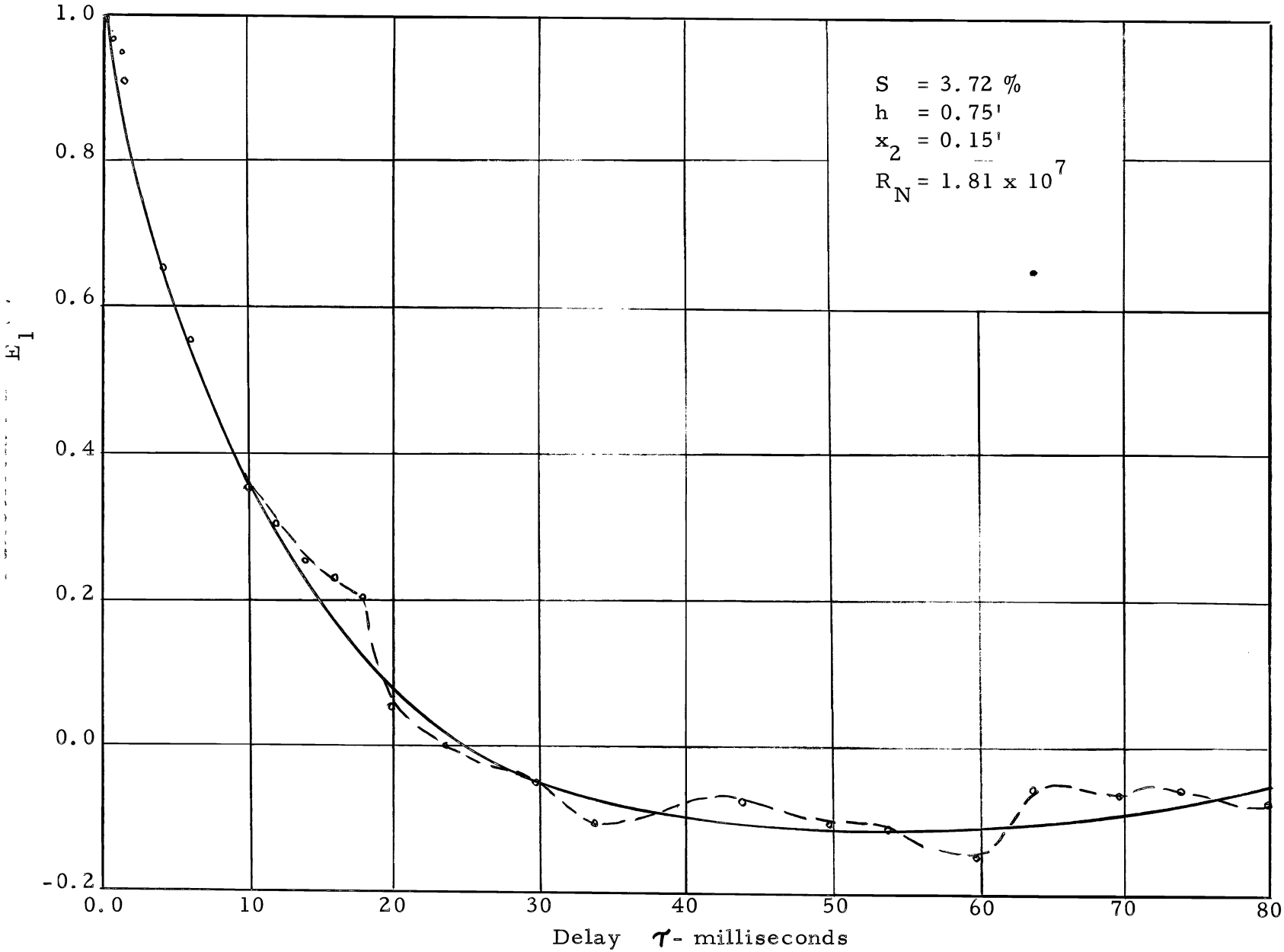

Figure 18. Autocorrelation curve.

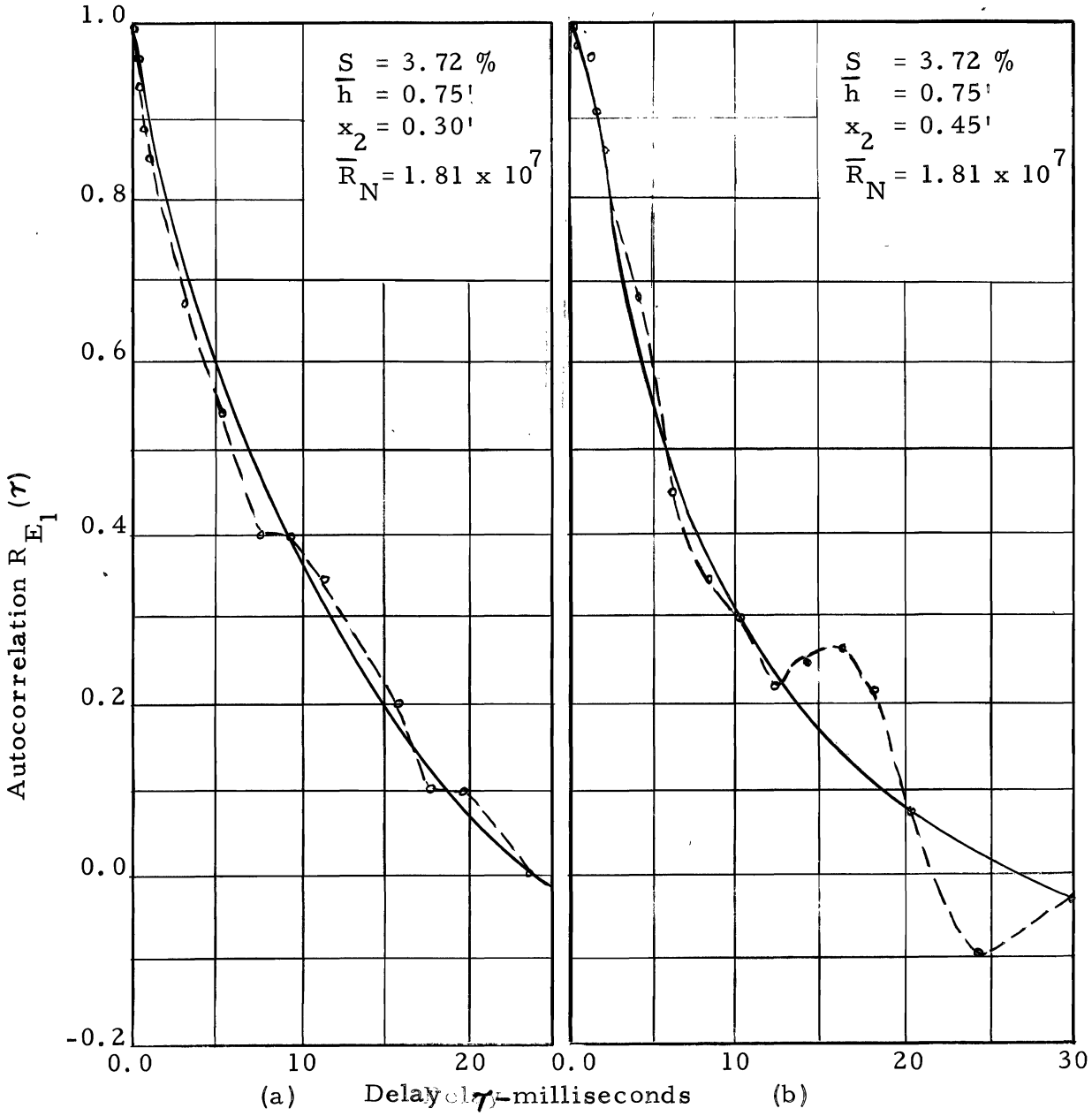

Figure 19. Autocorrelation curves.

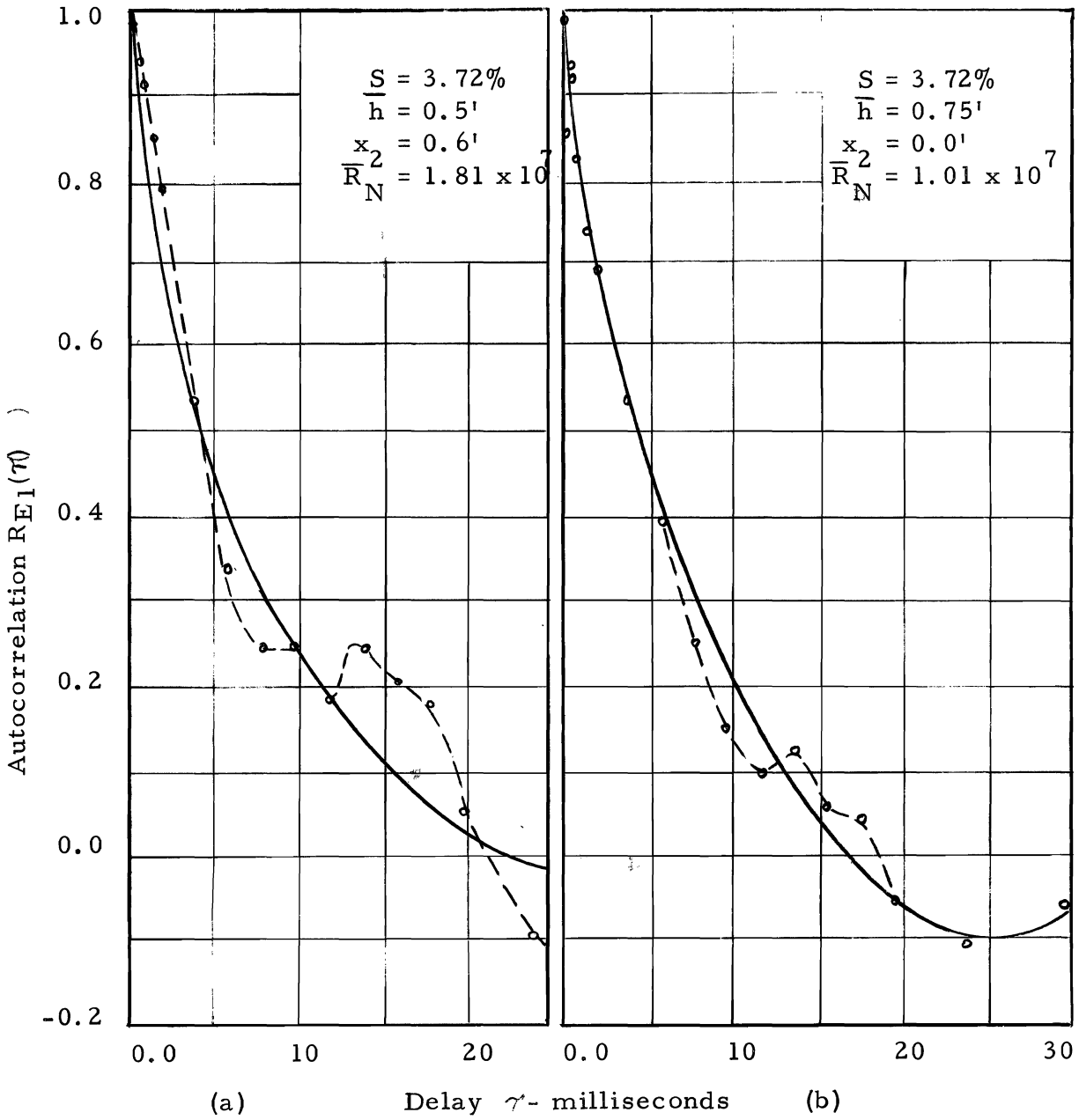

Figure 20. Autocorrelation curves.

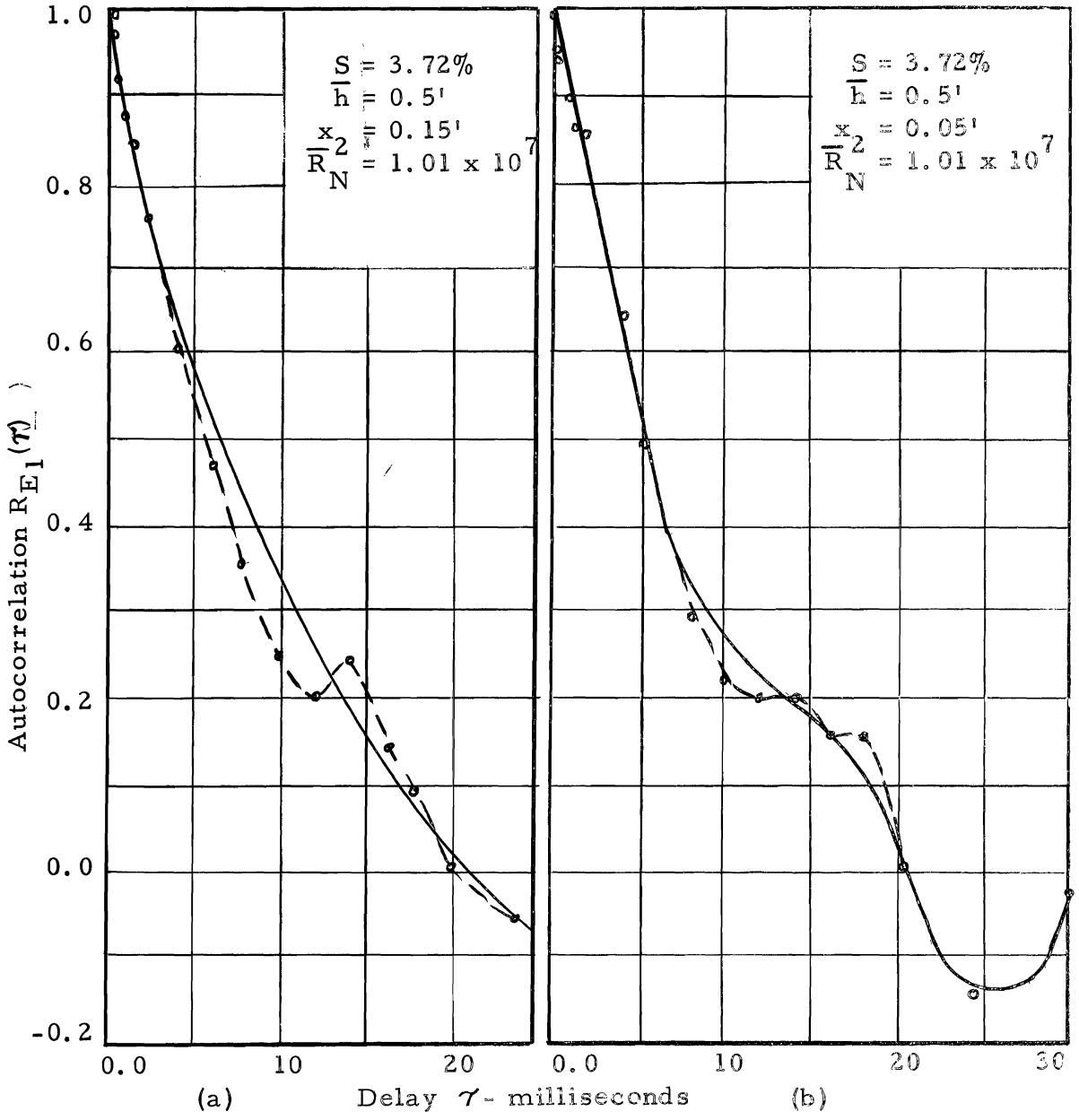

Figure 21. Autocorrelation curves.

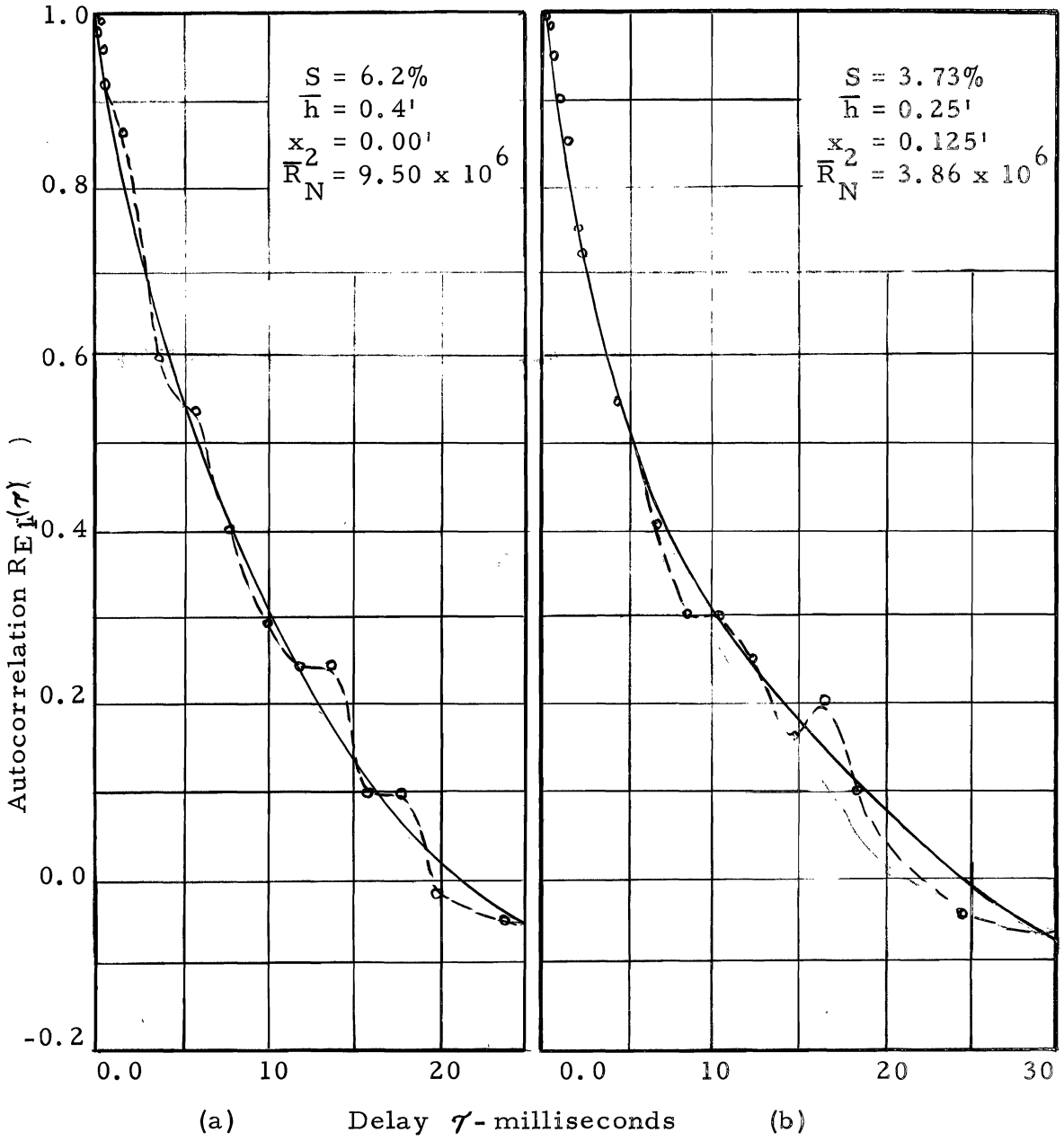

Figure 22. Autocorrelation curves.

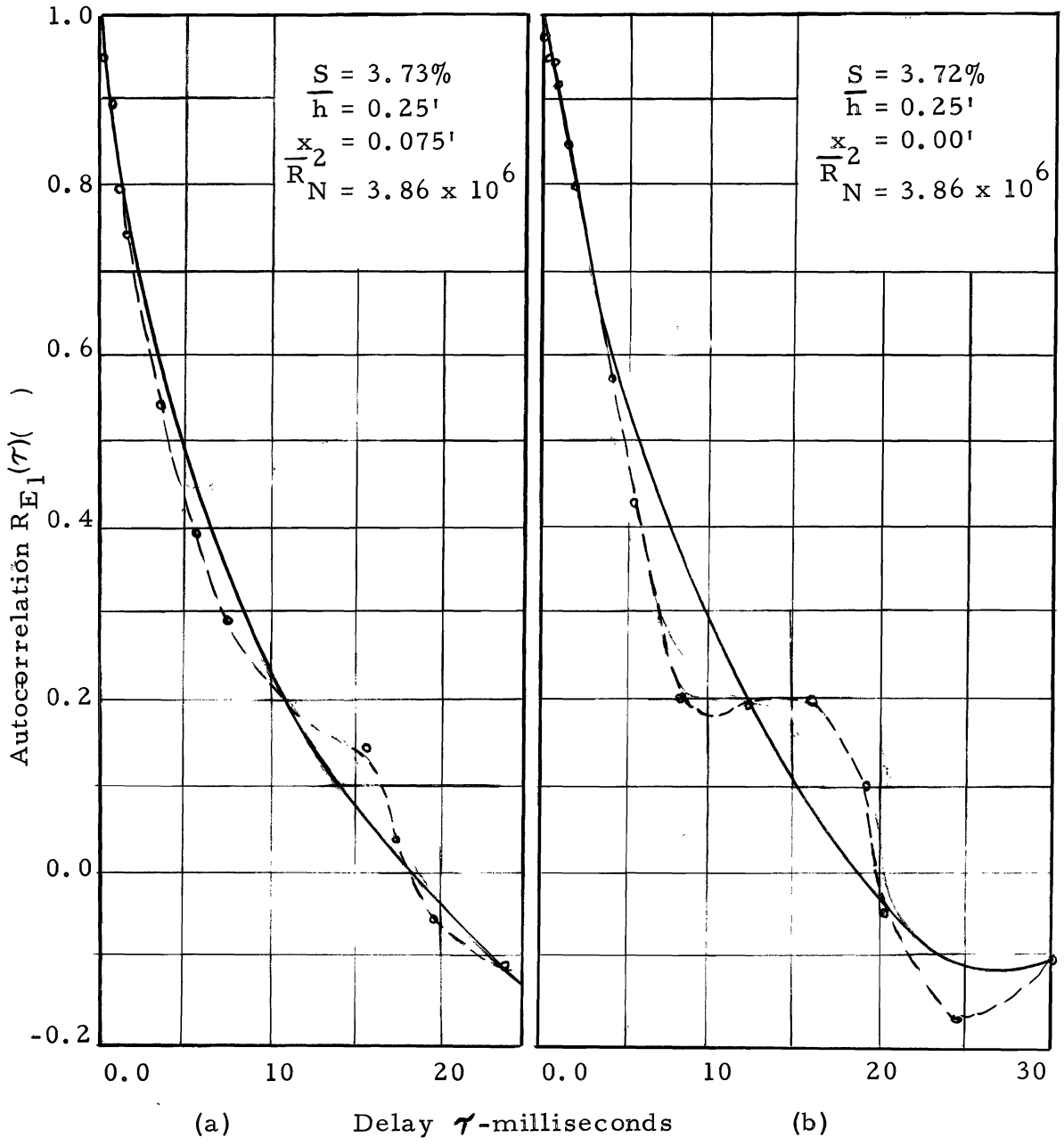

Figure 23. Autocorrelation curves.

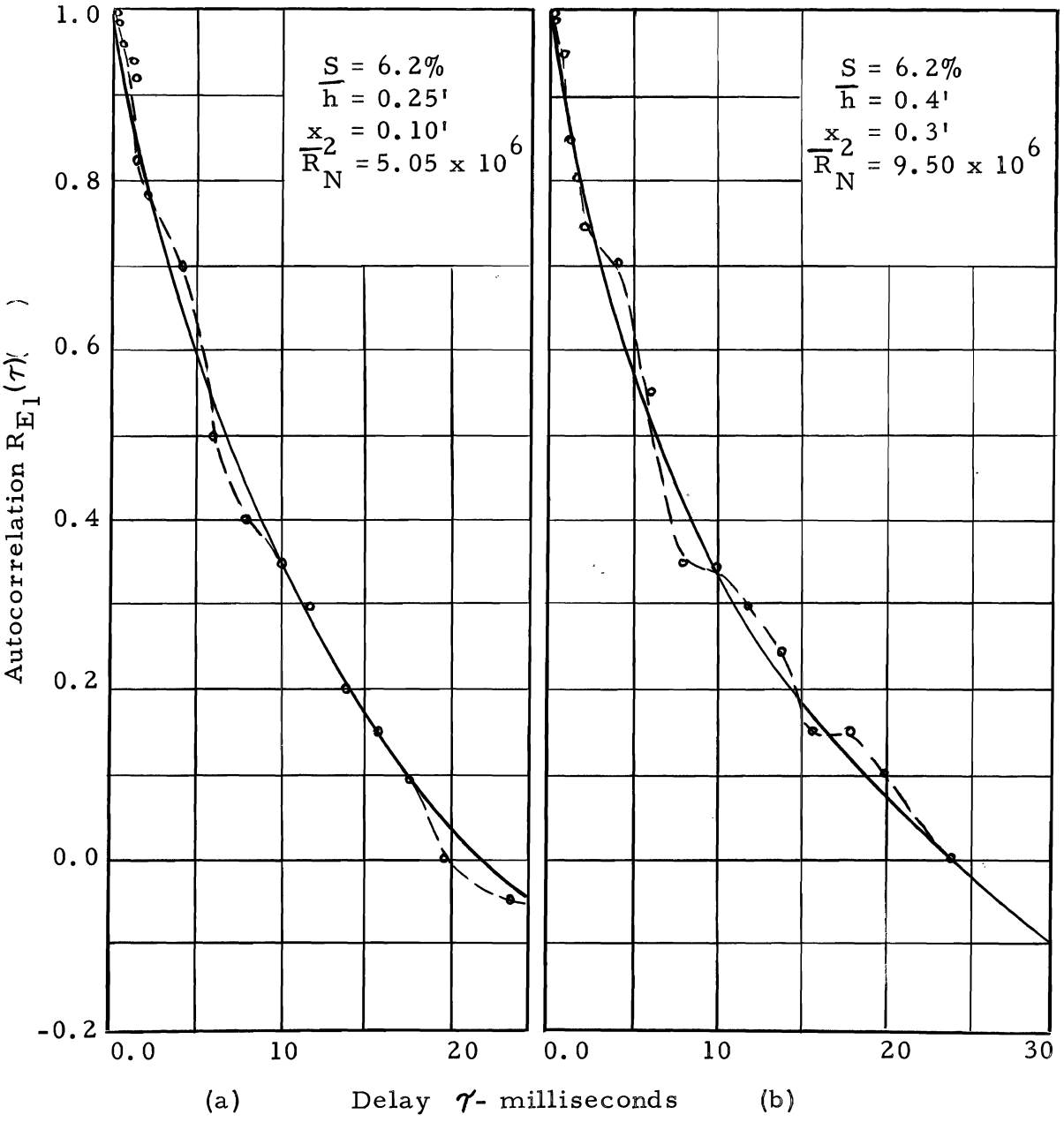

Figure 24. Autocorrelation curves.

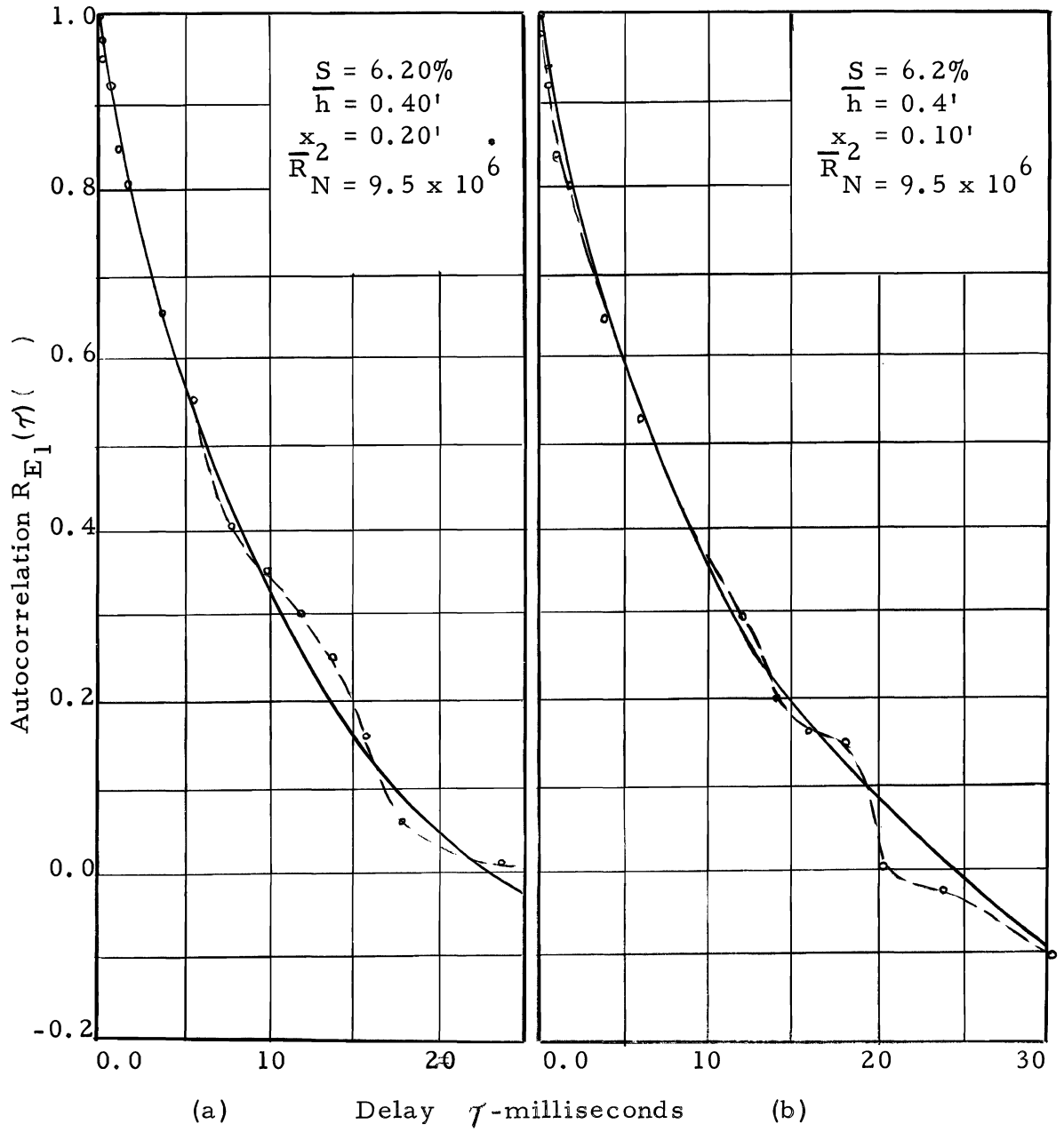

Figure 25. Autocorrelation curves.

Cross Correlation Curves

The cross correlation curves, as defined in Chapter III, are of much value for getting pressure correlations, scales of turbulence and energy distribution. A few cross curves measured for two different depths and slopes are shown in Figures 27 thru 35. These curves are divided into two sets--horizontal cross-correlation and vertical cross-correlation. It will be noticed that all the curves show a value of about 0.65 as the largest coefficient measured as the distance approached zero. The correlation coefficient should theoretically be one at zero distance. In fact, a zero distance was never attained because the piezoelectric probes had a maximum thickness of over 1/8 of an inch. Therefore, the closest distance to which they could be brought was a little more than 1/8 of an inch. This produced the decrease in maximum measured correlation value.

The cross correlation curves show that the rate of decrease of correlation is small for large probe separation distances and vica versa. It was observed that near the bed the horizontal correlation attains a negative value of 0.1. This shows that the flow field has some eddies of 4 inches diameter which rotate about a vertical axis above each sphere. Towards the surface the strength of these eddies decreases so that the correlation does not attain such large negative value.

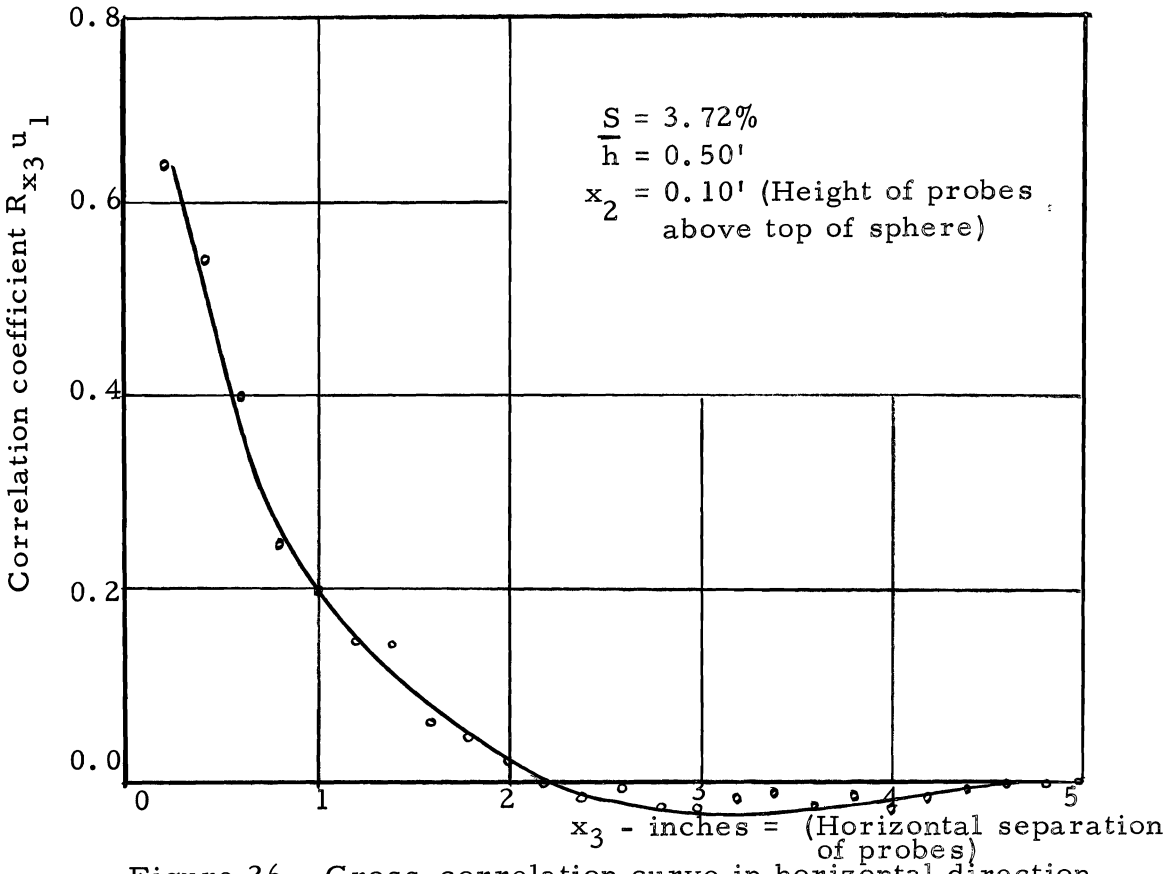

Figure 26. Cross-correlation curve in horizontal direction.

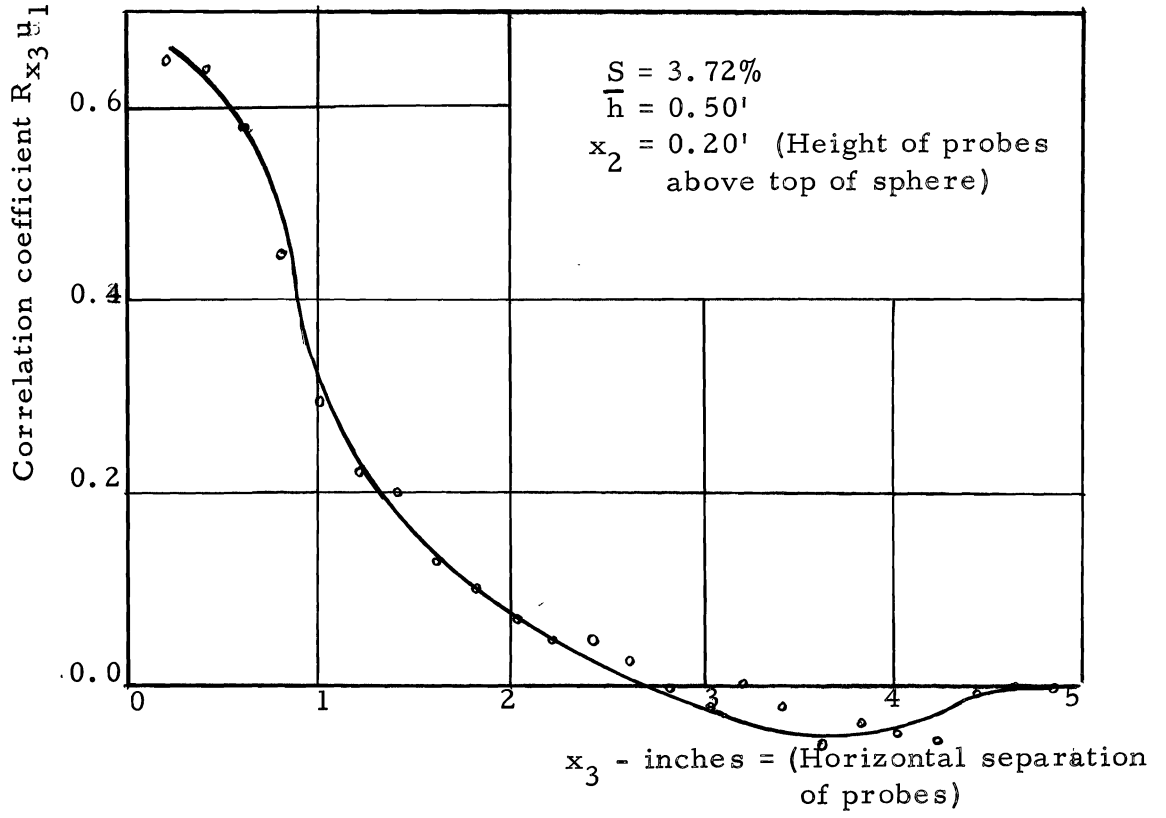

Figure 27. Cross-correlation curve in horizontal direction.

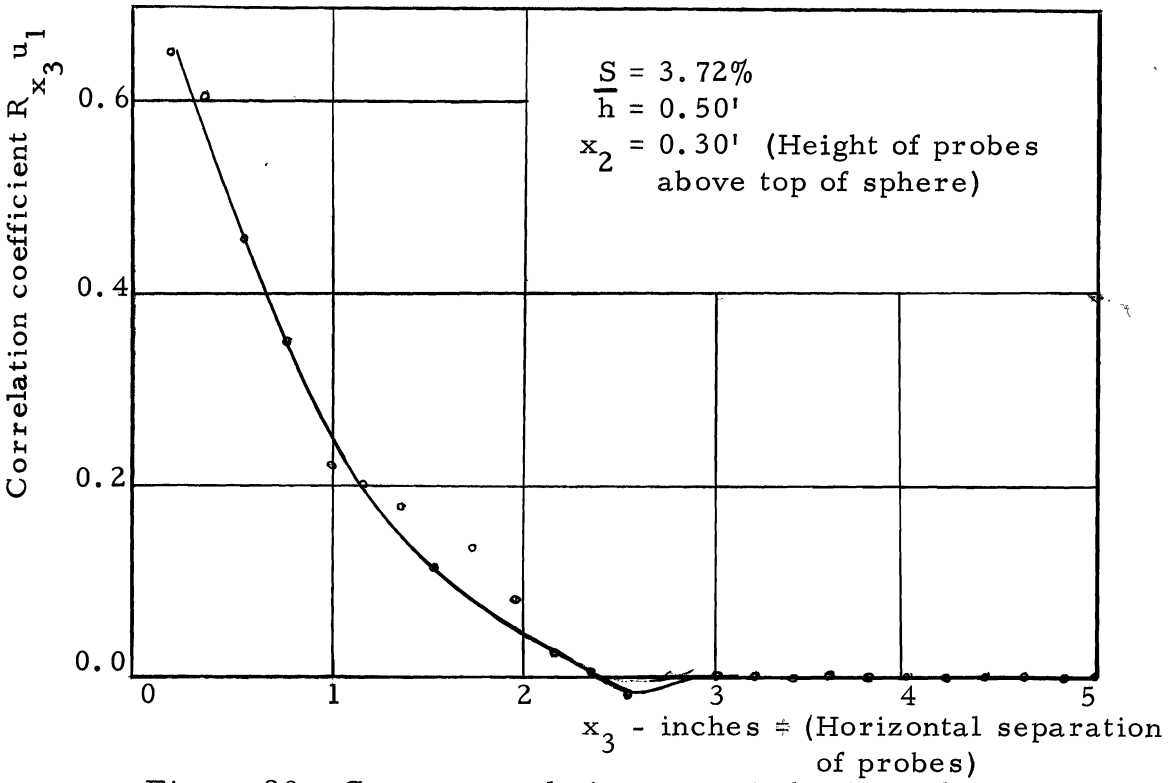

Figure 28. Cross-correlation curve in horizontal direction.

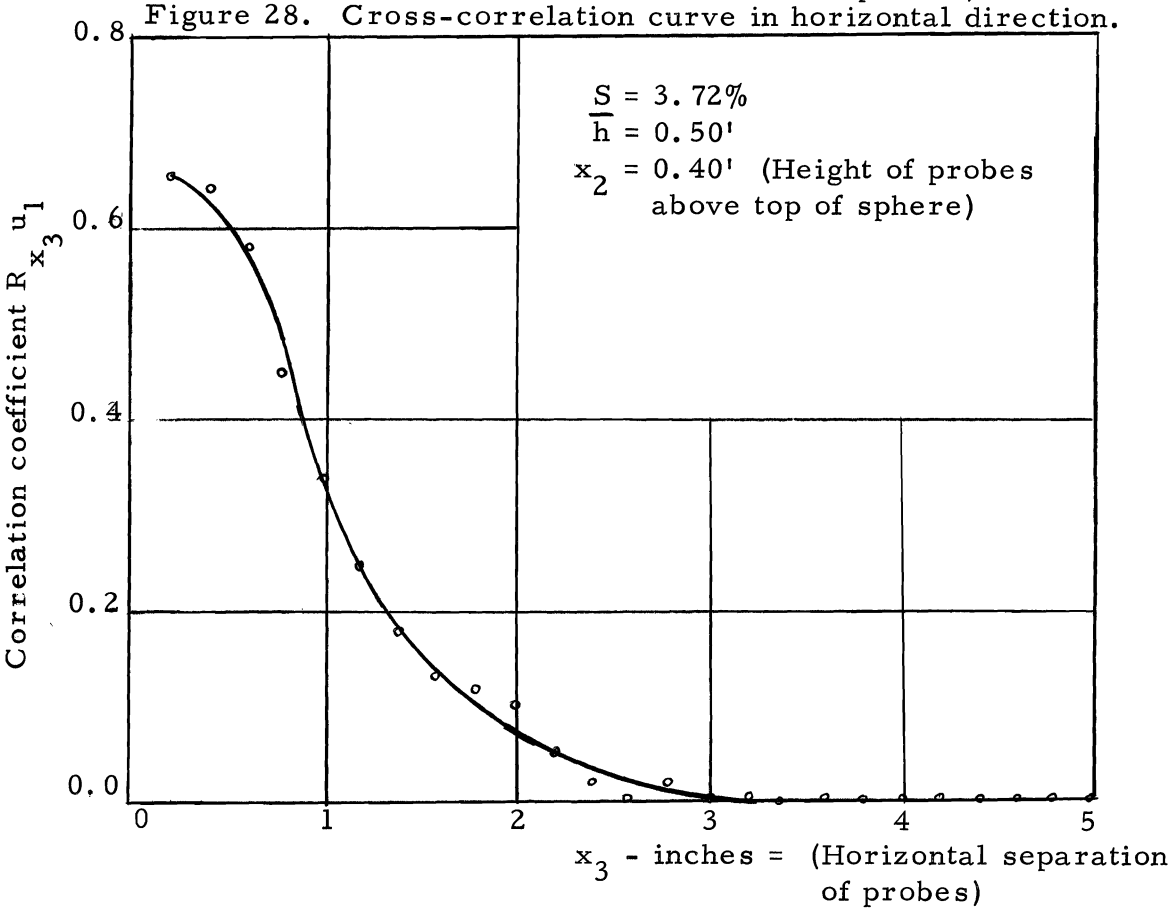

Figure 29. Cross-correlation curve in horizontal direction.

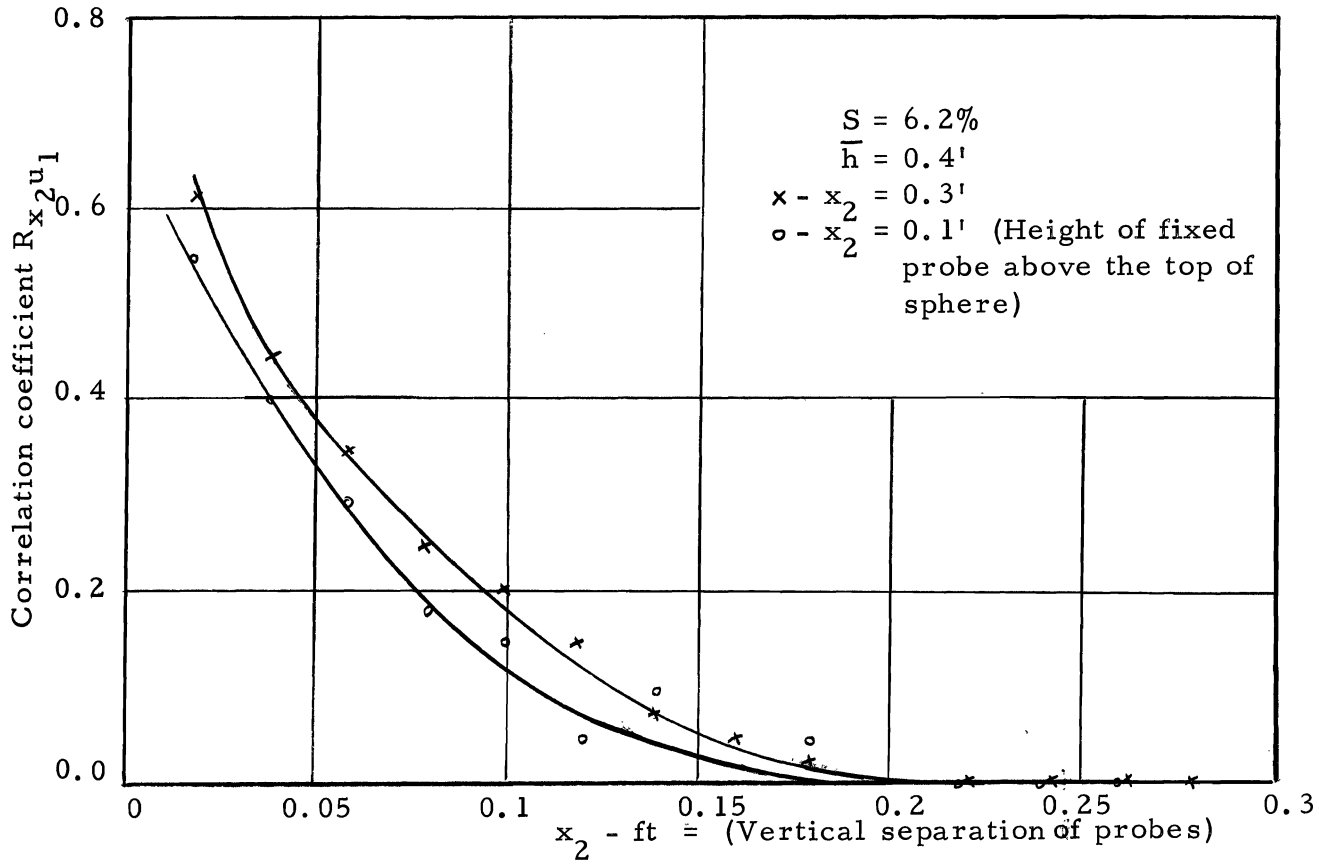

Figure 30. Cross-correlation in vertical direction

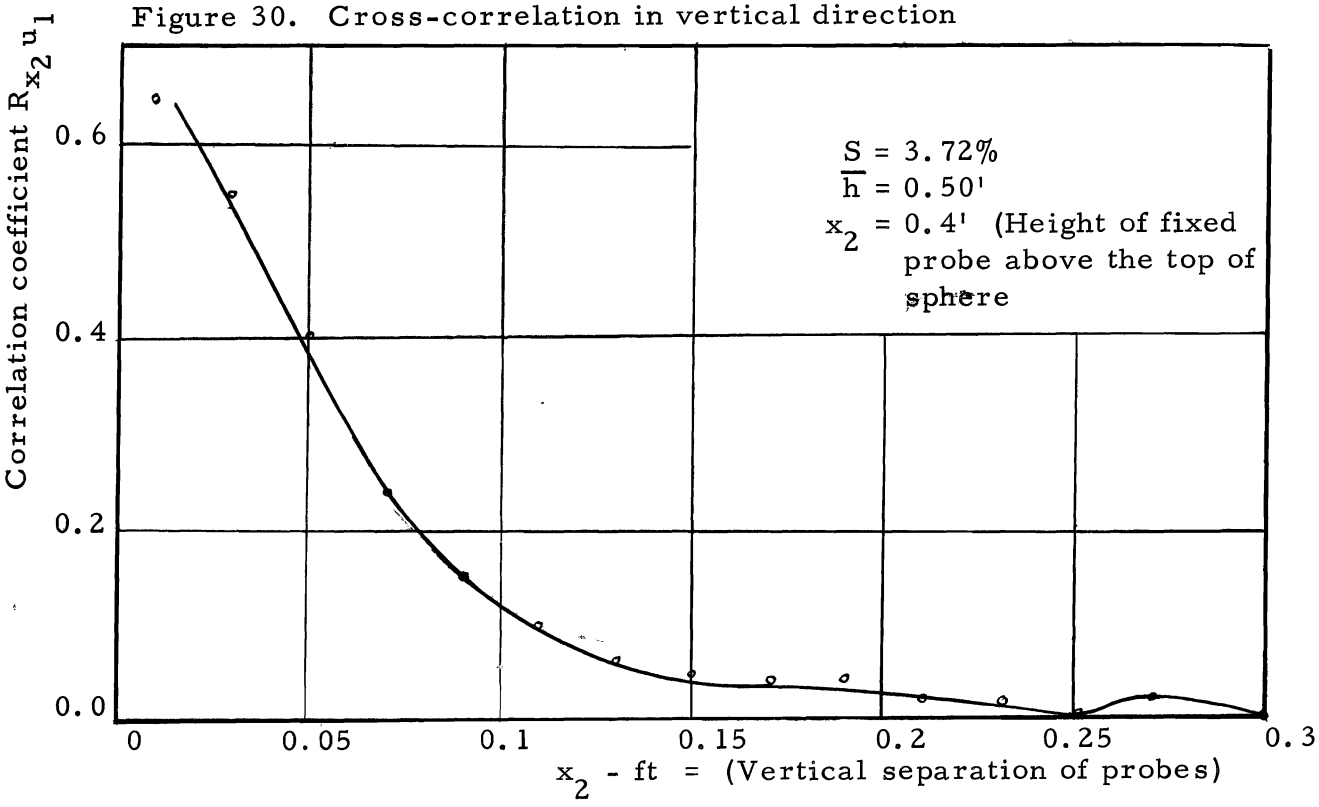

Figure 31. Cross-correlation curve in vertical direction

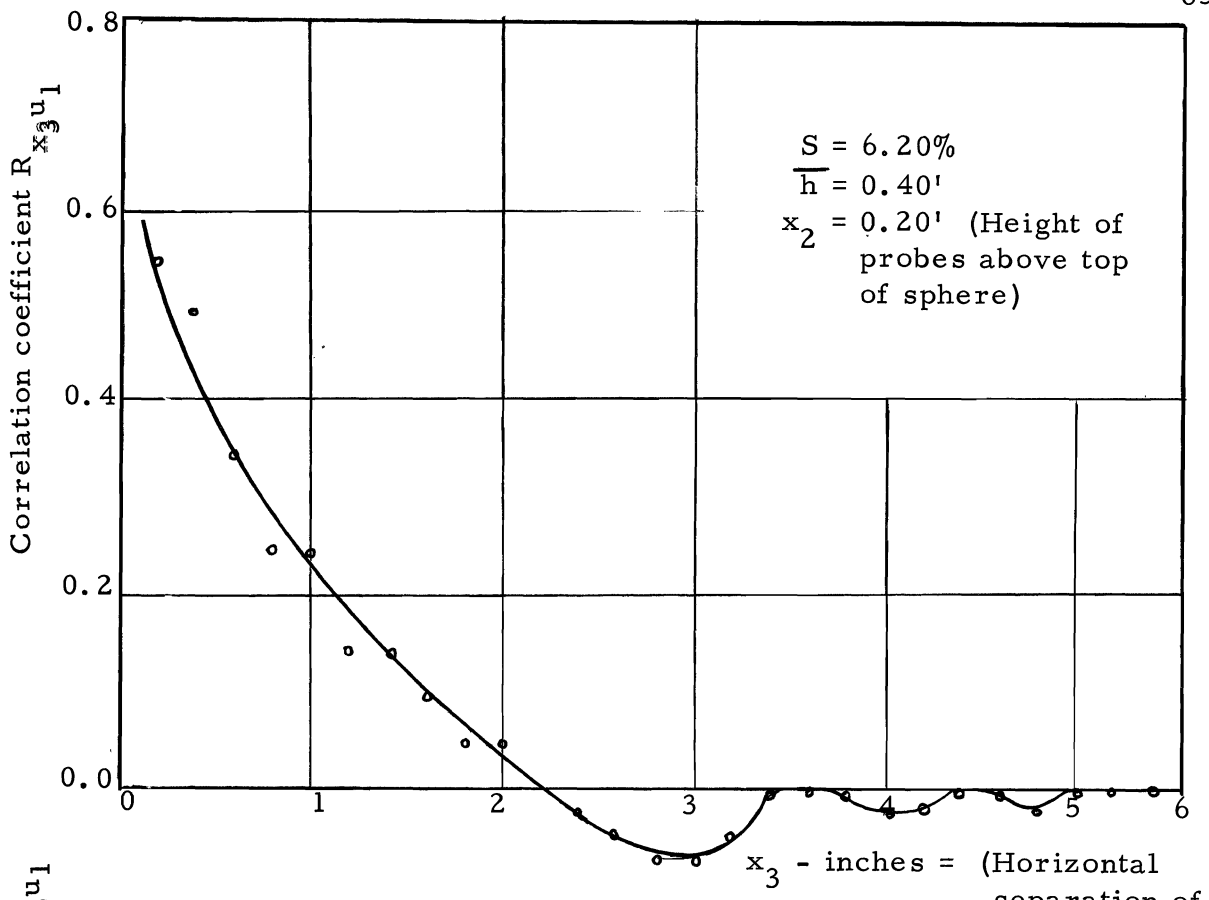

Figure 32. Cross-correlation in horizontal direction.

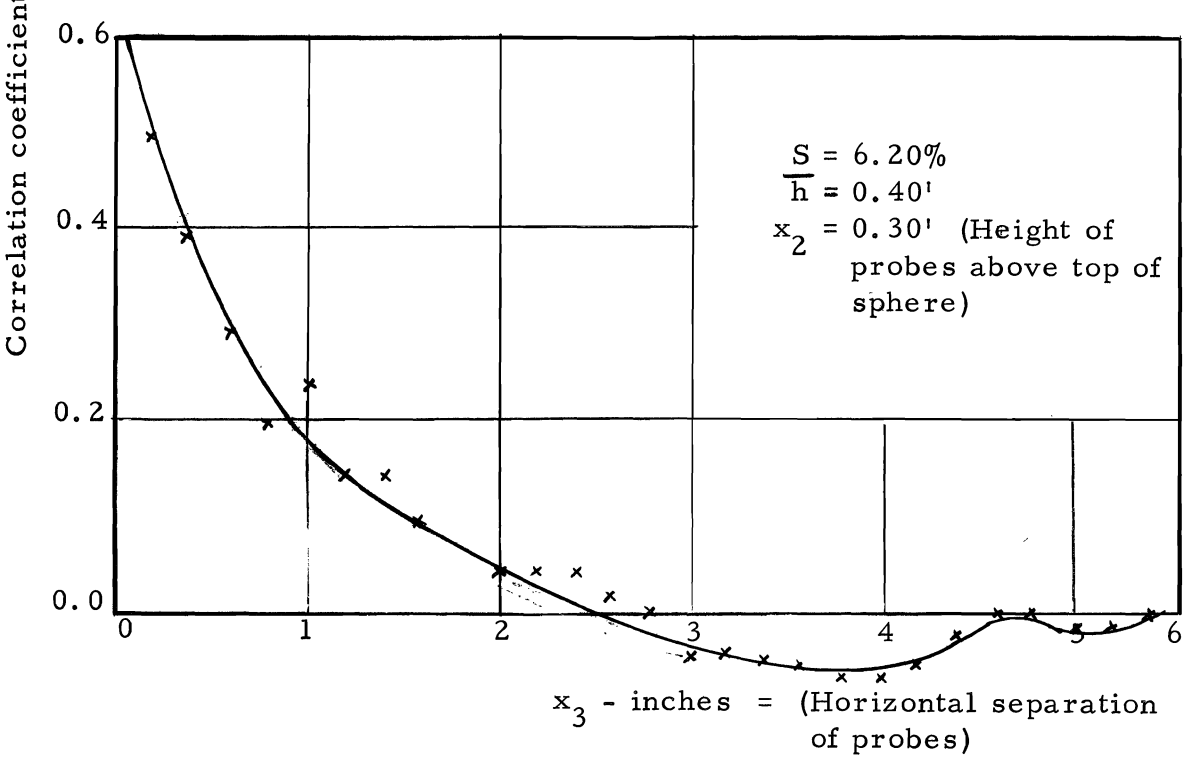

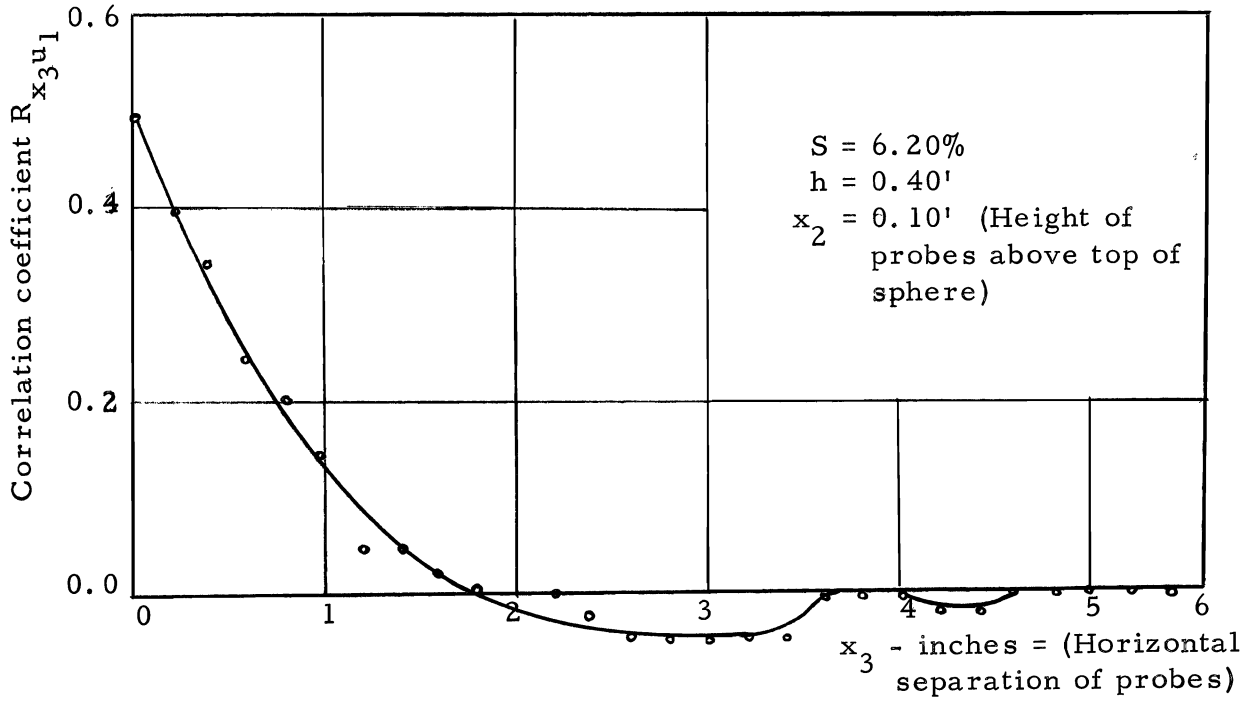

Figure 34. Cross-correlation in horizontal direction.

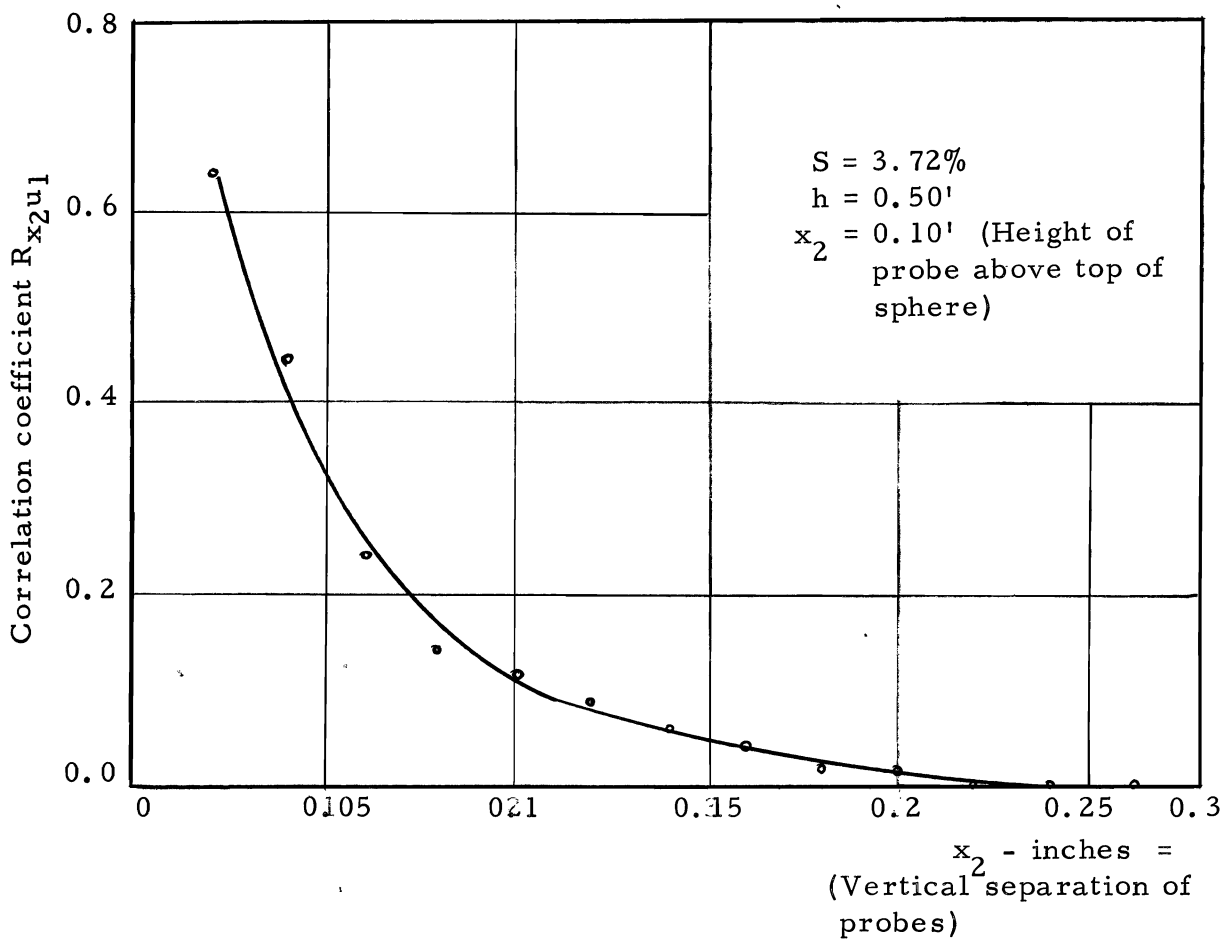

The vertical correlation curves do not show a negative value. This is because the flow depths are such that a system of eddies showing negative correlation could not develop.

There was very little effect of the change of position of the probes relative to the wall on the shape of these curves. A change in slope has also produced but little effect on the shape of the curves.

Cross-correlation curves have been measured by many persons in different types of turbulence. The curves obtained by Taylor (1935), Jordon (1963), and Favre (1963) are similar to the present curves.

Microscale of Turbulence

In Chapter III it was mentioned that the average size of eddies which are mainly responsible for dissipation of energy in a turbulent flow field is measured by microscale. The distribution of microscale of the turbulence for different Reynolds number are shown in Figure 37. All these curves are similar in shape. The microscale is small near the bed but increases to a maximum at about half the depth and then again falls to a lower value. These curves are quite similar to those measured by Jordon and Rao (1963). Figure 36 shows that microscale is independent of Reynolds number. Until now no satisfactory explanation about the distribution of microscale has been suggested, but it can be said that the maximum dissipation is in the region of considerable turbulence production.

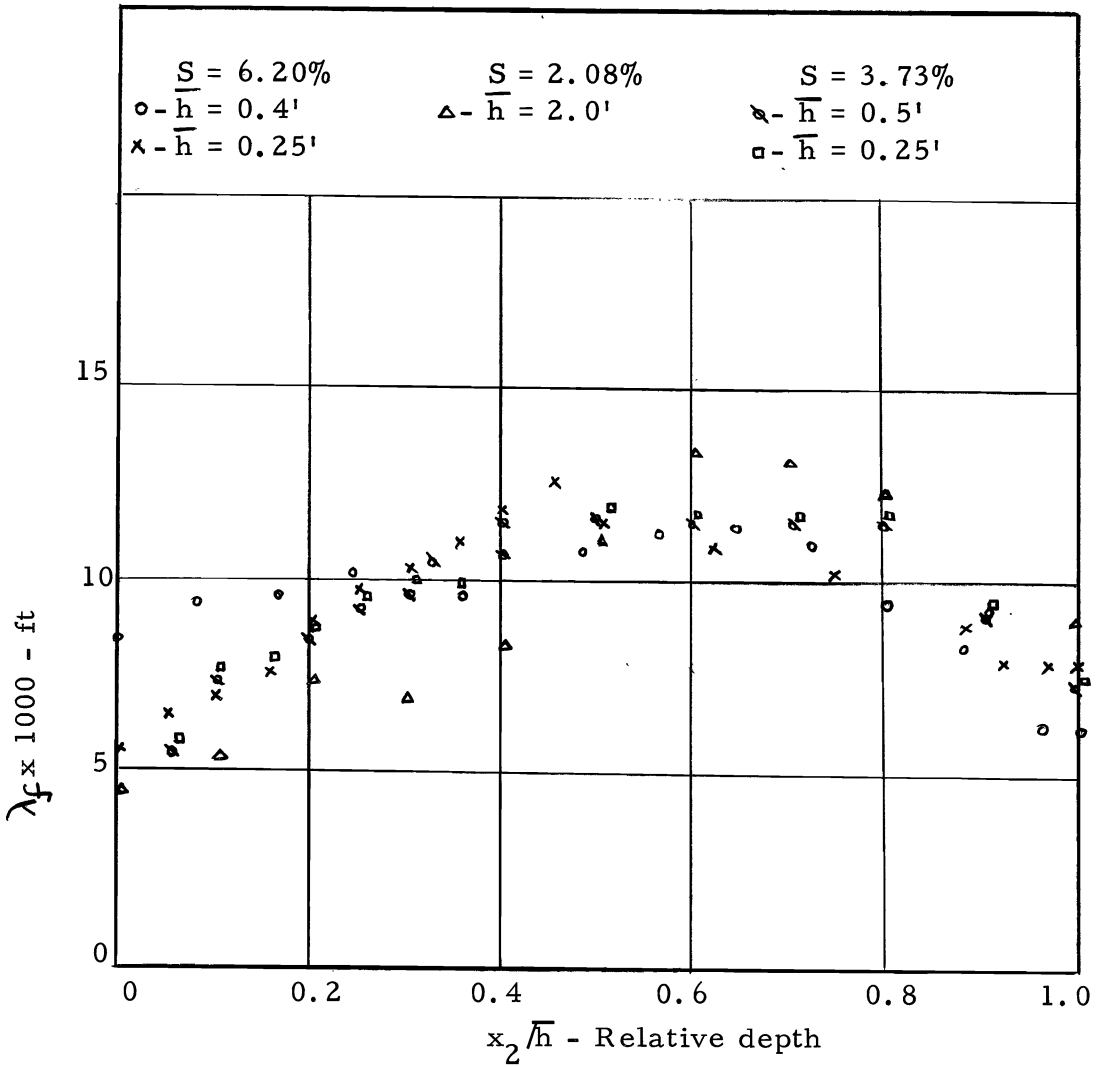

Figure 36. Variation of λ_f as a function of relative depth

Macroscale of Turbulence

Figure 37 shows the distribution of macroscale as a function of relative depth. These curves are for different Reynolds numbers. The value of ℓ_1 increases as one moves away from the bed but only up to a certain point. After attaining a maximum value, it again falls. Similar curves were obtained by Laufer (1953) while studying turbulence energy balance and dissipation in a channel 5 inches wide and 60 inches deep. One of his curves has been superimposed on figure 37.

One more curve obtained by Jordon (1963) has also been replotted. The shape of all these curves is similar to the curves obtained under the present study.

All these curves have been obtained from the Eulerian time correlation curves which give only average macroscale. The true macroscale is given by the curves of cross-correlation. Hence great care should be taken in drawing any conclusions from these curves.

The distribution of macroscale can be explained by dividing the channel into three parts which may be designated as outer, intermediate, and wall proximity zone. In the zone of wall proximity, a lot of turbulence production takes place but due to comparatively greater viscous effects the eddies cannot increase in size, hence macroscale remains small. As one comes to the intermediate zone, the viscous effects are dominated by the turbulence production causing a higher

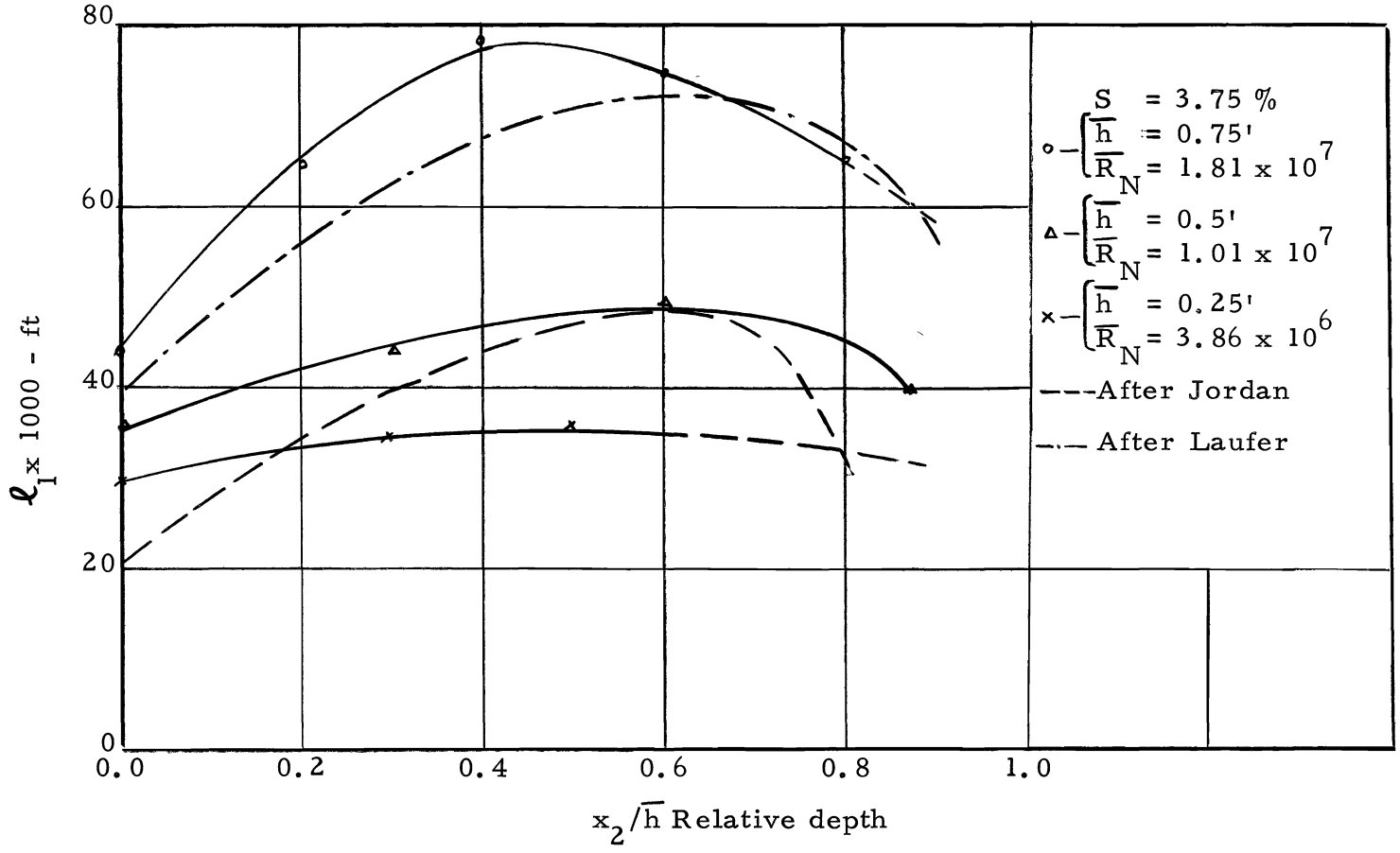

Figure 37. Variation of ℓ_1 (Macroscale) as a function of relative depth.

value of macroscale. In the outer zone, much energy is being dissipated, the eddies are growing smaller and smaller and this decreases the value of macroscale.

The maximum value of macroscale observed is nearly 0.08 ft. But a possibility of presence of macroscale of large size cannot be ruled out because the probe could not detect big eddies of low frequency.

One-Dimensional Energy Spectrum

In a turbulent field which is homogeneous with respect to time at a fixed point at any instant the energy is directly related to $\overline{u}_1^2$. This energy is distributed among the eddies in proportion to their size, i.e., large eddies carry more energy and small eddies carry less energy. A curve drawn between the size of eddies and energy clearly shows the distribution of energy in that flow field. It has been found that the size of eddies cannot be easily determined. So energy distribution curves are usually drawn with respect to frequency of the velocity fluctuations, this being inversly proportional to the size of eddies. This type of curve is called energy spectrum curve.

Let $E_1(n)$ be the contribution of energy to $\overline{u}_1^2$ of the frequencies between n and dn + n. Then function $E_1(n)$ is called one-dimensional energy spectrum function.

Then

$$\int_0^\infty dn \; E_1(n_1) = \overline{u}_1^2$$

The relation of $E_1(n)$ to other turbulence properties is shown in Chapter III.

The distribution of $E_1(n)$ cannot be determined easily by theoretical means. So investigators have formulated certain relations about it by analyzing three-dimensional energy spectrum function $E(n)$. In such a theoretical analysis it is more convenient to use wave number $K = \frac{2\pi n}{U}$ than n. Lin (1947) showed that from the von Karman-Howarth equation it is possible to arrive at the following result:

$$\frac{\partial}{\partial t} E(K) = F(K) - 2\nu K E(K) \quad . \quad . \quad . \quad . \quad (5\text{-}2)$$

This relation according to Hinze (1959) can be written as follows

$$\frac{\partial}{\partial t} \int_0^K E[K(r)]\, dK = \int_0^K F(K)\, dK - 2\nu \int_0^K K^2 E(K)\, dK \quad . \quad . \quad (5\text{-}3)$$

This can be reduced to

$$\frac{\partial}{\partial t} \int_0^K E(K)\, dK = \int_0^K F(K)\, dK - 2\nu \int_0^K K^2 E(K)\, dK + H(K) \quad . \quad . \quad . \quad . \quad (5\text{-}4)$$

In the equation the various terms have following meanings.

The left hand side of this equation represents the change of total kinetic energy of turbulence. The first term on the right represents the interaction of eddies of different wave numbers, thereby transferring energy by inertial effects to or from the eddies in the wave number region 0 to k and therefore $F(K)$ is referred as the transfer spectrum function. $H(K)$ is the energy supplied to turbulence. The second term can be shown to represent the dissipation of turbulence

energy into heat hence $K^2 E(k)$ is known as the dissipation spectrum function. The solution of the equation has been found by many persons. According to Kovaszray (1948)

$$E(K) = \left(\frac{\epsilon^2}{a^{10}}\right)^{\frac{1}{3}} K^{-5/3}\left[1 - \frac{a^{2/3}}{2}\left(\frac{K}{K_d}\right)^{4/3}\right]^2 \quad . \quad . \quad . \quad (5\text{-}5)$$

For the region of negligible viscosity effects this becomes, where K is of moderate value,

$$E(K) = \left(\frac{8\epsilon}{9a}\right)^{2/3} K^{-5/3} \quad . \quad . \quad . \quad . \quad . \quad . \quad . \quad . \quad . \quad (5\text{-}6)$$

For very large k where viscosity plays an important part, Heinseberg (1948) showed that

$$E(K) = \text{constant} \times K^{-7} \quad . \quad . \quad . \quad . \quad . \quad . \quad . \quad . \quad . \quad . \quad . \quad . \quad . \quad . \quad . \quad . \quad . \quad . \quad . \quad (5\text{-}7)$$

Similar solutions of the equation have been obtained by Bass (1949) and Chandrasekhar (1949).

Using Batchelor's (1953) equation for an isotropic turbulence which states

$$E(K) = K^3 \frac{d}{dK}\left[\frac{1}{K_1}\frac{dE(K_1)}{dK_1}\right] \quad . \quad . \quad . \quad . \quad (5\text{-}8)$$

one can obtain the following results from equation (5-6) and (5-7)

$$E_1(K_1) = \frac{9}{55}\left(\frac{8\epsilon}{9a}\right)^{2/3} K_1^{-5/3} \quad . \quad . \quad . \quad . \quad . \quad (5\text{-}9)$$

and

$$E_1(K_1) = \frac{1}{63}\left(\frac{8a}{2\nu^2}\right)^2 K_1^{-7} \quad \ldots\ldots \quad (5\text{-}10)$$

Kolmogoroff also gave the solution of equation (5-5) similar to equation (5-9). His equation is

$$E_1(K_1) = a' \epsilon^{2/3} K_1^{-5/3} \quad \ldots\ldots \quad (5\text{-}11)$$

Experimentally one-dimensional energy spectrum can be measured by using spectrum analyzer as described in Chapter IV. A few one-dimensional spectrum curves obtained at different discharges and slopes are shown in Figures 38 thru 44. These curves are quite similar to those obtained by Rao, Romano (1956) etc.

The conclusion from these curves should be drawn with great care due to following reasons: the spectrum analyzer used for the measurements was not sensitive to low frequencies. The instrument would not respond to frequencies below 30 cps and so data lying in that region is not reliable. The level of the probe signal was also increased by the noise picked up by equipment at various joints and connections. The vibrations induced in the probe due to impact of water also increased the probe signal.

The probe used was sensitive to pressure fluctuations as well as to the velocity. But the formula used for calculating the energy considers that the probe output is only due to velocity fluctuations. Thus energy which is being added due to pressure fluctuations was taken as energy

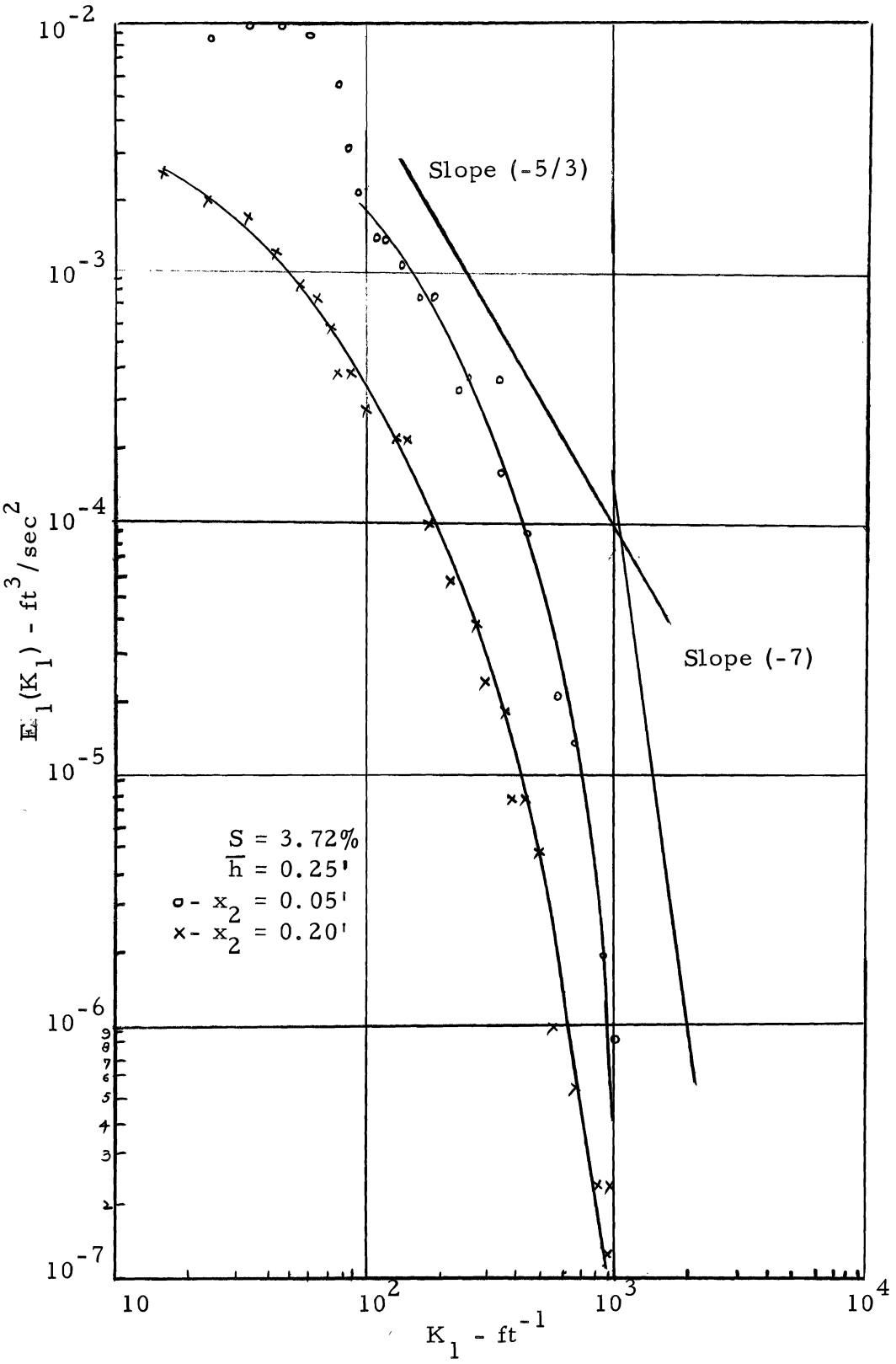

Figure 38. One-dimensional energy spectra.

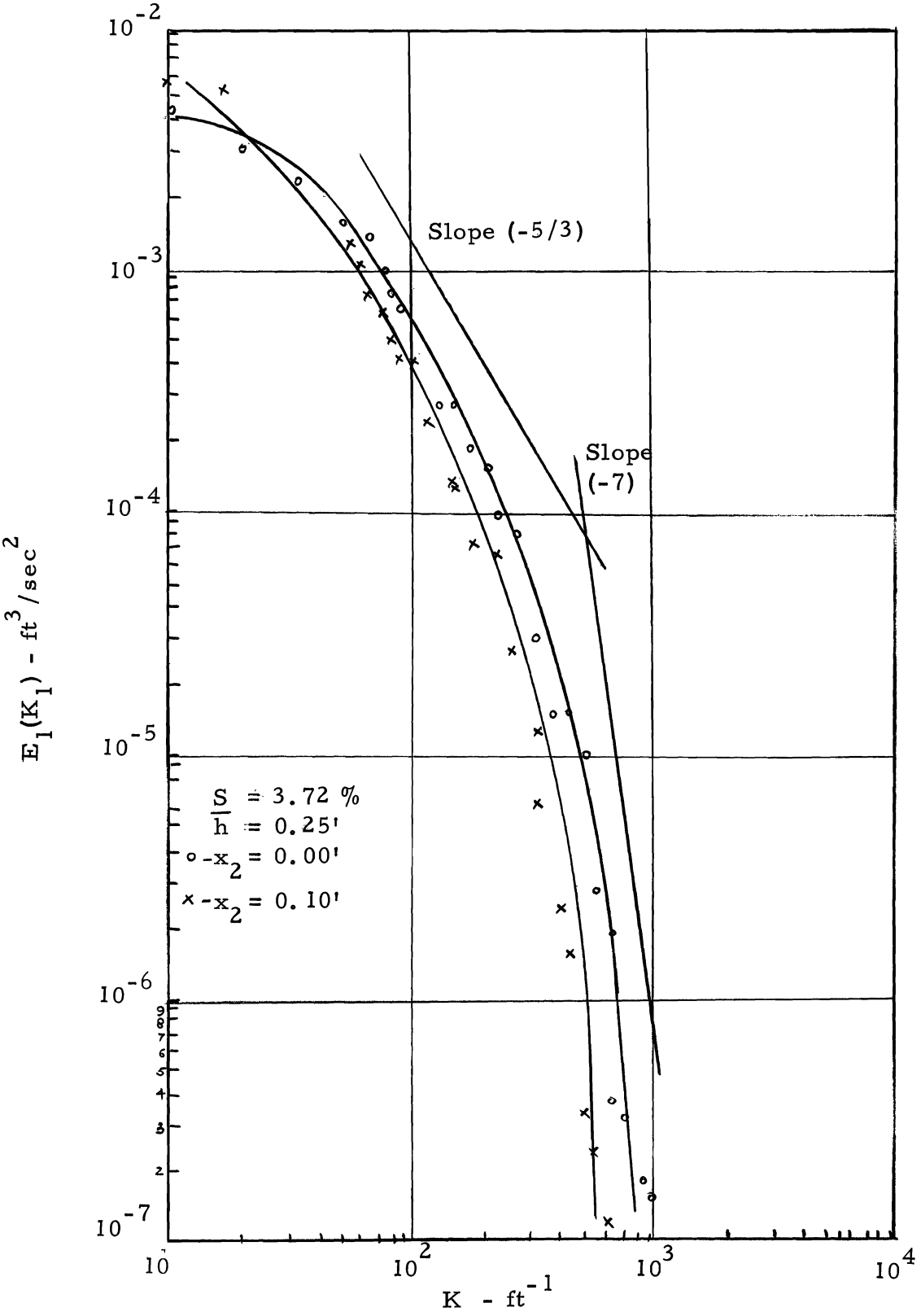

Figure 39. One-dimensional energy spectra.

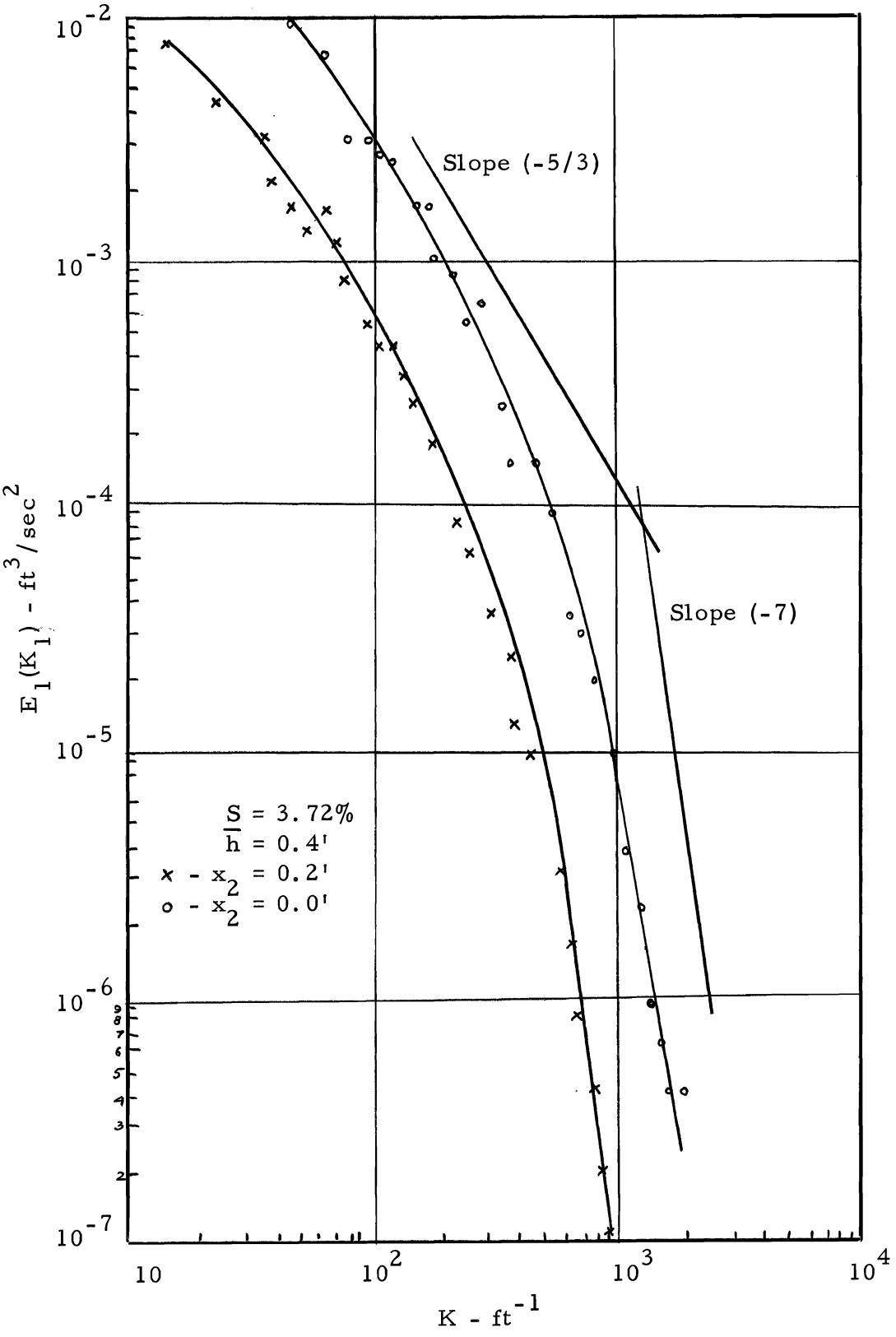

Figure 40. One-dimensional energy spectra.

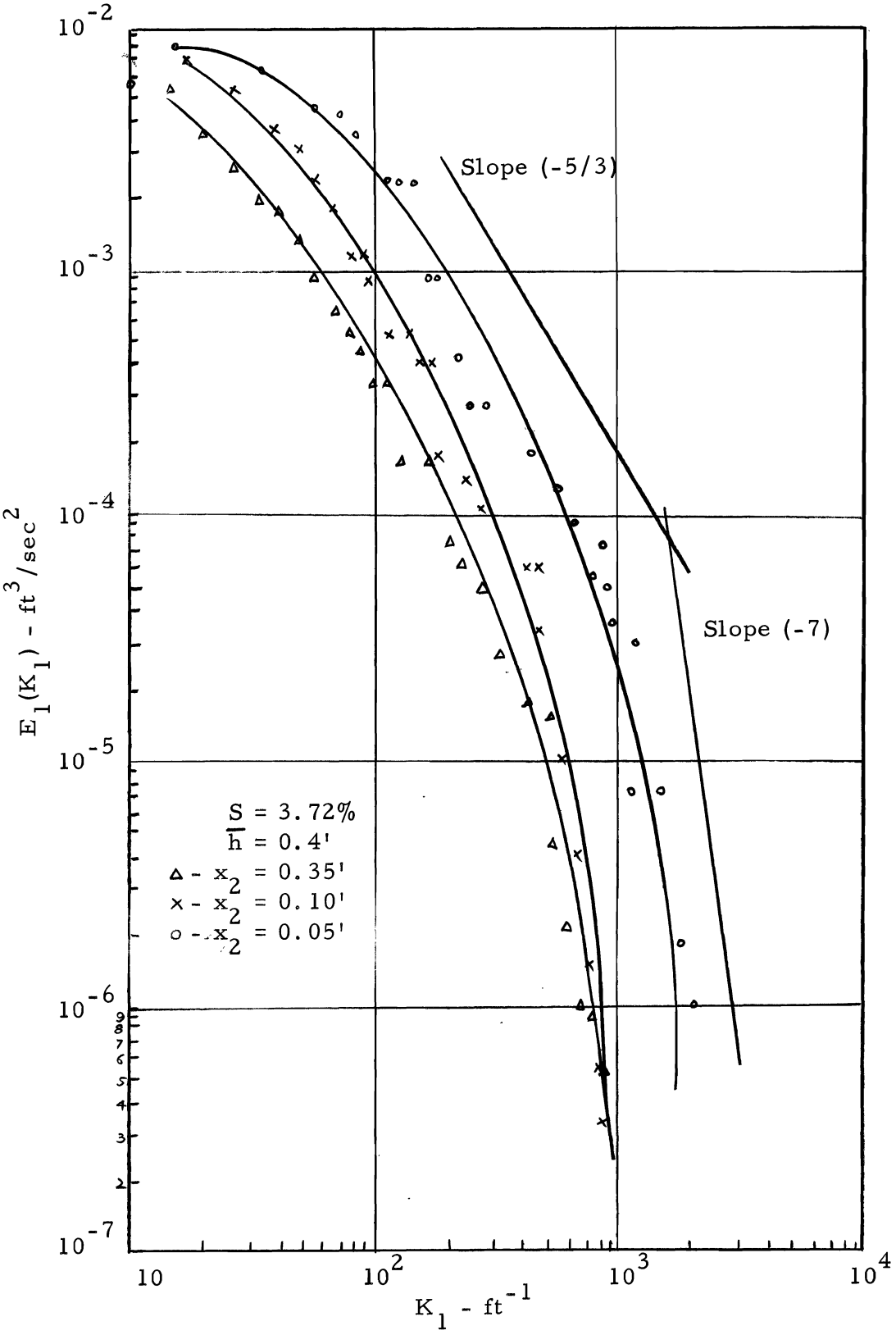

Figure 41. One-dimensional energy spectra.

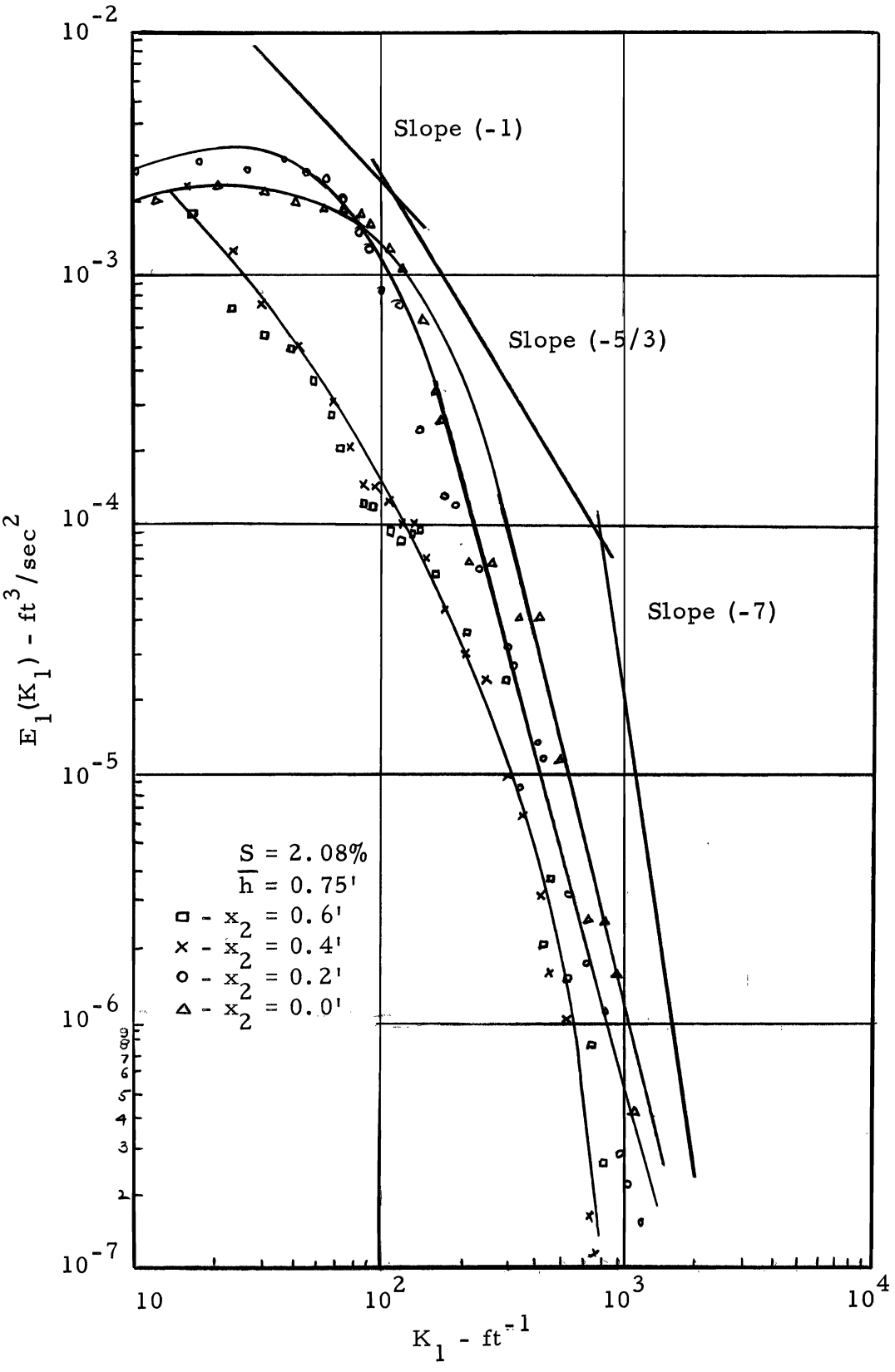

Figure 42. One-dimensional energy spectra.

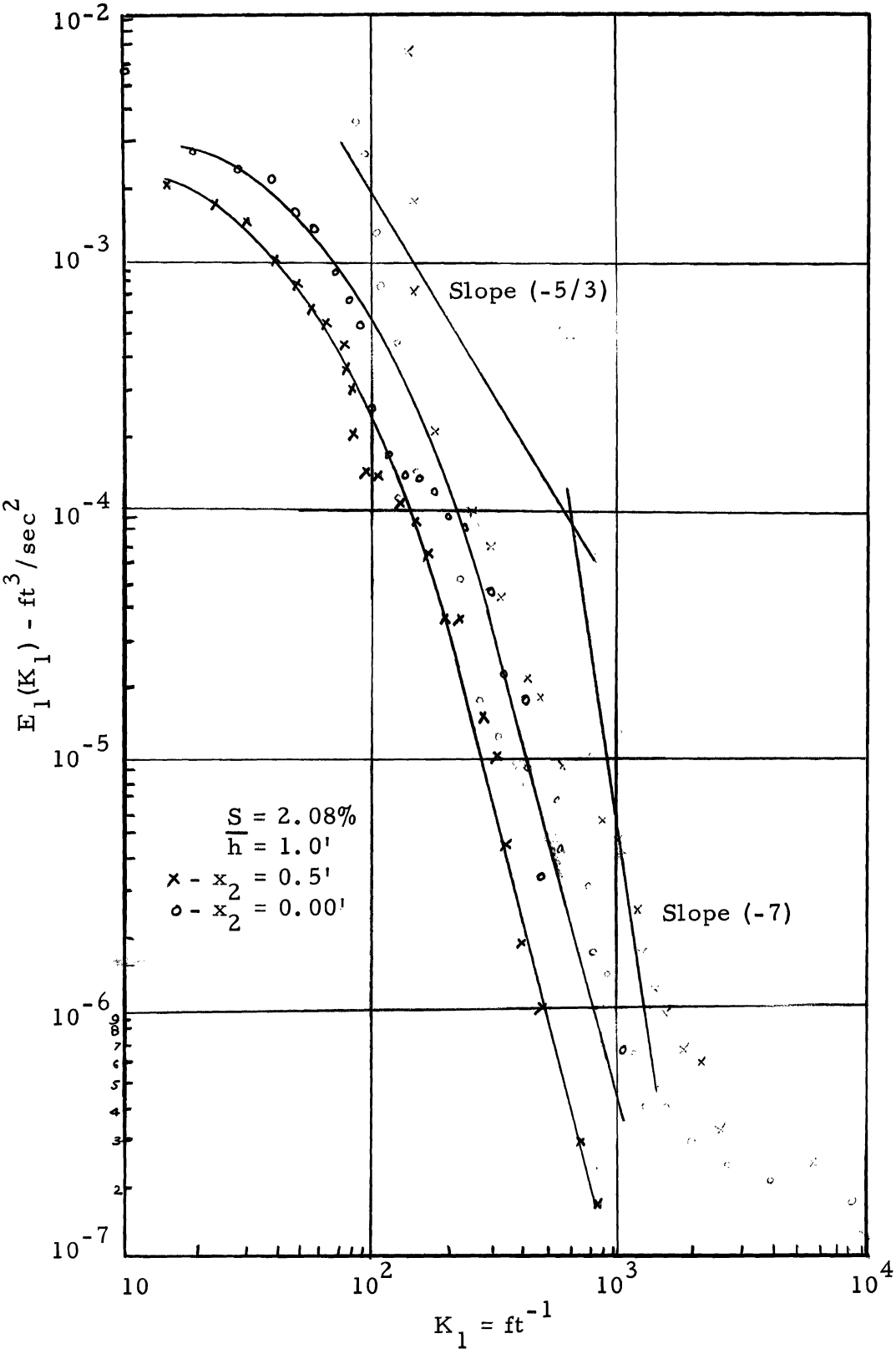

Figure 43. One-dimensional energy spectra.

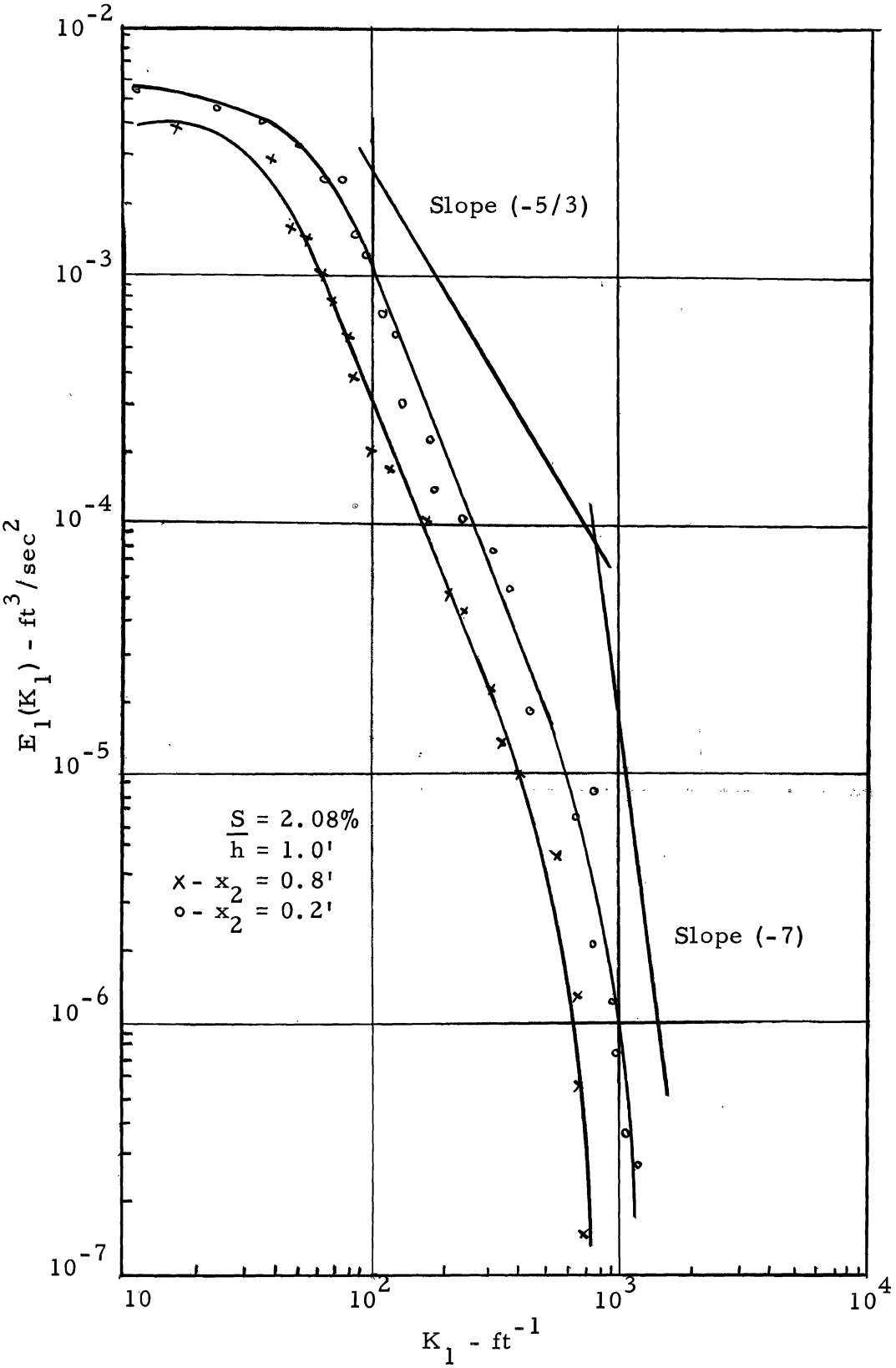

Figure 44. One-dimensional energy spectra.

carried by the eddies. Moreover the probe being insensitive to the low frequencies could not detect the energy carried by big eddies which might be in large quantity.

The spectrum curve show a definite decrease in energy with increase of wave number. The rate at which energy decreases in the low wave number range is small but increases rapidly in the higher wave number region. Thus, most of the energy is carried by the big eddies.

The data lying in the low wave number region cannot be compared with any theoretical curves because such a curve does not exist. For moderate wave number the curve follows equation (5-9) closely. The equation for higher wave number is also satisfied by most of the curves although the trend of curves is such that they move away from the line whose slope is (-7).

Dissipation Spectra

The functions $K_1^2 E_1(K_1)$ and $K^2 E(K)$ are referred as dissipation spectra and describe the distribution of rate of decay of turbulent energy with respect to heat. A few linear plots of this spectra are shown in Figure 45 to 46. The scatter in the points is due to experimental error. These curves do not differ much in form from those measured by Gibson (1962-1963) and Rao. These plots are used for determining the total rate of dissipation assuming that turbulence is isotropic because

$$\epsilon = 15 \nu \int_0^\infty K_1^2 \, E(K_1) \, dK_1 \quad . \qquad (5\text{-}12)$$

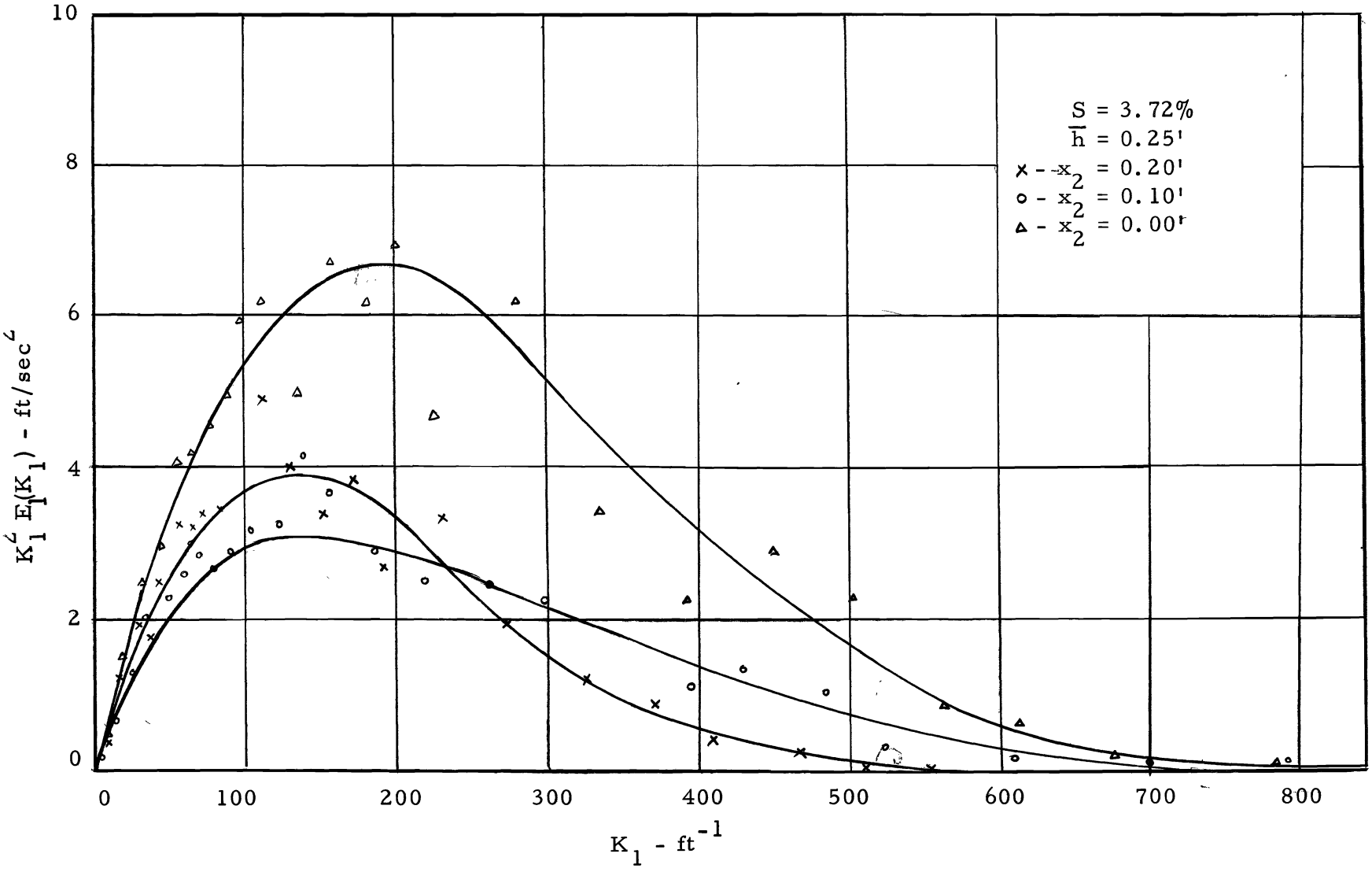

Figure 45. One-dimensional dissipation spectra.

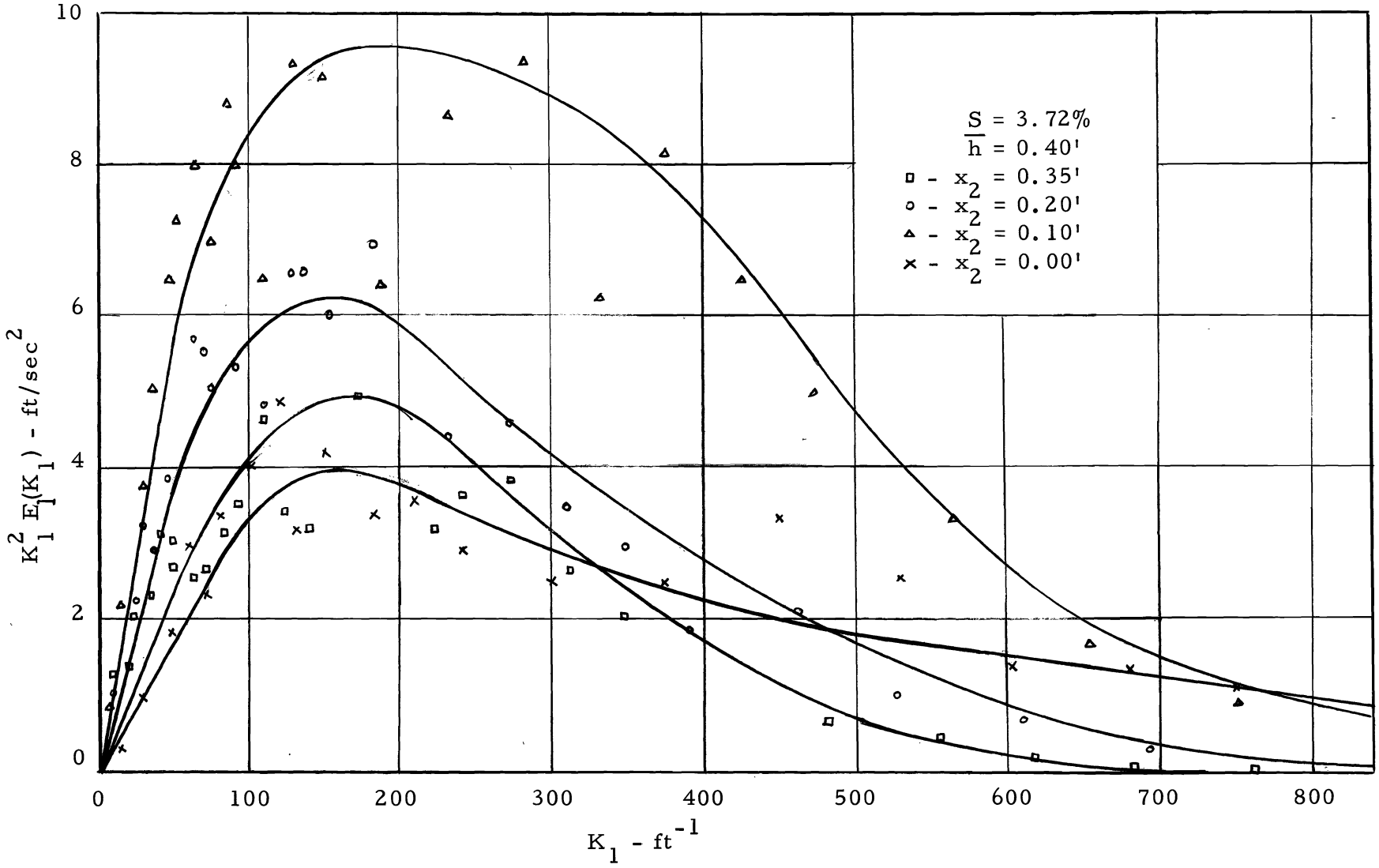

Figure 46. One-dimensional dissipation spectra.

CHAPTER VI

CONCLUSIONS

From the experimental investigation and the subsequent interpretation and discussion of results the following conclusions can be made concerning the structure of turbulence in a rough open channel.

1. The shape of dimensionless mean velocity curves is not effected by change in slope and Reynolds number.

2. The intensity of turbulence is high near the bed but decreases with increase in Reynolds number.

3. The maximum turbulence intensity occurs at that region where maximum turbulence is being produced.

4. An increase in slope causes more intense turbulence.

5. The autocorrelation decays faster near the bed than near the surface and roughness or slope does not have much effect on it.

6. The cross-correlation curves are not effected by the change of flow rate or slope for this kind of turbulence. The value of vertical correlation decreases faster than horizontal correlation. The vertical correlation never gets a negative value whereas horizontal correlation becomes negative when the correlation distance is 3 inches.

7. The longitudinal microscale increases from a small value which occurs at the bottom to a higher value and falls again as the surface is approached. The change in Reynolds number and slope does not effect

the shape of microscale curves.

8. The longitudinal macroscale of turbulence decreases as the bed is approached. It increases with increase in distance from the bed until a maximum value is reached and then decreases near the surface. The region of maximum macroscale is the region of small viscous action but of considerable turbulence generation.

9. The macroscale is a function of Reynolds number as well as of relative depth.

10. Spectrum curves show that most of the energy is carried by the eddies of frequencies lying between 0 and 100 cps.

11. The spectrum curves follow equation (5-9) to some extent. So there is a possibility that local isotropy exists.

12. The contribution to the turbulence energy increases as the bed of the channel is approached.

13. The dissipation spectra show that medium size eddies are the major cause of energy dissipation.

LITERATURE CITED

Bass, J. 1949. "Sur less bases mathemaliques de la theorie de la turbulence d' Hei senberg." Comtex Rendus des Seances, De L' Academe des Sciences, Paris.

Batchelor, G. K. 1946. "The theory of axisymetric turbulence." Proceedings Royal Society Series A.

Batchelor, G. K. 1953. "The theory of homogeneous turbulence." Cambridge University Press, Cambridge, Great Britain.

Bazin, H., and H. Darcy. 1865. "Rechevches hydrauliques," Mem. Pre. par. div. Sav., XXIII, Paris.

Brookshire, W. A. 1961. "A study of the structure of turbulent shear flow in pipes." Unpublished Ph. D. dissertation in chemical engineering, Louisiana State University, Baton Rouge, Louisiana.

Chandrasekhar, S. 1949. "On Heisenberg's elementary theory of turbulence." Proceedings of the Royal Society of London, Series A.

Clyde, Calvin G. 1961. "Fluctuations of total head near a smooth wall in a turbulent open channel flow." Unpublished Ph. D. dissertation in civil engineering, University of California, Berkeley, California.

Dryden, H. L. 1938. "Turbulence investigations at the National Bureau of Standards." Proceedings of Fifth International Congress of Applied Mechanics.

Favre, A., J. Gaviglio, and R. Dumas. 1953. "Recherche Aeroraut." Paris. No. 32, p. 21.

Gibson, M. M. 1962. "Spectrum of turbulence at high Reynolds number." Nature.

Gibson, M. M. 1963. "Spectra of turbulence in a round jet." Journal of Fluid Mechanics, Part II.

Heisenberg, W. 1948. "On the theory of statistical and isotropic turbulence." Proceedings of the Royal Society of London. Series A.

Hinze, J. O. 1959. "Turbulence," McGraw-Hill Book Company, Inc., New York.

Jordan, H. B. 1963. "A study of the scale of turbulence in a circular channel," Unpublished Ph. D. dissertation in chemical engineering, Louisiana State University, Baton Rouge, Louisiana.

Karman, Von T. and L. Howarth. 1938. "On the statistical theory of Isotropic turbulence." Proceedings of the Royal Society A164, 192-215.

Karman, Von T. 1948. "Progress in the statistical theory of turbulence." Journal of Marine Research 7, 252-264.

Kolmogoroff, A. N. 1941. "The local structure of turbulence in incompressible viscous fluid for very large Reynolds numbers, C. R. Acad. Sci. U.R.S.S. (Doklady)." English translation available in Turbulence classic papers on statistical theory. Edited by Friedlander, S. K. and L. Topper. Interscience Publishers, New York.

Kovanszney, L. S. G. 1948. "Spectrum of locally isotropic turbulence." Journal of the Aeronautical Sciences. 15(12):745-53.

Laufer, J. 1951. "Investigation of turbulent flow in a two dimensional channel." National Advisory Committee for Aeronautics Report, 1053.

Laufer, J. 1954. "The structure of turbulence in fully developed pipe flow." National Advisory Committee for Aeronautics Report 1174.

Lee, J. J. 1966. "A preliminary experimental study of the turbulence decay in the wake of a hemisphere in free surface flow." An unpublished report submitted at Utah State University, Logan, Utah.

Lin, C. C. 1947. "Remarks on the spectrum of turbulence." Proceedings of the First Symposium of Applied Mathematics, American Mathematical Society.

Martin, G. C. 1963. "An investigation into the turbulence characteristic of fluids in pipe flow." Ann Arbor, Michigan. University Microfilm.

Pai, S. I. 1957. Viscous flow theory (II turbulent flow)." D. Van Nostrand Company, Inc., Princeton, New Jersey.

Prandtl, L. 1926. "Uber die ausgebildete turbulenz." Proceeding of the Second International Congress of Applied Mechanics, Zurich.

Rao, M. V. 1965. "A study of the structure of shear turbulence in free surface flow." Dissertation for Doctor of Philosophy in Fluid Mechanics, Utah State University, Logan, Utah.

Reynold, Osborne. 1894. "On the dynamical theory of incompressible viscous fluids and the determination of the criterion." Proceedings of the Royal Society of London, Series A.

Romano, John Emilio. 1954. "Spectrum of turbulence in axisymmetrical flow." Ann Arbor, Michigan, University Microfilm.

Roshko, A. 1954. "On the development of turbulent wakes from vortex streets." National Advisory Committee for Aeronautical, Technical Report Number 1191.

Rouse, H. 1938. "Fluid mechanics for hydraulic engineers." McGraw-Hill Book Company, Inc., New York.

Schlichting, Hermann. 1955. "Boundary layer theory." Translated by J. Kestin, New York, McGraw-Hill.

Taylor, G. I. 1935. "Statistical theory of turbulence." Proceedings of the Royal Society A 151, 421-478.

Taylor, G. I. 1938. "The spectrum of turbulence." Proceedings of the Royal Society, A 164, 476-490.

Townsend, A. A. 1956. "The structure of turbulent shear flow." Cambridge University Press, Cambridge, Great Britain.

LIST OF SYMBOLS AND DEFINITIONS

Symbol	Definition	Dimension
A	Area	L^2
A	Instantaneous value of a fluctuating quantity	--
$\overline{A}$	Mean value of A	--
a	Deviation of A from its mean value	--
a_{x_1}	Acceleration in x_1 direction	(L/T^2)
$\overline{a}_{x_1}$	Mean value of a_{x_1}	(L/T^2)
a_{x_2}	Acceleration in x_2 direction	(L/T^2)
$\overline{a}_{x_2}$	Mean value of a_{x_2}	(L/T^2)
a_{x_3}	Acceleration in x_3 direction	(L/T^2)
$\overline{a}_{x_3}$	Mean value of a_{x_3}	(L/T^2)
B	Instantaneous value of a fluctuating quantity	--
$\overline{B}$	Mean value of B	--
b	Deviation of B from its mean value	--
C	Constant in equation (4-7)	$(\frac{\text{Millivolts}}{L})$
c	Constant	--
$E(K)$	Three-dimensional turbulence energy spectrum function in wave number domain	(L^5/T^2)
$E_1(n)$	Longitudinal one-dimensional turbulence energy spectrum function in frequency domain	(L^2/T)

Symbol	Definition	Dimension
$E_1(K_1)$	Longitudinal one-dimensional turbulence energy spectrum function in wave number domain	(L^3/T^2)
e	Absolute roughness	(L)
F(K)	Three-dimensional transfer energy spectrum function	(L^3/T^2)
f(r)	Longitudinal cross-correlation coefficient	--
g	Gravitational acceleration	(L/T^2)
g(r)	Lateral cross-correlation coefficient	--
H	Instantaneous value of head	(L)
H(K)	Function representing energy supplied to the turbulence	(M/LT^2)
$\overline{H}$	Mean value of head H	(L)
H'	Fluctuating component of total head	(L)
h	Height of any point	(L)
h	Instantaneous flow depth	(L)
$\overline{h}$	Mean depth of flow	(L)
h'	Deviation of flow depth from mean depth	(L)
i, j, k	Coordinate axes. Each one is equal to 1, 2, 3	--
k	Universal constant in equation (2-21)	--
K	Wave number = $\frac{2\pi n}{\overline{U}}$	$(\frac{1}{L})$
K_1	Longitudinal component of wave number vector	$(\frac{1}{L})$
K_d	Wave number range of main dissipation of energies	$(\frac{1}{L})$

Symbol	Definition	Dimension
ΔK	Effective band width established by the analyzer in wave number	$(\frac{1}{L})$
L_a	Pressure correlation coefficient	--
ℓ	Prandtl's mixing length	(L)
ℓ_i	Instantaneous mixing length	(L)
ℓ_1	Longitudinal integral scale or macroscale	(L)
m	Mass	(M)
n	Frequency	$(\frac{1}{T})$
Δn	Effective band width established by analyzer in cycles per second	$(\frac{1}{T})$
P	Pressure at an instant	(F/T^2)
$\overline{P}$	Mean value of P	(F/T^2)
P_R	Deviation of pressure from mean value	(F/T^2)
R	Ratio observed from R.M.S. meter $= \frac{\sqrt{\overline{u_1^2}}}{\sqrt{\overline{\left(\frac{\partial u_j}{\partial t}\right)^2}}}$	--
$\overline{R_N}$	Reynold's number	--
$R_{ij}(r)$	Eulerian cross-correlation	--
$R_E(t)$	Eulerian time correlation	--
$\vec{r}$	Distance vector	(L)
S	Slope	--
$(S_{ijk})_{AB}$	Triple cross correlation	--
t	Time	(T)
Δt	Small increment of time	(T)
U	Instantaneous velocity vector	(L/T)

Symbol	Definition	Dimension
$\overline{U}$	Temporal mean value of	(L/T)
U_A, U_B	Mean velocities at level A and B	(L/T)
U_1	Instantaneous velocity along x_1 direction	(L/T)
$\overline{U}_1$	Temporal mean value of U_1	(L/T)
U_2	Instantaneous velocity along x_2 direction	(L/T)
$\overline{U}_2$	Temporal mean value of U_2	(L/T)
U_3	Instantaneous velocity along x_3 direction	(L/T)
$\overline{U}_3$	Temporal mean value of U_1	(L/T)
u	Deviation of velocity from its mean value $\overline{U}$	(L/T)
u_1	Deviation of velocity from mean velocity along x_1 direction	(L/T)
u_2	Deviation of velocity from mean velocity along x_2 direction	(L/T)
u_3	Deviation of velocity from mean velocity along x_3 direction	(L/T)
$u_1' u_2'$	Root mean square of velocity fluctuations	(L/T)
u_f	Friction velocity	(L/T)
V	Overall mean velocity in an open channel	(L/T)
V_T	Instantaneous value of the total head transducer probe	(Volts)
V_R	Instantaneous value of real turbulence signal of the probe	(Volts)
V_N	Instantaneous value of noise	(Volts)
v_T'	Root mean square value of transducer probe output	(Volts)

Symbol	Definition	Dimension
v'_R	Root mean square value of real turbulence signal of the probe	(Volts)
v'_N	Root mean square value of the noise	(Volts)
W	Instantaneous vorticity	$(\frac{\text{Revolution}}{T})$
$\overline{w}$	Mean value of W	$(\frac{\text{Revolution}}{T})$
w	Deviation of vorticity from mean value	$(\frac{\text{Revolution}}{T})$
x_1, x_2, x_3 ξ_1, ξ_2, ξ_3	Cartesian coordinate axes	(L)
Δx	Small increment of distance	(L)
a	Heisenberg absolute constant in relations to eddy viscosity	--
a'	Absolute constant in equation (5-11)	--
γ	Specific weight of water	(M/L^2T^2)
λ	Eulerian microscale or dissipation length	(L)
λ_f	Longitudinal Eulerian microscale	(L)
λ_g	Lateral Eulerian microscale	(L)
ε	Rate of turbulent energy dissipation per unit mass	(L^2/T^3)
ε_t	Turbulent exchange coefficient	--
ρ	Density of fluid	(M/L^3)
$\bar{\rho}$	Time mean value of density	(M/L^3)
ρ'	Fluctuating component of density	(M/L^3)
τ	Shear stress	(M/LT^2)
τ	Preselected time constant in determining microscale with the correlator	(T)

Symbol	Definition	Dimension
τ	Time delay	(T)
τ_i	Instantaneous shear stress	(M/LT^2)
μ	Dynamic viscosity of fluid	(M/LT)
η	Eddy viscosity	(M/LT)
ν	Kinematic viscosity of fluid	(L^2/T)
$\mathfrak{L}$	Center line	--

APPENDIXES

Appendix A

Theory of Operation of Transducer Probe

The total instantaneous head which acts on the piezoelectric probe is expressed as

$$H = \bar{H} + H' = (\bar{h} + h') + \left(\frac{\bar{P}}{\gamma} + \frac{p}{\gamma}\right) + \left(\frac{\bar{U}_1 + u_1}{2g}\right) \quad . \quad . \quad . \quad (1)$$

It was observed by Perkins and Eagleson (1959) that $\bar{H}$ did not cause an effect on this probe. Therefore

$$H = h' + \frac{p}{\gamma} + \frac{2\bar{U}_1 u_1}{2g} + \frac{u_1^2}{2g} \quad . \quad . \quad . \quad . \quad (2)$$

In this equation it was found by Townsend (1947), Roshko (1954), and Ippen (1957) that the quantities h', $\frac{P}{\gamma}$, and $\frac{u_1^2}{2g}$ forms a very small part of h'.

Thus

$$H = \frac{\bar{U}_1 u_1}{g} \quad . \quad . \quad . \quad . \quad . \quad . \quad . \quad . \quad . \quad . \quad (3)$$

If V_R is the output of probe in volts at an instant, then

$$V_R = \frac{C \bar{U}_1 u_1}{g} \qquad u_1 = \frac{g V_R}{C \bar{U}_1} \quad . \quad . \quad . \quad . \quad . \quad . \quad (4)$$

where C is a calibration constant.

Taking R.M.S. value of equation (4)

$$u_1' = \frac{g V_R'}{C \bar{U}_1} \quad . \quad . \quad . \quad . \quad . \quad . \quad . \quad . \quad (5)$$

For the two probes used in the study the value of C was found to be equal to 6.066 and 7.140 millivolts per foot.

The equation (4) can also be written as

$$\Delta \overline{V_R}^2 = \Delta u_1^2 \frac{C \bar{U}_1^2}{g^2}$$

or

$$\Delta u_1^2 = \frac{g}{C^2 \bar{U}_1^2} \overline{\Delta V_R^2}$$

Similarly

$$\overline{\Delta u_1^2 (n)} = \frac{g}{C^2 \bar{U}_1^2} \overline{\Delta V_R^2 (n)} \quad \ldots\ldots\ldots (6)$$

Now the wave number has been defined as

$$K_1 = \frac{2\pi n}{\bar{U}_1}$$

$$\Delta K_1 = \frac{2\pi}{\bar{U}_1} \Delta n \quad \ldots\ldots\ldots (7)$$

So equation (6) may also be written as

$$\overline{\Delta u_1^2 (K_1)} = \frac{g^2}{C^2 \bar{U}_1} \overline{\Delta V_R^2 (K_1)} \quad \ldots\ldots\ldots (8)$$

where

$\overline{\Delta V_R^2 (K_1)}$ = mean square of the output of the wave analyzer in volts resulting from turbulence fluctuations contained within the band width provided by the analyzer at wave number k_1 corresponding

to the frequency set on the wave analyzer.

$\overline{\Delta u_1^2(K_1)}$ = turbulence energy of fluctuations contained in the band width at K_1 corresponding frequency set on wave analyzer.

Dividing (8) by (7) we get

$$\frac{\Delta u_1^2(K)}{\Delta K_1} = E_1(K_1) = \frac{g\,\overline{\Delta V_R^2(K_1)}\,\bar{U}_1}{C^2\bar{U}_1^2\,2\pi\,\Delta n}$$

$$= E_1(K_1) = \frac{g^2\,\overline{\Delta V_R^2(K_1)}}{C^2\bar{U}_1\,2\pi\,\Delta n} \quad \ldots\ldots (9)$$

This equation can be used for the spectrum measurements.

Appendix B

Properties of Averaged Quantities

If there is some fluctuating quantity then the average value of this quantity is usually denoted by placing a bar above its symbol.

Such average values have the following properties

Let $A = \bar{A} + a \qquad B = \bar{B} + b$

where $\bar{A}$ and $\bar{B}$ are considered constant mean value quantities and a and b are the fluctuating components.

Then

$$\bar{A} = \overline{\bar{A} + a} = \bar{\bar{A}} + \bar{a} = \bar{A} + \bar{a} = \bar{A} \quad . \quad . \quad . \quad . \quad . \quad . \quad . \quad . \quad . \quad (1)$$

It is usual to consider "a" as random variable such that $\bar{a} = 0$

$$\overline{AB} = \bar{\bar{A}}\bar{\bar{B}} \triangleq \bar{A}\bar{B} \quad . \quad . \quad . \quad . \quad . \quad . \quad . \quad . \quad . \quad . \quad . \quad . \quad . \quad . \quad (2)$$

$$\overline{\bar{A}b} = \bar{\bar{A}}\bar{b} = \bar{A}\bar{b} = 0 \quad \text{Since } \bar{b} = 0 \quad . \quad . \quad . \quad . \quad . \quad . \quad . \quad . \quad . \quad (3)$$

Similarly

$$\overline{\bar{B}a} = \bar{\bar{B}}\bar{a} = \bar{B}\bar{a} = 0$$

$$\overline{AB} = \overline{(\bar{A} + a)\ (\bar{B} + b)}$$

$$= \overline{\bar{A}\bar{B}} + \overline{\bar{A}b} + \overline{\bar{B}a} + \overline{ab}$$

$$= \bar{A}\bar{B} + \overline{ab} \quad . \quad . \quad . \quad . \quad . \quad . \quad . \quad . \quad . \quad . \quad . \quad . \quad . \quad . \quad . \quad (4)$$

$$\overline{(ca)} = c\bar{a} \qquad \text{where c is a constant} \quad . \quad . \quad . \quad . \quad . \quad . \quad . \quad . \quad . \quad (5)$$

$$\overline{\frac{da}{dt}} = \frac{d\bar{a}}{dt} \quad . \quad . \quad . \quad . \quad . \quad . \quad . \quad . \quad . \quad . \quad . \quad . \quad . \quad . \quad . \quad . \quad (6)$$

Appendix C

Details of Electronic Instruments

Name

Wave and noise spectrum analyzer

Type 303

No. 21 Y

Manufacturer:

Quan-Tech Laboratories Inc.
Boonton, New Jersey

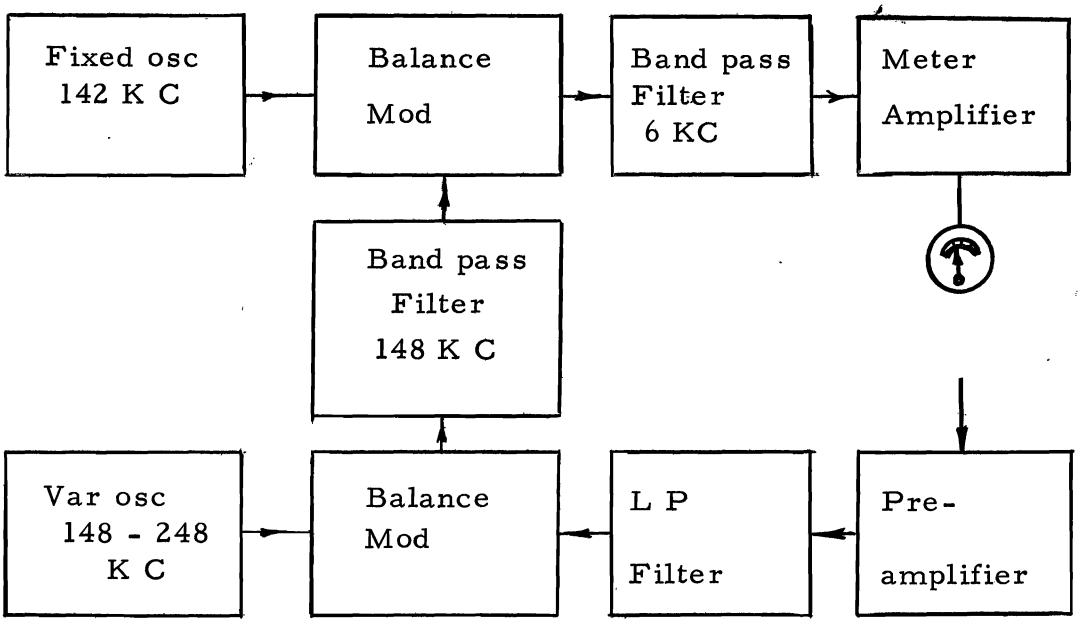

Figure 47. Simplified block diagram of spectrum analyzer internal circuit

Name:

Decade variable delay network

Type 801 j

No. 30-32146

Manufacturer:

AD-YU Electronics Inc.
249 - 259 Terhone Avenue
Passaic, New Jersey U.S.A.

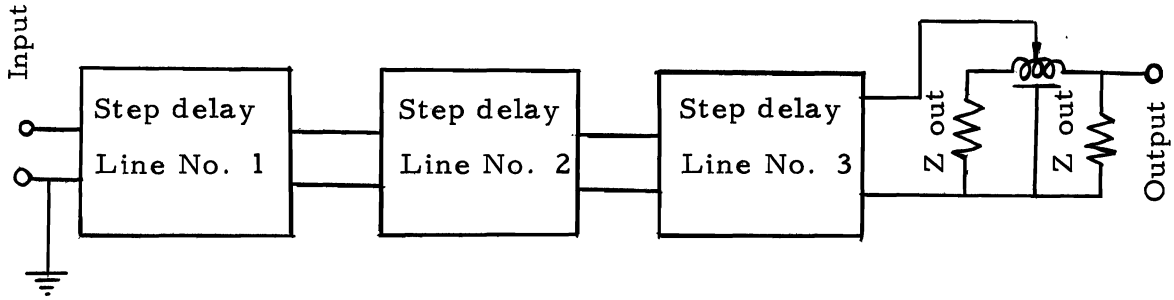

Figure 48. Block diagram of internal circuit of variable time delay.

Name:

Disa random signal indicator and correlator

Type 55A 0 6

No. 112

Manufacturer:

Dias Elektronic A/S Herlev
Copenhagen, Denmark

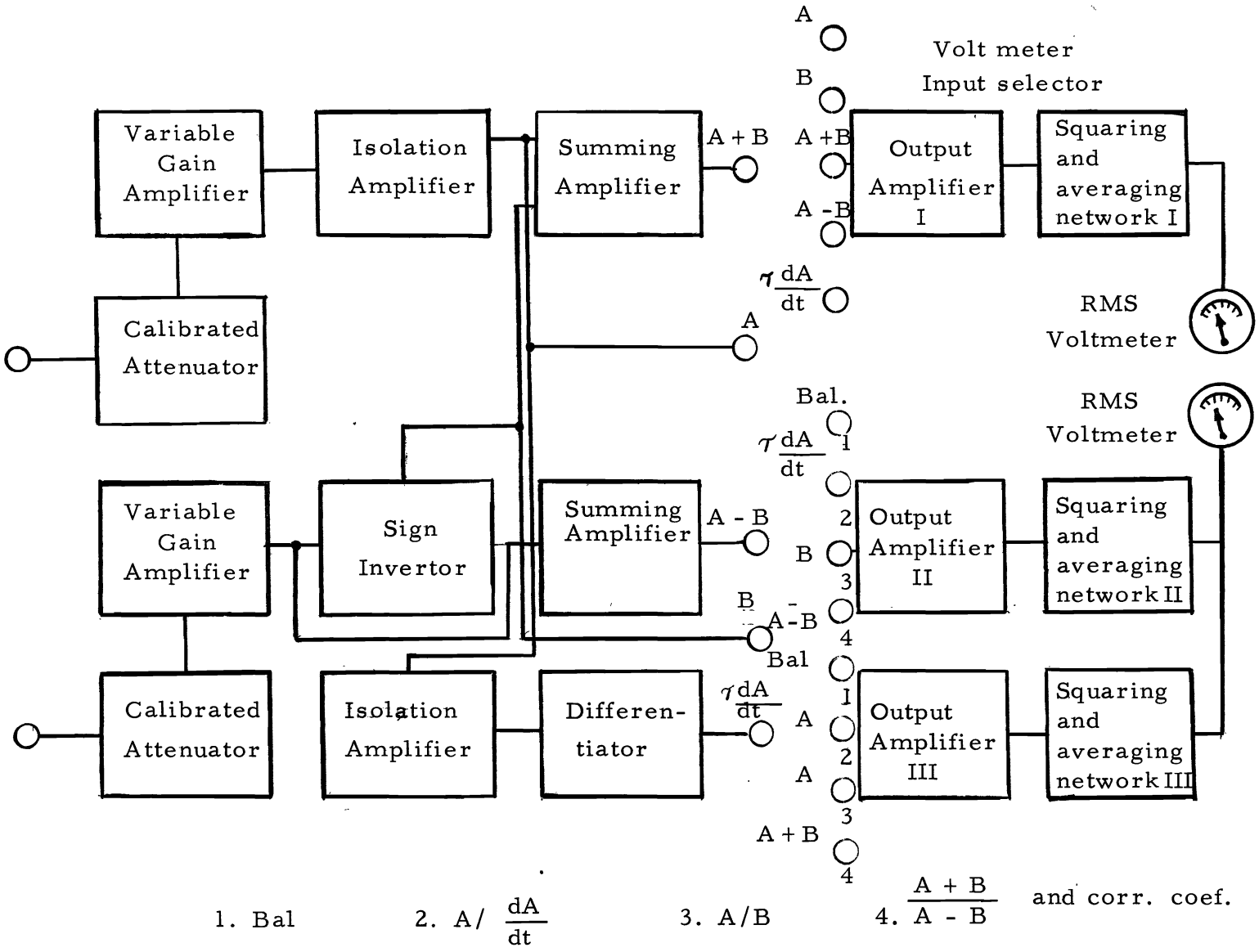

Figure 49. Block diagram of the internal circuit of the random signal indicator and correlator.

VITA

Farooq Nazir

Candidate for the Degree of

Master of Science

Thesis: The Structure of Turbulence in an Open Channel with Large Spherical Roughness Elements.

Major Field: Hydraulics.

Biographical Information:

Personal Data: Born at Sialkot, West Pakistan, October 11, 1943, son of Nazir Ahmad and Sughra Nazir; unmarried.

Education: Attended elementary school in Lahore, West Pakistan; received F. Sc. certificate from Government College Lahore; received the Bachelor of Engineering Degree from West Pakistan University of Engineering and Technology, in 1964; presently working toward Master of Science degree in hydraulics at Utah State University.

Professional Experience: Served West Pakistan Water and Power Development Authority from July 1964 to December 1965.